

Numerical methods for light scattering in plasmonic structures with corners

Camille Carvalho

A.S. Bonnet-Ben Dhia¹, L. Chesnel², P. Ciarlet Jr.¹

¹POEMS, UMR CNRS-ENSTA-INRIA, Université Paris Saclay, France

²DEFI, INRIA, Université Paris Saclay, France

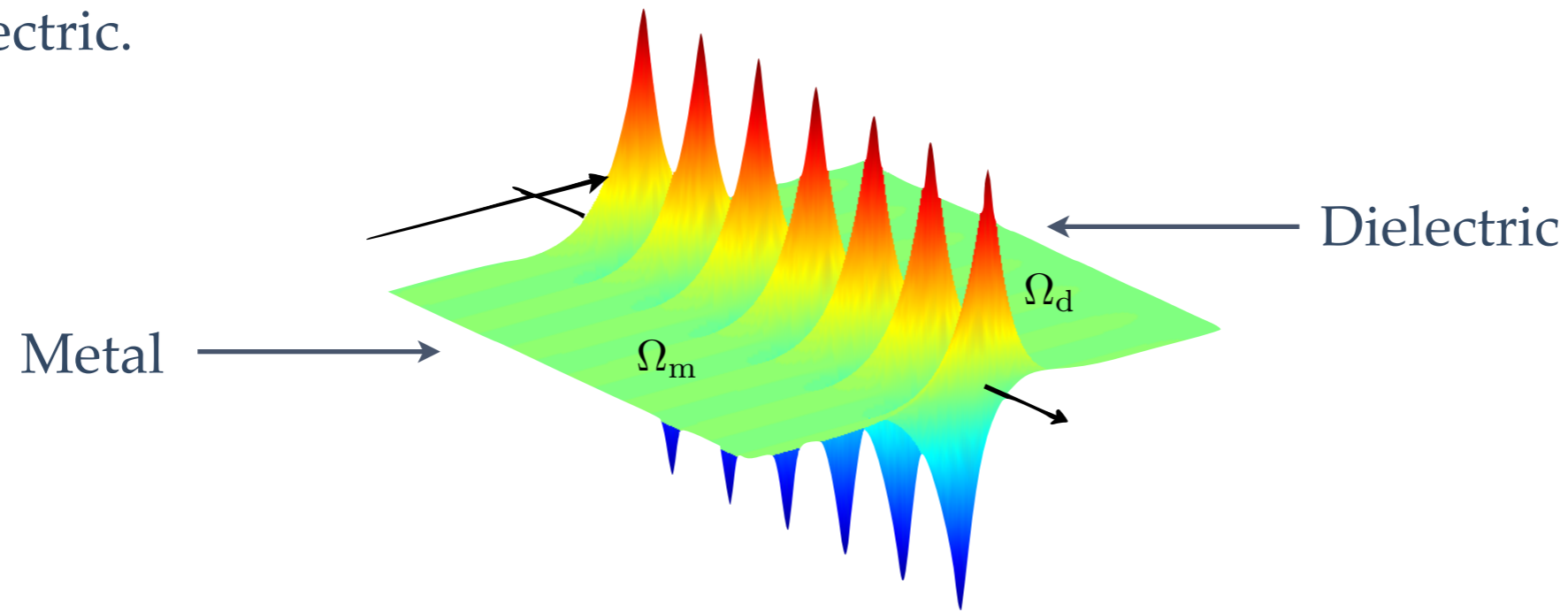


INRIA, september 2018

What are surface plasmons ?

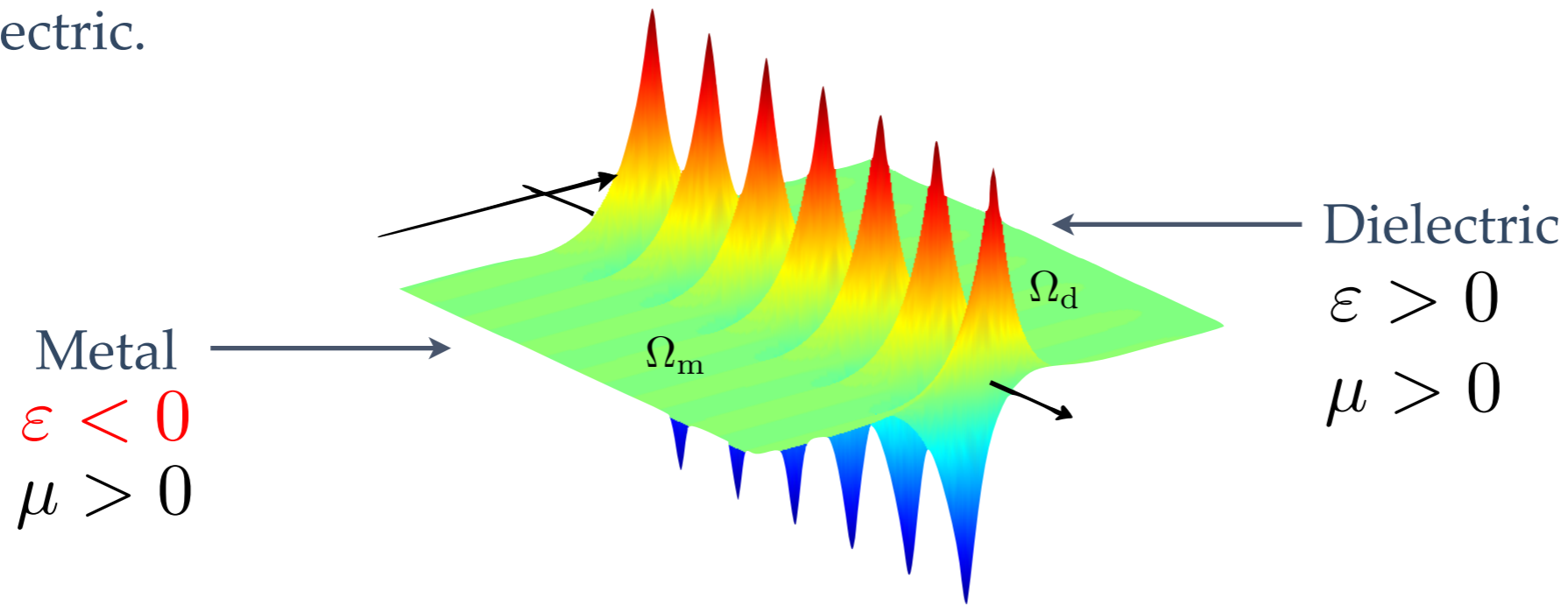
What are surface plasmons ?

Surface plasmons are **confined electromagnetic waves** at the interface between a metal and a dielectric.



What are surface plasmons ?

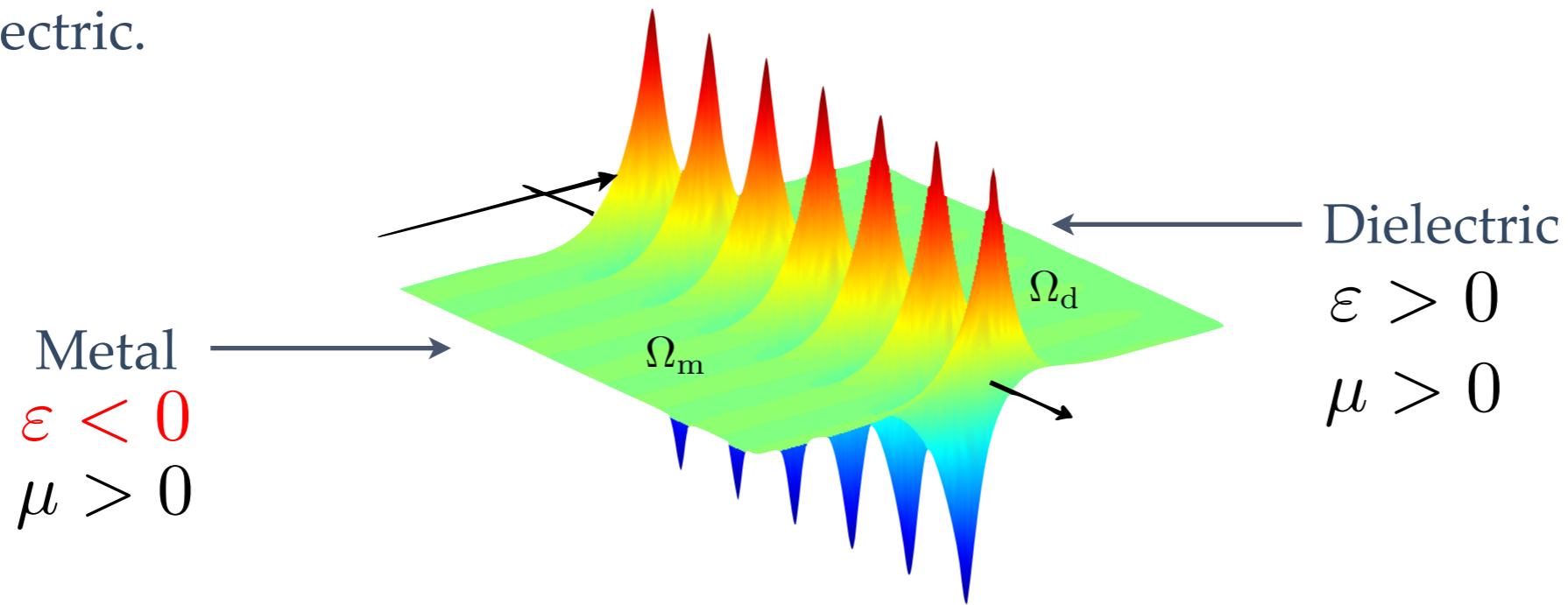
Surface plasmons are **confined electromagnetic waves** at the interface between a metal and a dielectric.



Such waves exist **at optical frequencies**, where the permittivity **changes sign**.

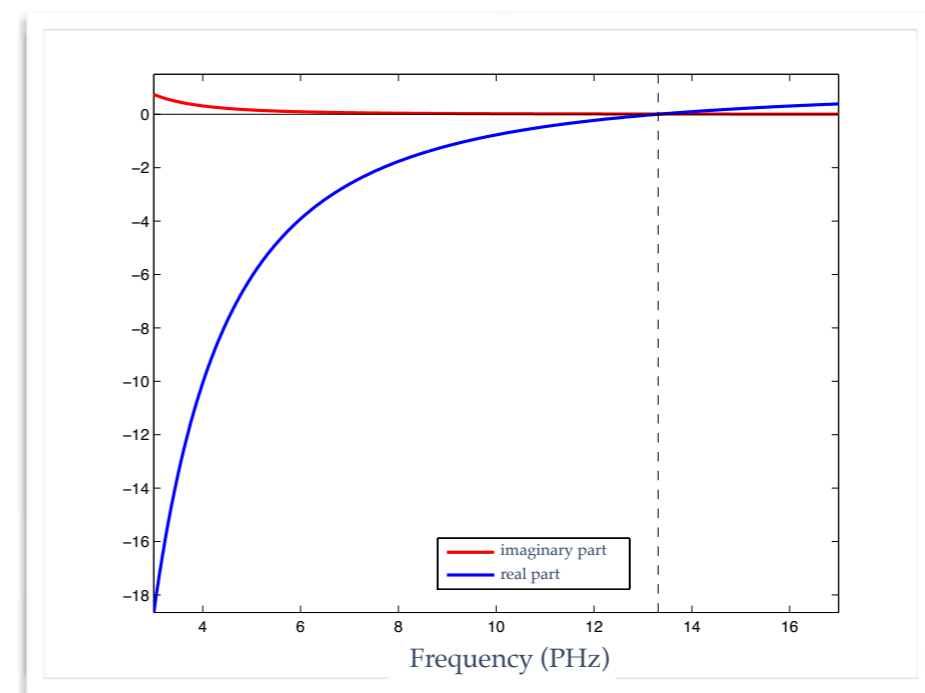
What are surface plasmons ?

Surface plasmons are **confined electromagnetic waves** at the interface between a metal and a dielectric.



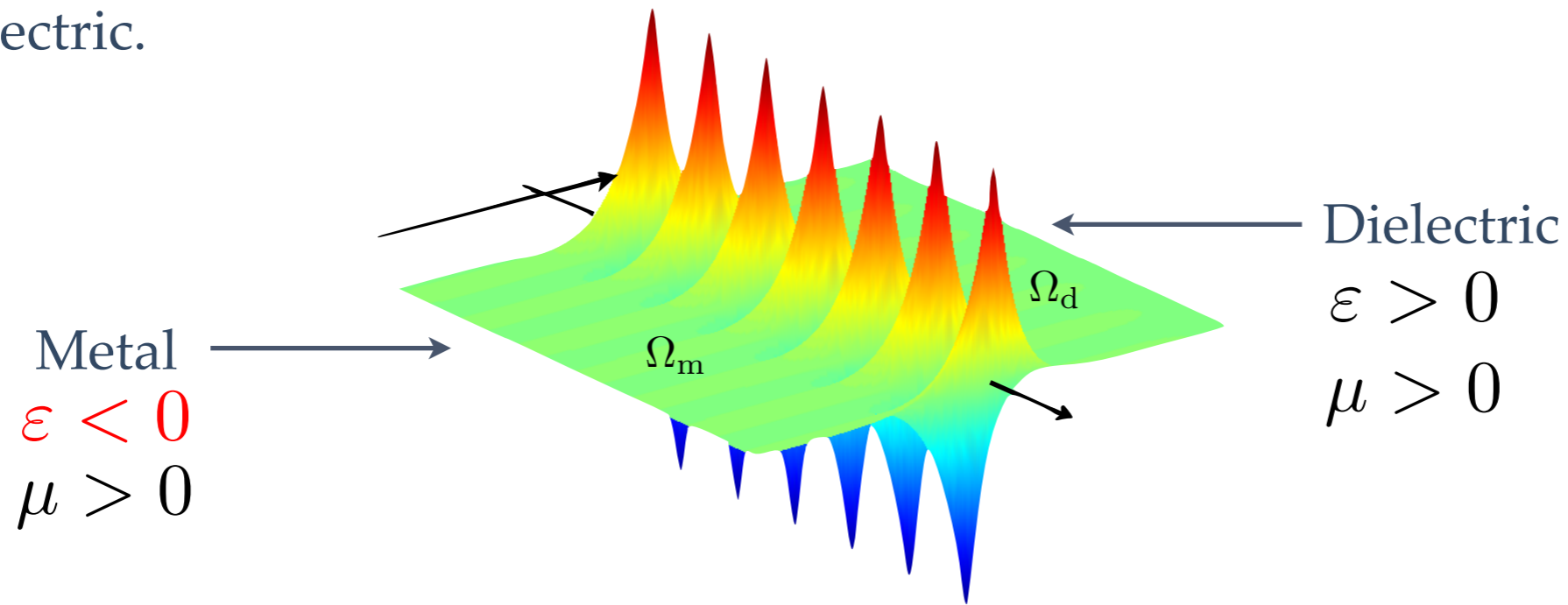
Such waves exist **at optical frequencies**, where the permittivity **changes sign**. One simple model of permittivity: Drude's model (convention $e^{-i\omega t}$).

$$\epsilon = \epsilon^\gamma(\omega) := 1 - \frac{\omega_p^2}{\omega^2 + i\omega\gamma}$$



What are surface plasmons ?

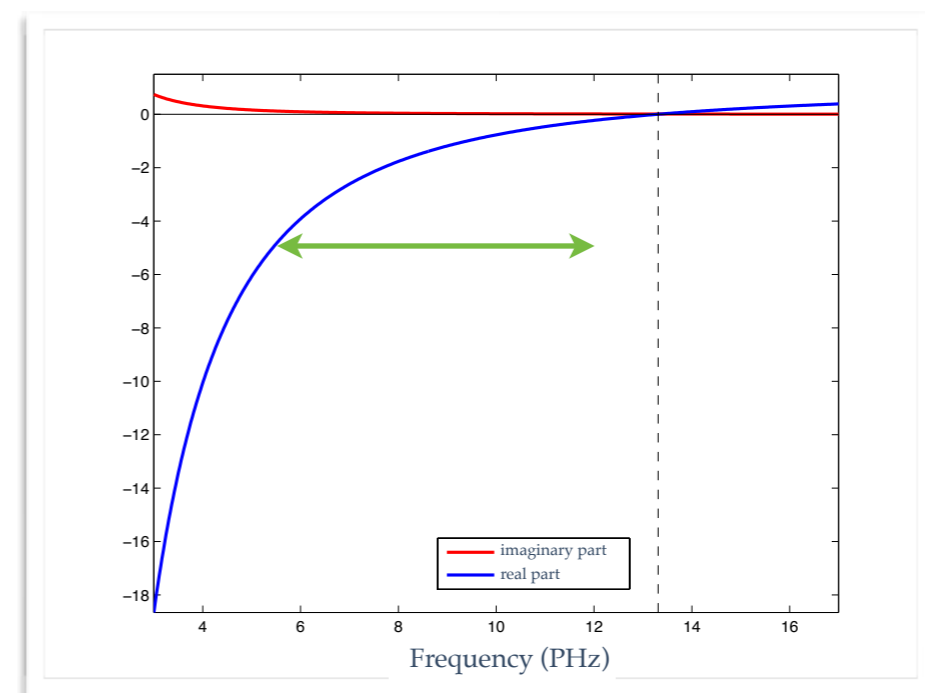
Surface plasmons are **confined electromagnetic waves** at the interface between a metal and a dielectric.



Such waves exist **at optical frequencies**, where the permittivity **changes sign**. One simple model of permittivity: Drude's model (convention $e^{-i\omega t}$).

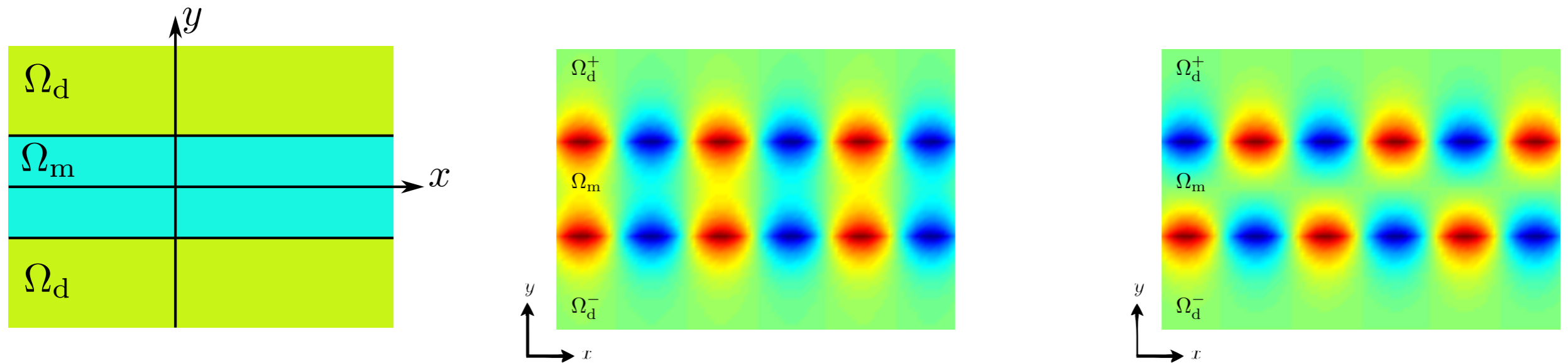
$$\epsilon = \epsilon^\gamma(\omega) := 1 - \frac{\omega_p^2}{\omega^2 + i\omega\gamma}$$

At optical frequencies ($\gamma \ll \omega < \omega_p$), ϵ has a **negative** real part and a neglectable imaginary part.



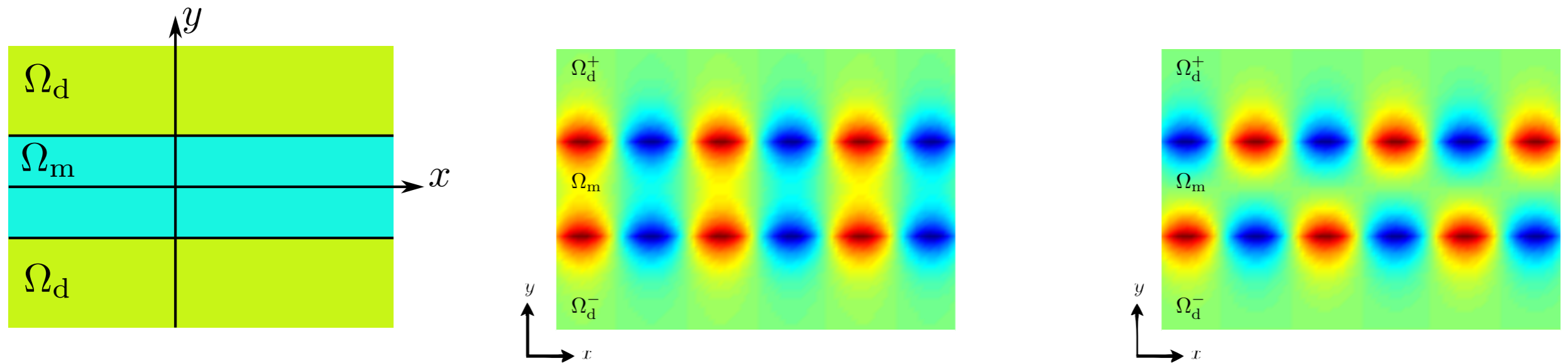
Surface plasmons and geometries

For **simple geometries**, one can get the expression of surface plasmons (use of separation of variables and deal with ODEs).



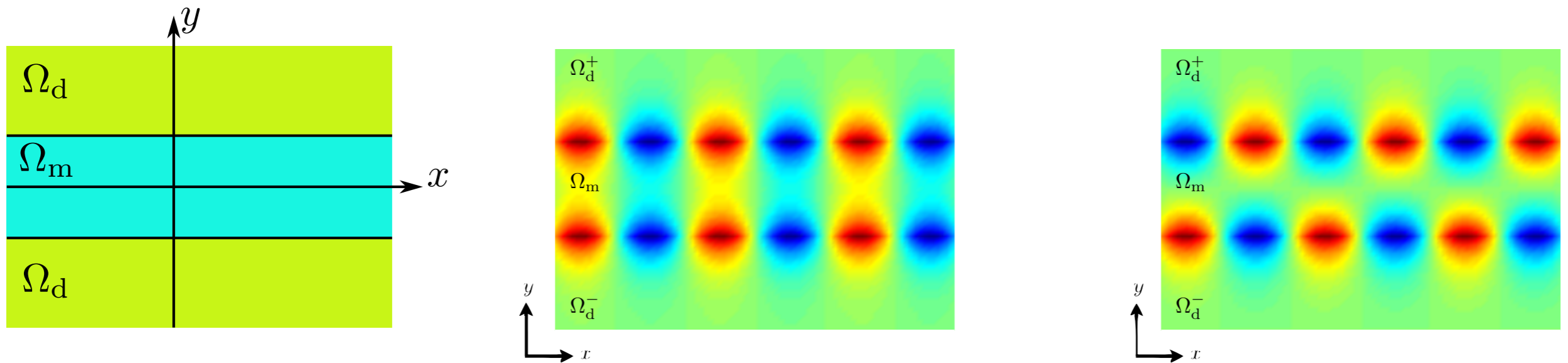
Surface plasmons and geometries

For **simple geometries**, one can get the expression of surface plasmons (use of separation of variables and deal with ODEs).



Surface plasmons and geometries

For **simple geometries**, one can get the expression of surface plasmons (use of separation of variables and deal with ODEs).

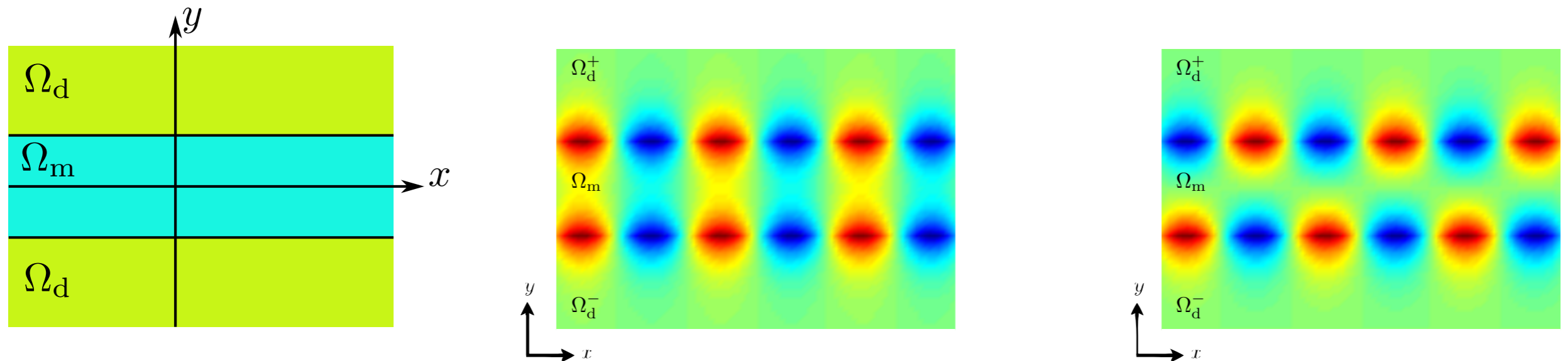


In more complex geometries:

- one has to solve **PDEs with sign-changing coefficients** (mathematical challenges)
- for non regular geometry **singular behaviors appear**
- phenomenon of **nanofocusing at sub-wavelength** (multiple scales to handle)

Surface plasmons and geometries

For **simple geometries**, one can get the expression of surface plasmons (use of separation of variables and deal with ODEs).



In more complex geometries:

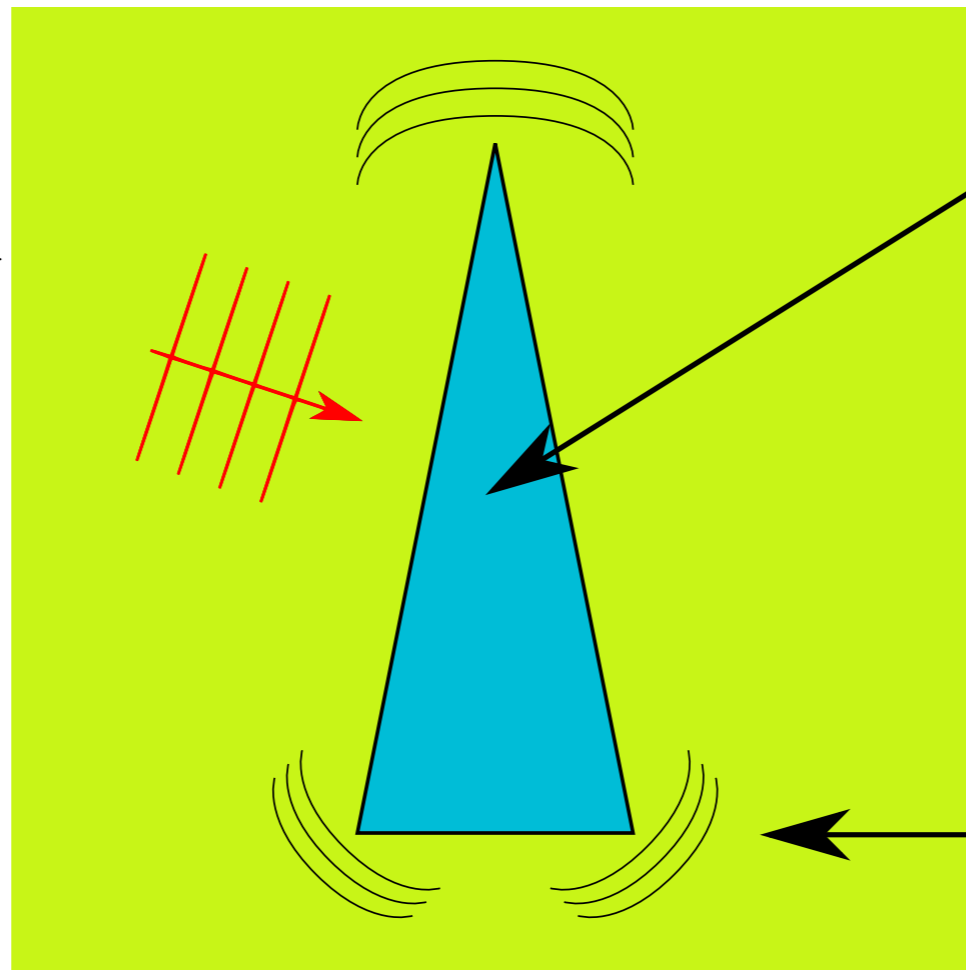
- one has to solve **PDEs with sign-changing coefficients** (mathematical challenges)
- for non regular geometry **singular behaviors appear**
- phenomenon of **nanofocusing at sub-wavelength** (multiple scales to handle)

Goal: develop accurate methods that take into account the multiple scales inherent.

The plasmonic scattering problem

The goal is to compute the scattered field by a polygonal metallic obstacle.

$$u^{inc} = e^{i \vec{k} \cdot \vec{x}}$$

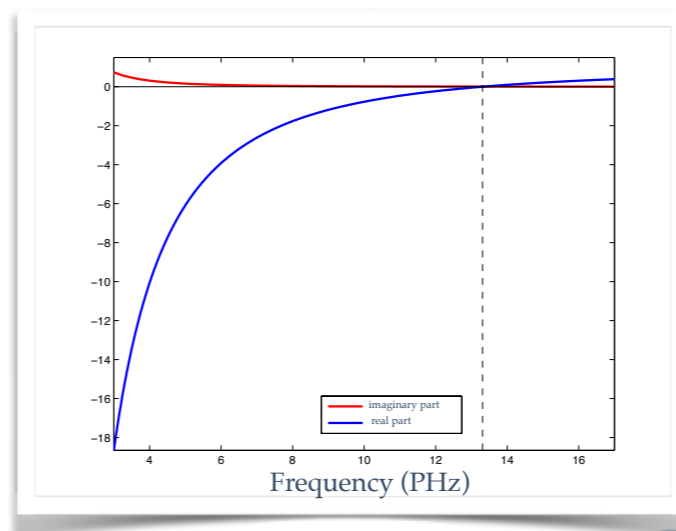


Metal
 $\epsilon_m(\omega)$ $\mu_m > 0$

Dielectric
 $\epsilon_d > 0$ $\mu_d > 0$

Metal's permittivity follows the Drude's model (convention $e^{-i\omega t}$):

$$\epsilon = \epsilon^\gamma(\omega) := 1 - \frac{\omega_p^2}{\omega^2 + i\omega\gamma}$$



Time-harmonic equations for the TM polarization

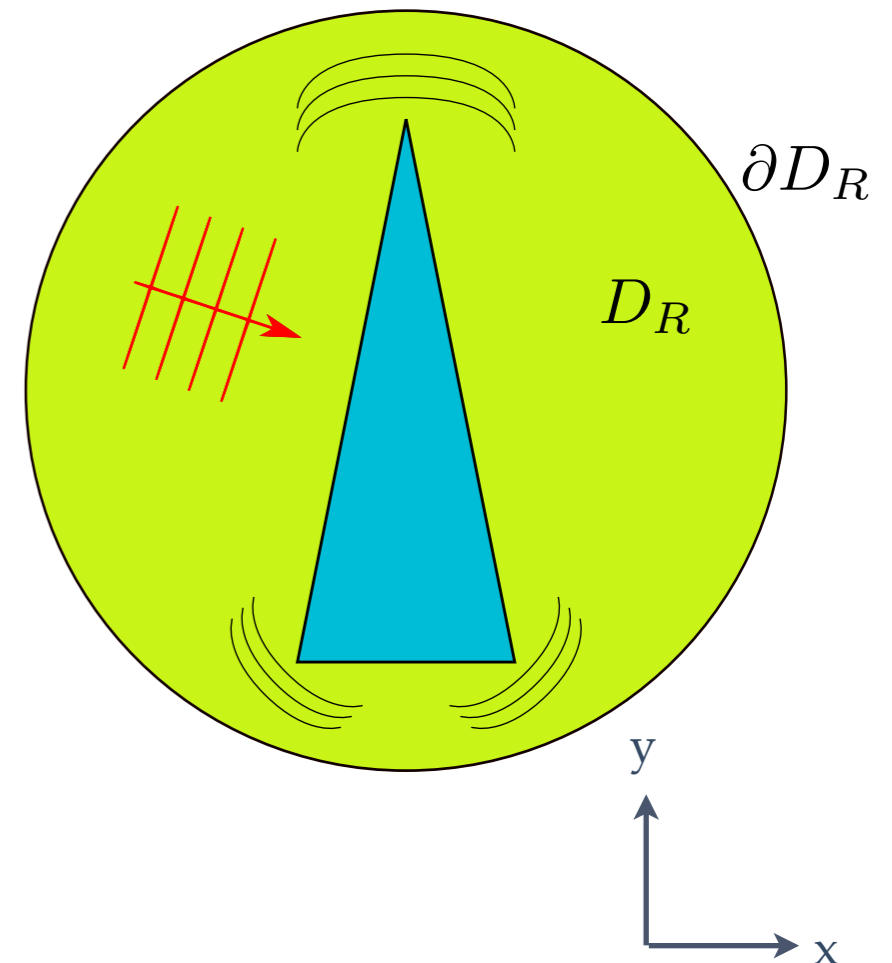
$$H_z = u^{\text{inc}} + u^{\text{sca}} \quad k = \frac{\omega}{c} \sqrt{\epsilon_d \mu_d}$$

$$\operatorname{div} \left(\frac{1}{\epsilon(\omega)} \nabla H_z \right) + \frac{\omega^2}{c^2} \mu H_z = 0 \text{ in } D_R$$

$$\partial_n H_z - ik H_z = \partial_n u^{\text{inc}} - ik u^{\text{inc}} \text{ on } \partial D_R$$

- * Radiation condition at finite distance

Work at a chosen frequency.



Time-harmonic equations for the TM polarization

$$H_z = u^{\text{inc}} + u^{\text{sca}} \quad k = \frac{\omega}{c} \sqrt{\epsilon_d \mu_d}$$

$$\operatorname{div} \left(\frac{1}{\epsilon(\omega)} \nabla H_z \right) + \frac{\omega^2}{c^2} \mu H_z = 0 \text{ in } D_R$$

$$\partial_n H_z - ik H_z = \partial_n u^{\text{inc}} - ik u^{\text{inc}} \text{ on } \partial D_R$$

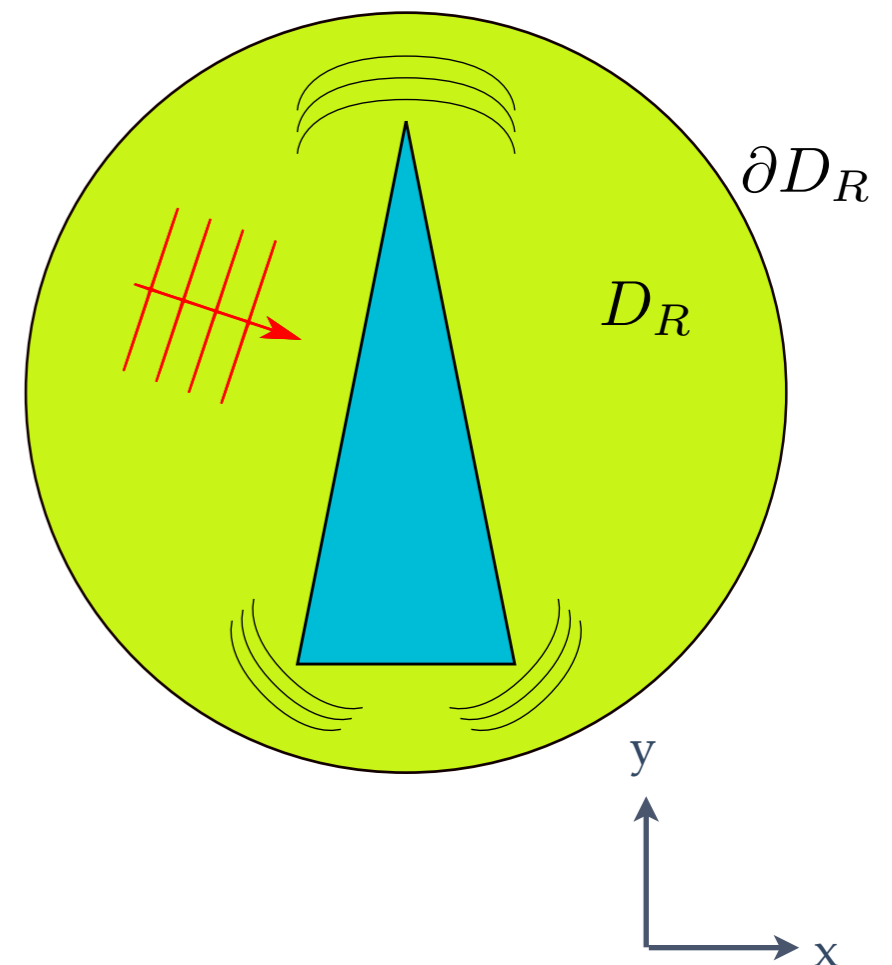
- * Radiation condition at finite distance

Work at a chosen frequency.

Mathematically:

-due to the dissipation, the problem has a unique solution
(Variational formulation + Fredholm theory)

-one can approximate the solution with Finite Elements Methods



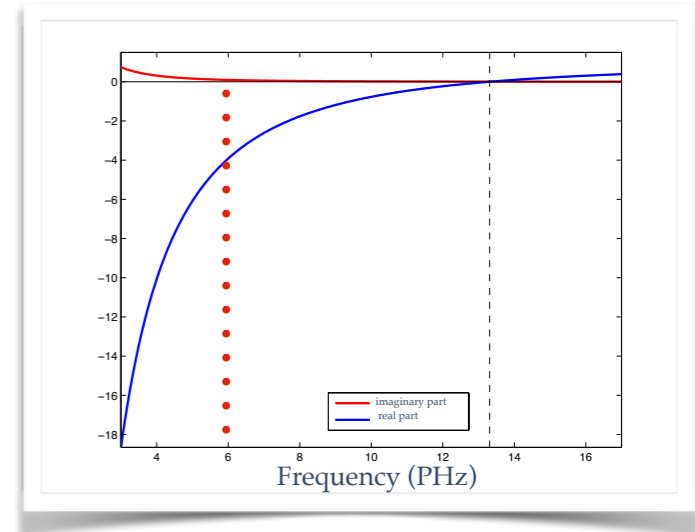
Numerical illustrations

We computed the total field for a triangular silver inclusion embedded in vacuum. We use Finite Element of order 2, with a plane wave of incidence $-\pi/12$.

Numerical illustrations

We computed the total field for a triangular silver inclusion embedded in vacuum. We use Finite Element of order 2, with a plane wave of incidence $-\pi/12$.

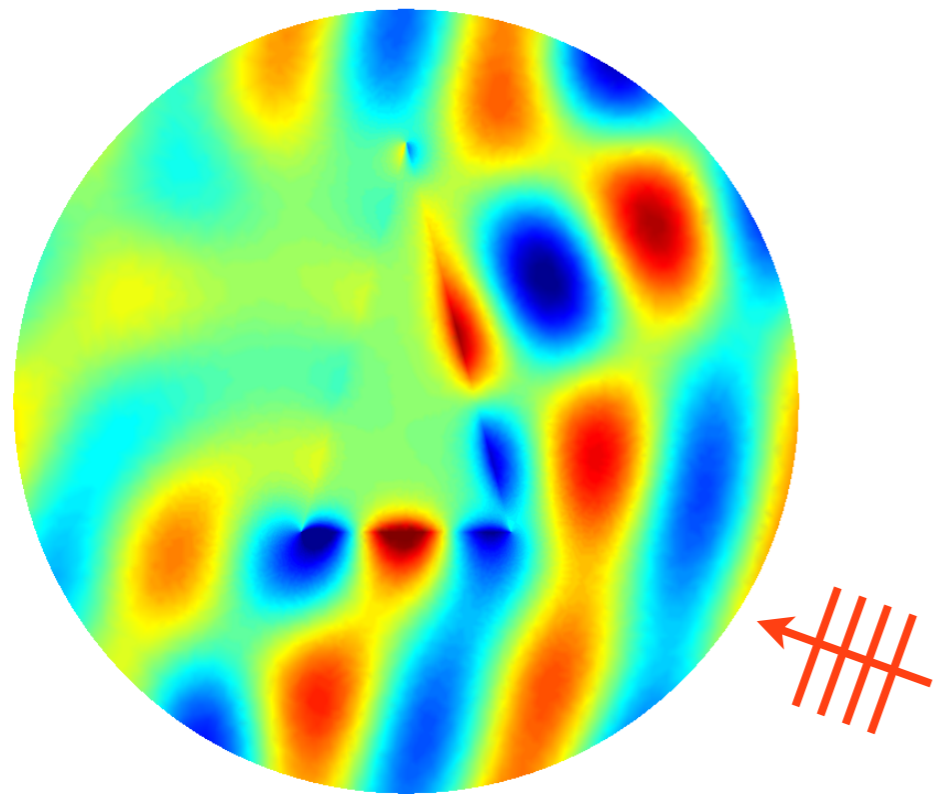
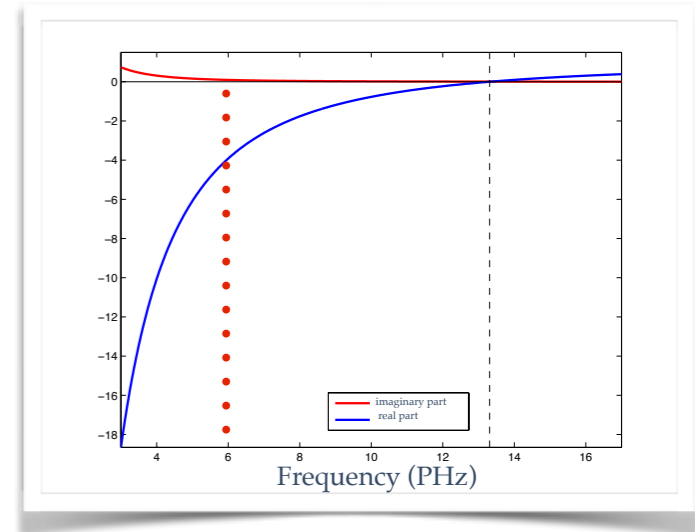
$$\omega_p = 13.3 \text{ PHz} \quad \omega = 6 \text{ PHz} \quad \gamma = 0.113 \text{ PHz}$$
$$\varepsilon_m(\omega) = -3.9193 + 0.0926i \quad \varepsilon_d = \mu_d = \mu_m = 1$$



Numerical illustrations

We computed the total field for a triangular silver inclusion embedded in vacuum. We use Finite Element of order 2, with a plane wave of incidence $-\pi/12$.

$$\begin{aligned} \omega_p &= 13.3 \text{ PHz} & \omega &= 6 \text{ PHz} & \gamma &= 0.113 \text{ PHz} \\ \varepsilon_m(\omega) &= -3.9193 + 0.0926i & \varepsilon_d &= \mu_d = \mu_m = 1 \end{aligned}$$

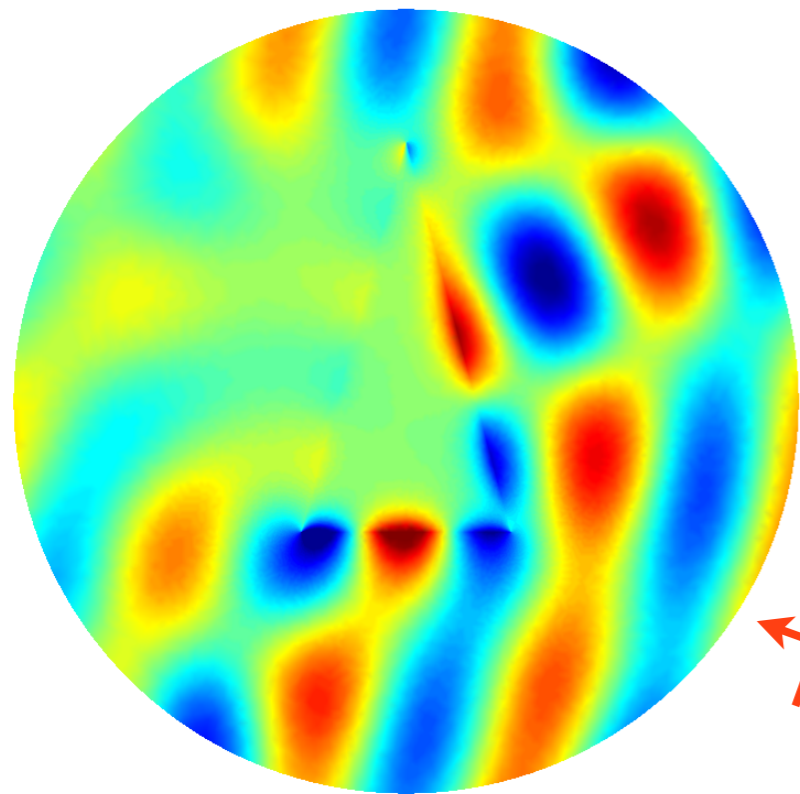
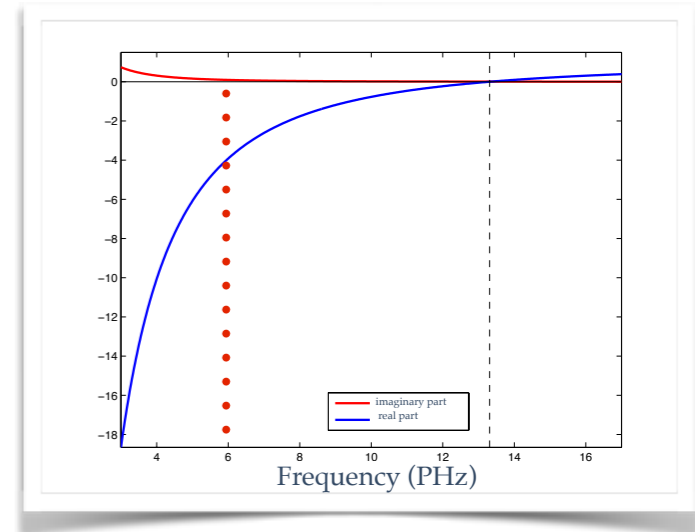


coarse mesh

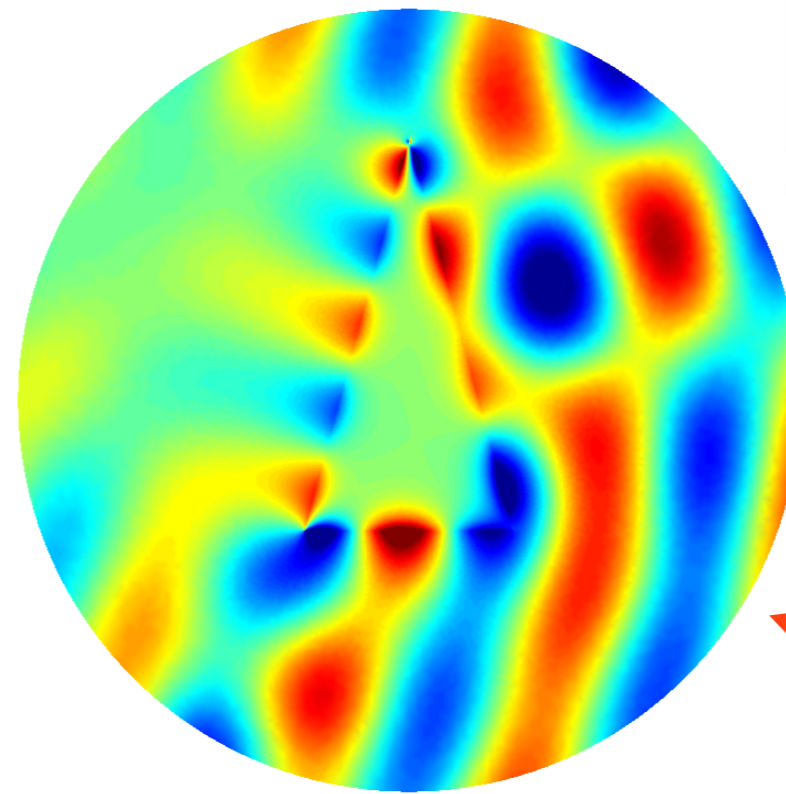
Numerical illustrations

We computed the total field for a triangular silver inclusion embedded in vacuum. We use Finite Element of order 2, with a plane wave of incidence $-\pi/12$.

$$\omega_p = 13.3 \text{ PHz} \quad \omega = 6 \text{ PHz} \quad \gamma = 0.113 \text{ PHz}$$
$$\varepsilon_m(\omega) = -3.9193 + 0.0926i \quad \varepsilon_d = \mu_d = \mu_m = 1$$



coarse mesh

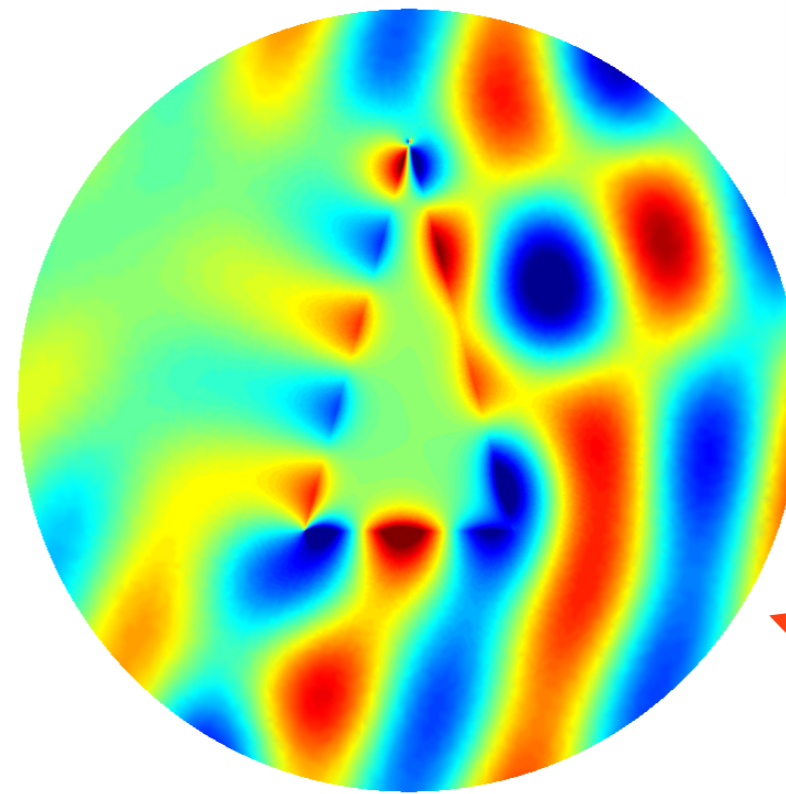
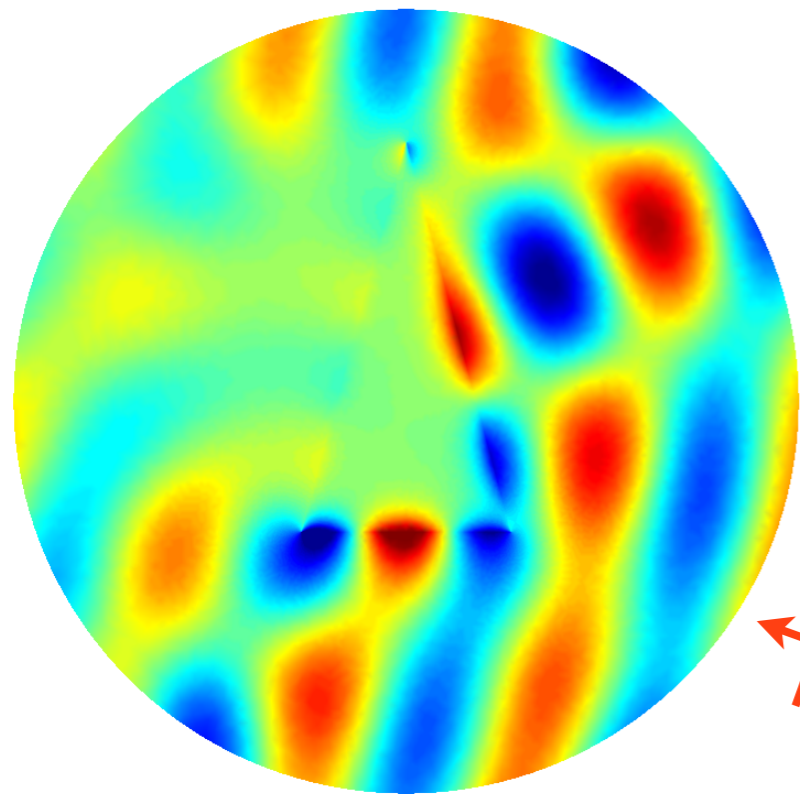
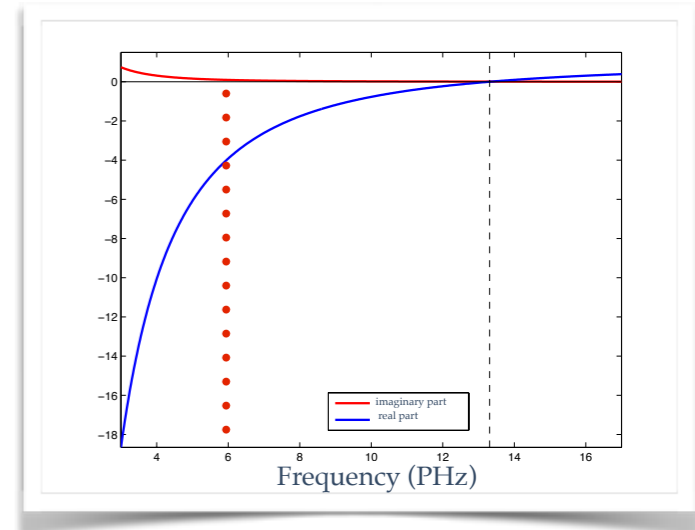


refined mesh

Numerical illustrations

We computed the total field for a triangular silver inclusion embedded in vacuum. We use Finite Element of order 2, with a plane wave of incidence $-\pi/12$.

$$\omega_p = 13.3 \text{ PHz} \quad \omega = 6 \text{ PHz} \quad \gamma = 0.113 \text{ PHz}$$
$$\varepsilon_m(\omega) = -3.9193 + 0.0926i \quad \varepsilon_d = \mu_d = \mu_m = 1$$

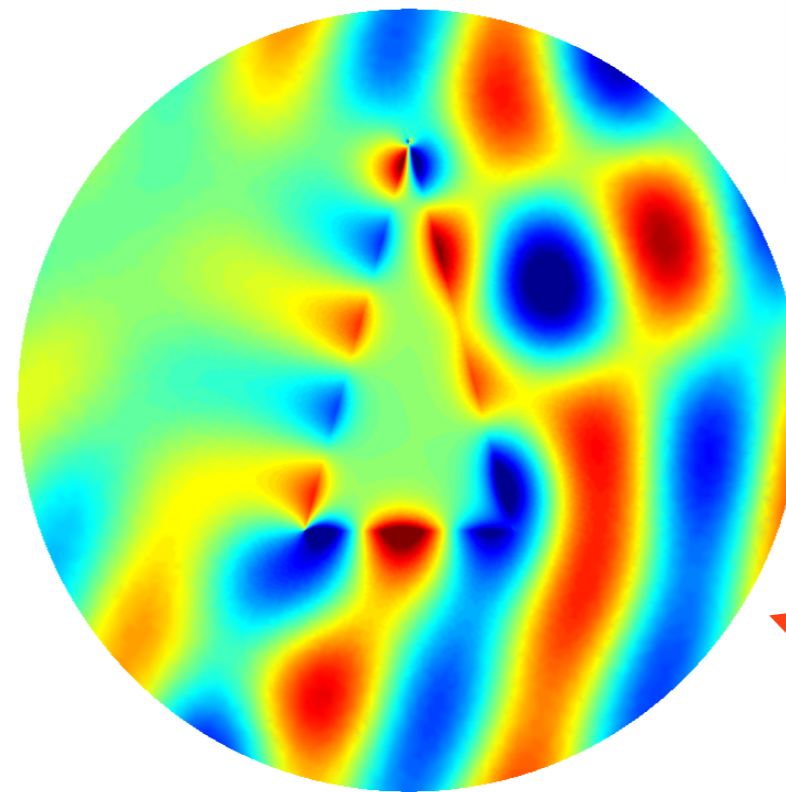
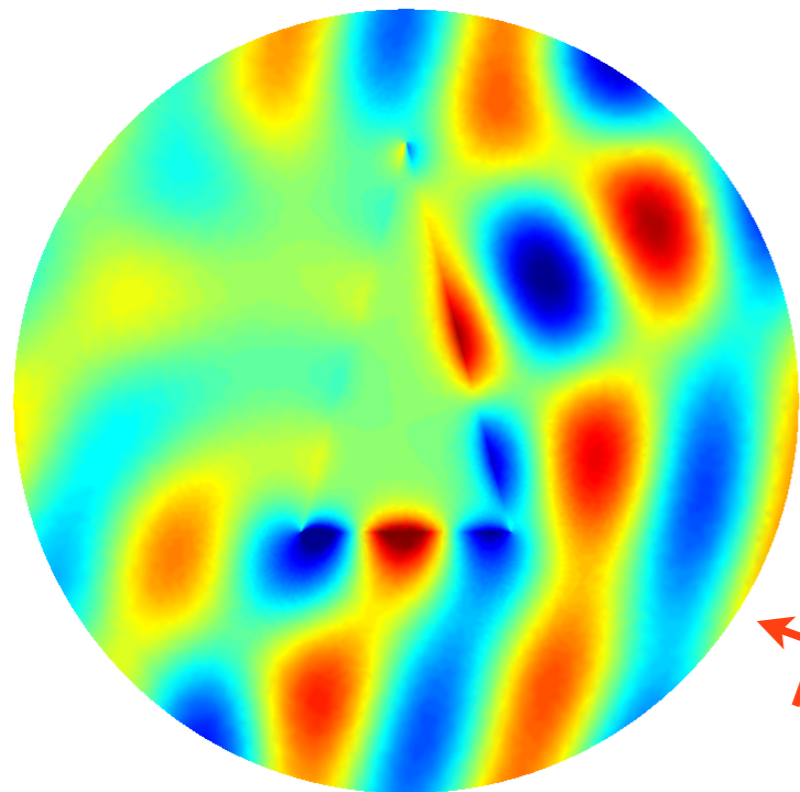
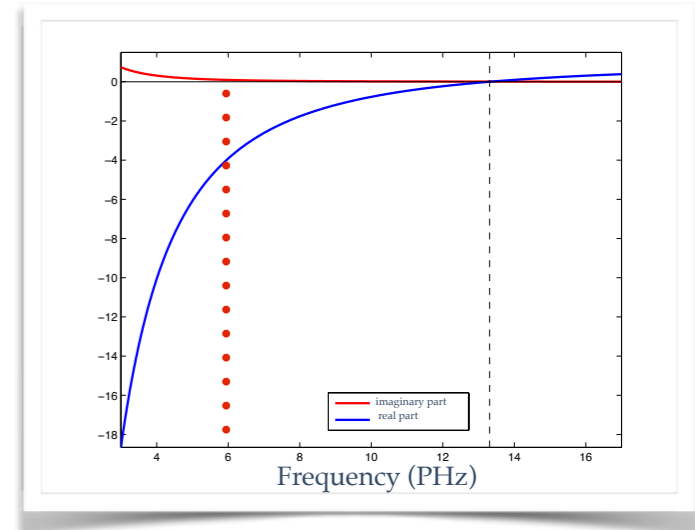


The solution is not stable ! Strong oscillations near the corners.

Numerical illustrations

We computed the total field for a triangular silver inclusion embedded in vacuum. We use Finite Element of order 2, with a plane wave of incidence $-\pi/12$.

$$\omega_p = 13.3 \text{ PHz} \quad \omega = 6 \text{ PHz} \quad \gamma = 0.113 \text{ PHz}$$
$$\varepsilon_m(\omega) = -3.9193 + 0.0926i \quad \varepsilon_d = \mu_d = \mu_m = 1$$



The solution is not stable ! Strong oscillations near the corners.
To understand the reasons of such instabilities and how to avoid them, we study a limit problem by neglecting dissipation.

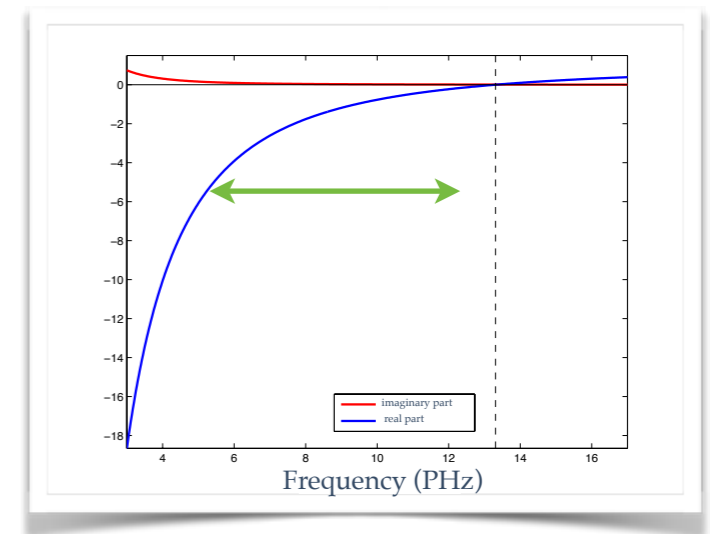
Outline

- ❖ Introduction
- ❖ The limit problem
- ❖ Analysis at the corners
- ❖ Multiscale-FEM approach
- ❖ Extensions

The dissipationless Drude's model

At optical frequencies one can neglect dissipation so that the metal's permittivity follows the law:

$$\varepsilon = \varepsilon^0(\omega) := 1 - \frac{\omega_p^2}{\omega^2} < 0$$

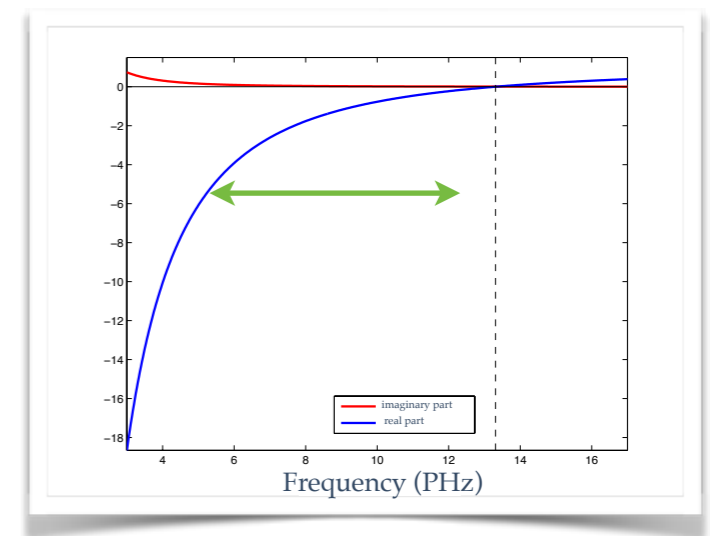


The dissipationless Drude's model

At optical frequencies one can neglect dissipation so that the metal's permittivity follows the law:

$$\varepsilon = \varepsilon^0(\omega) := 1 - \frac{\omega_p^2}{\omega^2} < 0$$

Now we consider the scattering problem with **sign-changing coefficient** (chosen frequency):



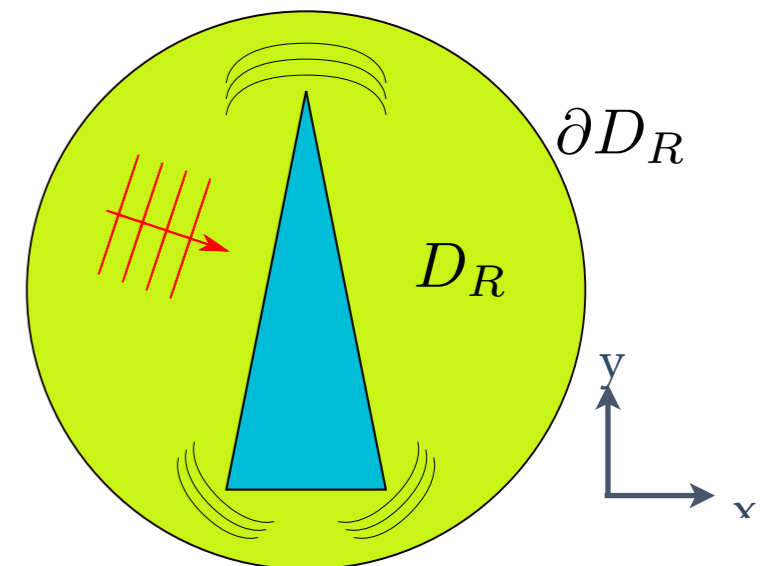
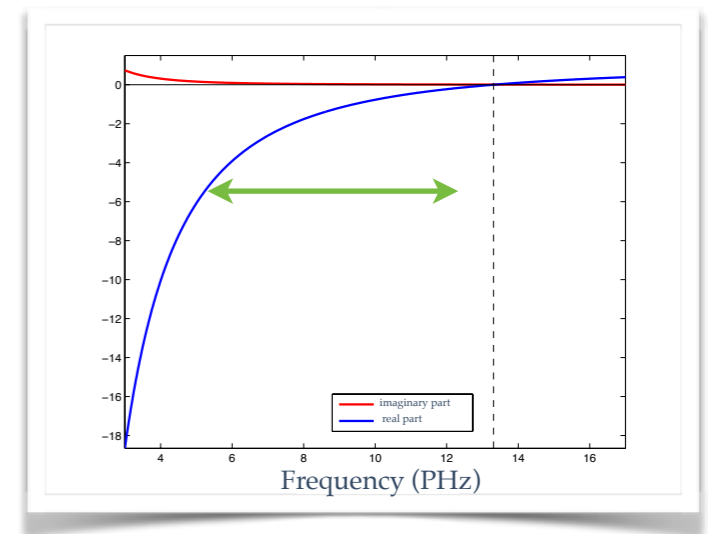
The dissipationless Drude's model

At optical frequencies one can neglect dissipation so that the metal's permittivity follows the law:

$$\varepsilon = \varepsilon^0(\omega) := 1 - \frac{\omega_p^2}{\omega^2} < 0$$

Now we consider the scattering problem with **sign-changing coefficient** (chosen frequency):

$$\operatorname{div} \left(\frac{1}{\varepsilon(\omega)} \nabla H_z \right) + \frac{\omega^2}{c^2} \mu H_z = 0 \text{ in } D_R$$
$$\partial_n H_z - ik H_z = \partial_n u^{\text{inc}} - ik u^{\text{inc}} \text{ on } \partial D_R$$



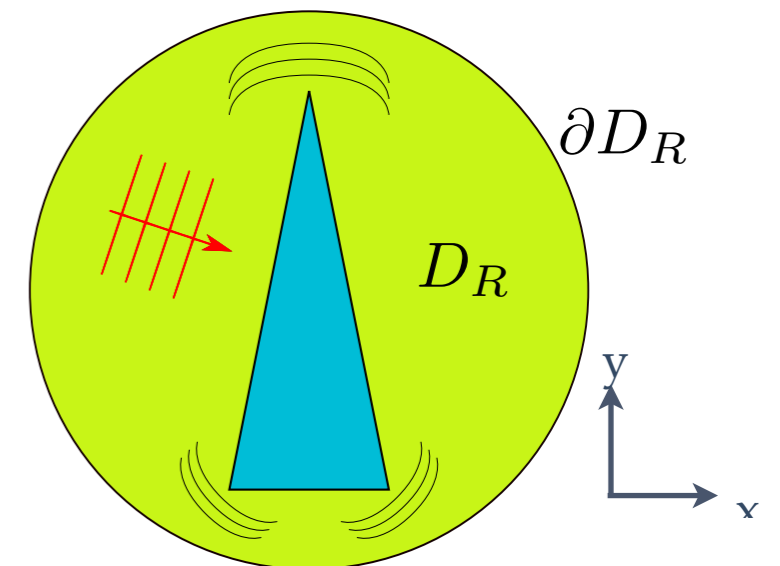
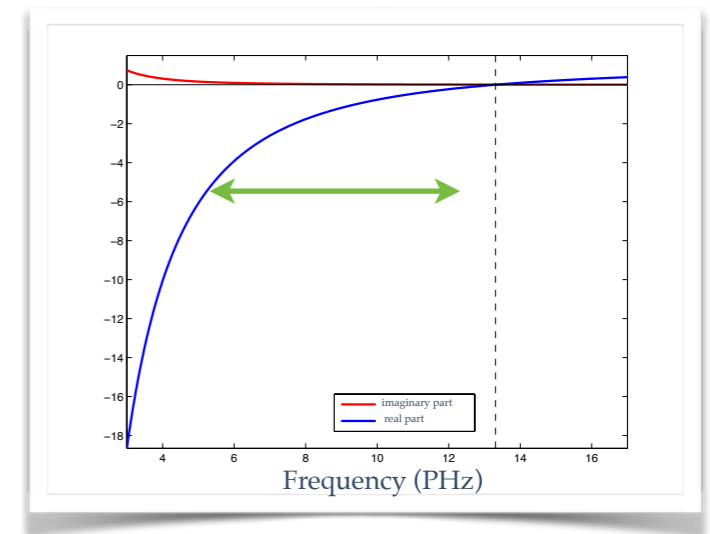
The dissipationless Drude's model

At optical frequencies one can neglect dissipation so that the metal's permittivity follows the law:

$$\varepsilon = \varepsilon^0(\omega) := 1 - \frac{\omega_p^2}{\omega^2} < 0$$

Now we consider the scattering problem with **sign-changing coefficient** (chosen frequency):

$$\operatorname{div} \left(\frac{1}{\varepsilon(\omega)} \nabla H_z \right) + \frac{\omega^2}{c^2} \mu H_z = 0 \text{ in } D_R$$
$$\partial_n H_z - ik H_z = \partial_n u^{\text{inc}} - ik u^{\text{inc}} \text{ on } \partial D_R$$



Mathematically this implies for our problem:

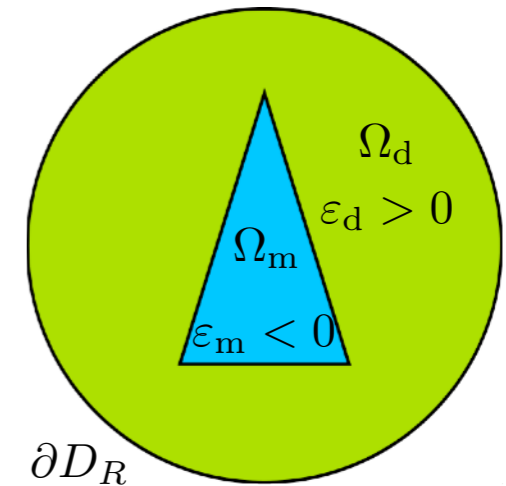
- difficulties to prove existence and uniqueness of the solution
- the corners of the inclusion may cause strong singular behavior
- standard approximation with Finite Elements Methods may fail

Well-posedness of the problem

Find $u := u^{\text{inc}} + u^{\text{sc}} \in H^1(D_R)$ such that: $H^1(D_R) := \{u \mid \int_{D_R} |u|^2 + |\nabla u|^2 d\mathbf{x} < +\infty\}$

$\text{div}(\varepsilon^{-1} \nabla u) + \frac{\omega^2}{c^2} \mu u = 0$ in D_R ,

$\partial_n u - iku = \partial u^{\text{inc}} - iku^{\text{inc}}$ on ∂D_R .

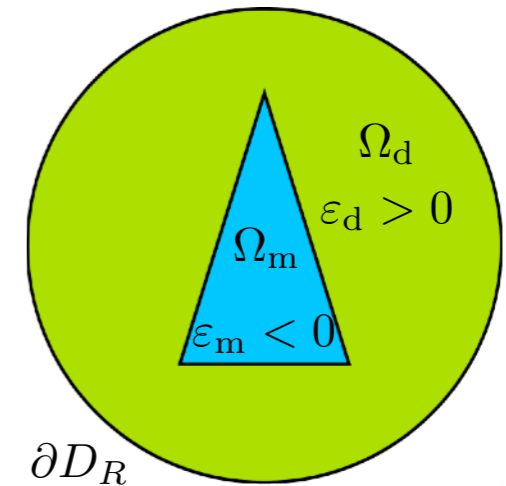


Well-posedness of the problem

Find $u := u^{\text{inc}} + u^{\text{sac}} \in H^1(D_R)$ such that: $H^1(D_R) := \{u \mid \int_{D_R} |u|^2 + |\nabla u|^2 d\mathbf{x} < +\infty\}$

$\text{div}(\varepsilon^{-1} \nabla u) + \frac{\omega^2}{c^2} \mu u = 0$ in D_R ,

$\partial_n u - iku = \partial u^{\text{inc}} - iku^{\text{inc}}$ on ∂D_R .



Thanks to the **T-coercivity theory**, one can prove well-posedness **under some conditions** on ε and the geometry.

Idea: build ad hoc isomorphisms to compensate the change of sign.



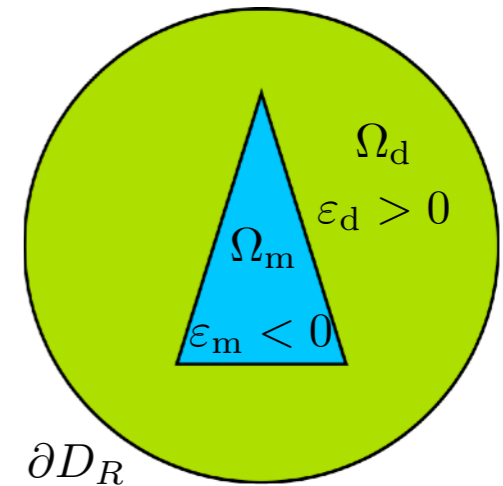
Bonnet-Ben Dhia, Ciarlet, Zwölf (2010), Bonnet-Ben Dhia, Chesnel, Ciarlet (2012).

Well-posedness of the problem

Find $u := u^{\text{inc}} + u^{\text{sac}} \in H^1(D_R)$ such that: $H^1(D_R) := \{u \mid \int_{D_R} |u|^2 + |\nabla u|^2 d\mathbf{x} < +\infty\}$

$\text{div}(\varepsilon^{-1} \nabla u) + \frac{\omega^2}{c^2} \mu u = 0$ in D_R ,

$\partial_n u - iku = \partial u^{\text{inc}} - iku^{\text{inc}}$ on ∂D_R .



Thanks to the **T-coercivity theory**, one can prove well-posedness **under some conditions** on ε and the geometry.

Idea: build ad hoc isomorphisms to compensate the change of sign.

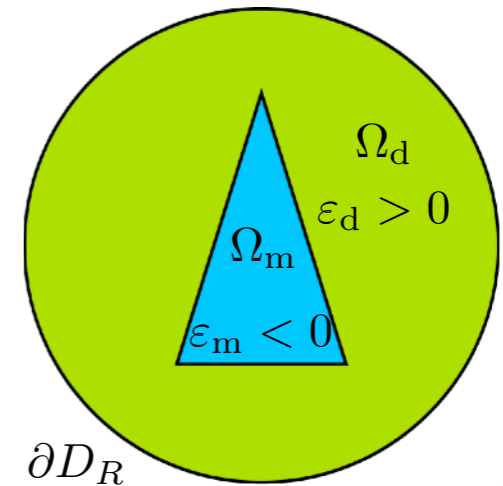
In our case: **YES if and only if** $\kappa_\varepsilon := \frac{\varepsilon_m}{\varepsilon_d} \notin I_c$



Bonnet-Ben Dhia, Ciarlet, Zwölf (2010), Bonnet-Ben Dhia, Chesnel, Ciarlet (2012).

Well-posedness of the problem

$$\left| \begin{array}{l} \text{Find } u := u^{\text{inc}} + u^{\text{sac}} \in H^1(D_R) \text{ such that: } H^1(D_R) := \{u \mid \int_{D_R} |u|^2 + |\nabla u|^2 d\mathbf{x} < +\infty\} \\ \text{div}(\varepsilon^{-1} \nabla u) + \frac{\omega^2}{c^2} \mu u = 0 \quad \text{in } D_R, \\ \partial_n u - iku = \partial u^{\text{inc}} - iku^{\text{inc}} \quad \text{on } \partial D_R. \end{array} \right.$$



Thanks to the **T-coercivity theory**, one can prove well-posedness **under some conditions** on ε and the geometry.

Idea: build ad hoc isomorphisms to compensate the change of sign.

In our case: **YES if and only if** $\kappa_\varepsilon := \frac{\varepsilon_m}{\varepsilon_d} \notin I_c$ I_c is called **critical interval**.



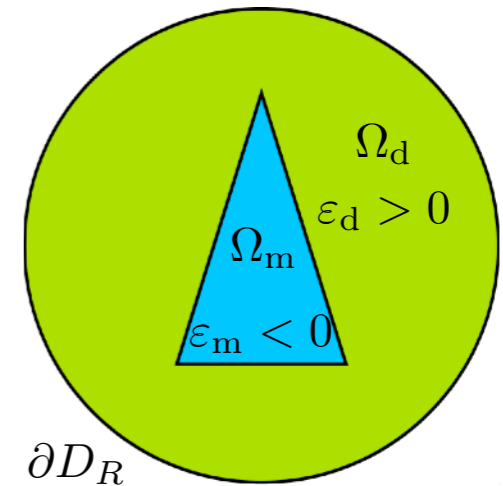
Bonnet-Ben Dhia, Ciarlet, Zwölf (2010), Bonnet-Ben Dhia, Chesnel, Ciarlet (2012).

Well-posedness of the problem

Find $u := u^{\text{inc}} + u^{\text{sac}} \in H^1(D_R)$ such that: $H^1(D_R) := \{u \mid \int_{D_R} |u|^2 + |\nabla u|^2 d\mathbf{x} < +\infty\}$

$$\text{div}(\varepsilon^{-1} \nabla u) + \frac{\omega^2}{c^2} \mu u = 0 \quad \text{in } D_R,$$

$$\partial_n u - iku = \partial u^{\text{inc}} - iku^{\text{inc}} \quad \text{on } \partial D_R.$$

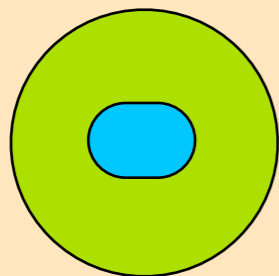


Thanks to the **T-coercivity theory**, one can prove well-posedness **under some conditions** on ε and the geometry.

Idea: build ad hoc isomorphisms to compensate the change of sign.

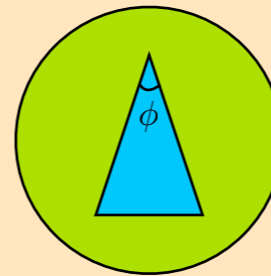
In our case: **YES if and only if** $\kappa_\varepsilon := \frac{\varepsilon_m}{\varepsilon_d} \notin I_c$ I_c is called **critical interval**.

If the interface is smooth:



$$I_c = \{-1\}$$

If the interface has corners:



$$I_c = \left[\frac{\phi - 2\pi}{\phi}; \frac{\phi}{\phi - 2\pi} \right]$$

$$\phi \rightarrow 0, I_c \rightarrow \mathbb{R}^-$$

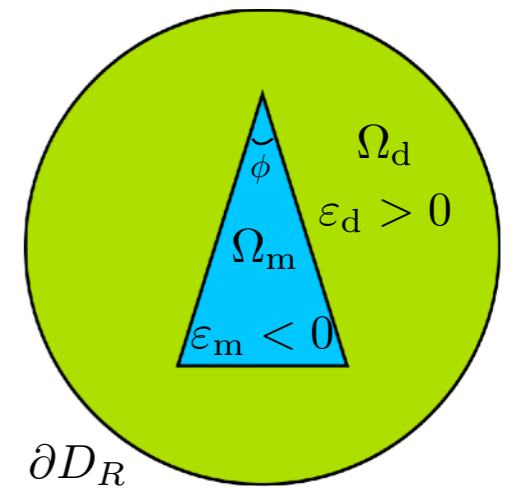
$$\phi \rightarrow \pi, I_c \rightarrow \{-1\}$$



Bonnet-Ben Dhia, Ciarlet, Zwölf (2010), Bonnet-Ben Dhia, Chesnel, Ciarlet (2012).

Critical interval and critical frequencies

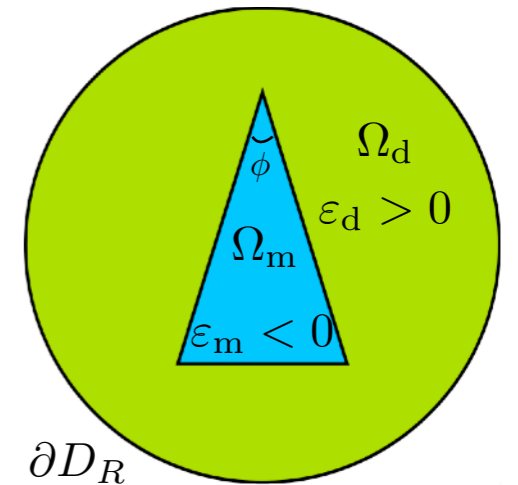
$$I_c = \left[\frac{\phi - 2\pi}{\phi}; \frac{\phi}{\phi - 2\pi} \right]$$



Critical interval and critical frequencies

The critical interval is related to **critical frequencies**:
for dissipationless Drude's we have

$$I_c = \left[\frac{\phi - 2\pi}{\phi}; \frac{\phi}{\phi - 2\pi} \right]$$

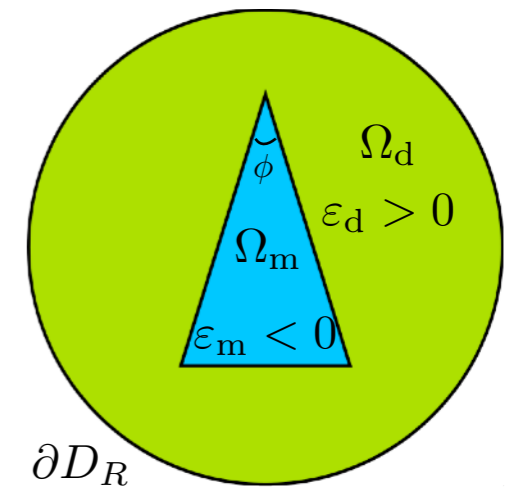


Critical interval and critical frequencies

The critical interval is related to **critical frequencies**:
for dissipationless Drude's we have

$$\kappa_{\varepsilon} \in \left[\frac{\phi - 2\pi}{\phi}; \frac{\phi}{2\pi - \phi} \right] \iff \omega \in \left[\frac{\omega_p}{\sqrt{1 + \frac{\phi}{\varepsilon_d(2\pi - \phi)}}}; \frac{\omega_p}{\sqrt{1 + \frac{\varepsilon_d \phi}{2\pi - \phi}}} \right]$$

$$I_c = \left[\frac{\phi - 2\pi}{\phi}; \frac{\phi}{\phi - 2\pi} \right]$$



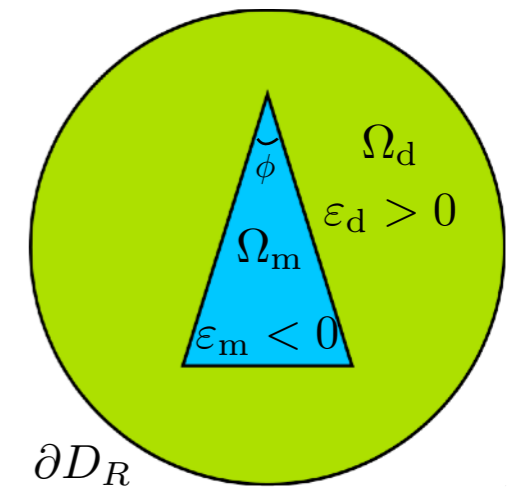
Critical interval and critical frequencies

The critical interval is related to **critical frequencies**:
for dissipationless Drude's we have

$$\kappa_{\varepsilon} \in \left[\frac{\phi - 2\pi}{\phi}; \frac{\phi}{2\pi - \phi} \right] \iff \omega \in \left[\frac{\omega_p}{\sqrt{1 + \frac{\phi}{\varepsilon_d(2\pi - \phi)}}}; \frac{\omega_p}{\sqrt{1 + \frac{\varepsilon_d \phi}{2\pi - \phi}}} \right]$$

$$\kappa_{\varepsilon} = -1 \iff \omega = \omega_{sp} := \frac{\omega_p}{\sqrt{1 + \varepsilon_d}} \text{ Surface plasmons frequency}$$

$$I_c = \left[\frac{\phi - 2\pi}{\phi}; \frac{\phi}{\phi - 2\pi} \right]$$



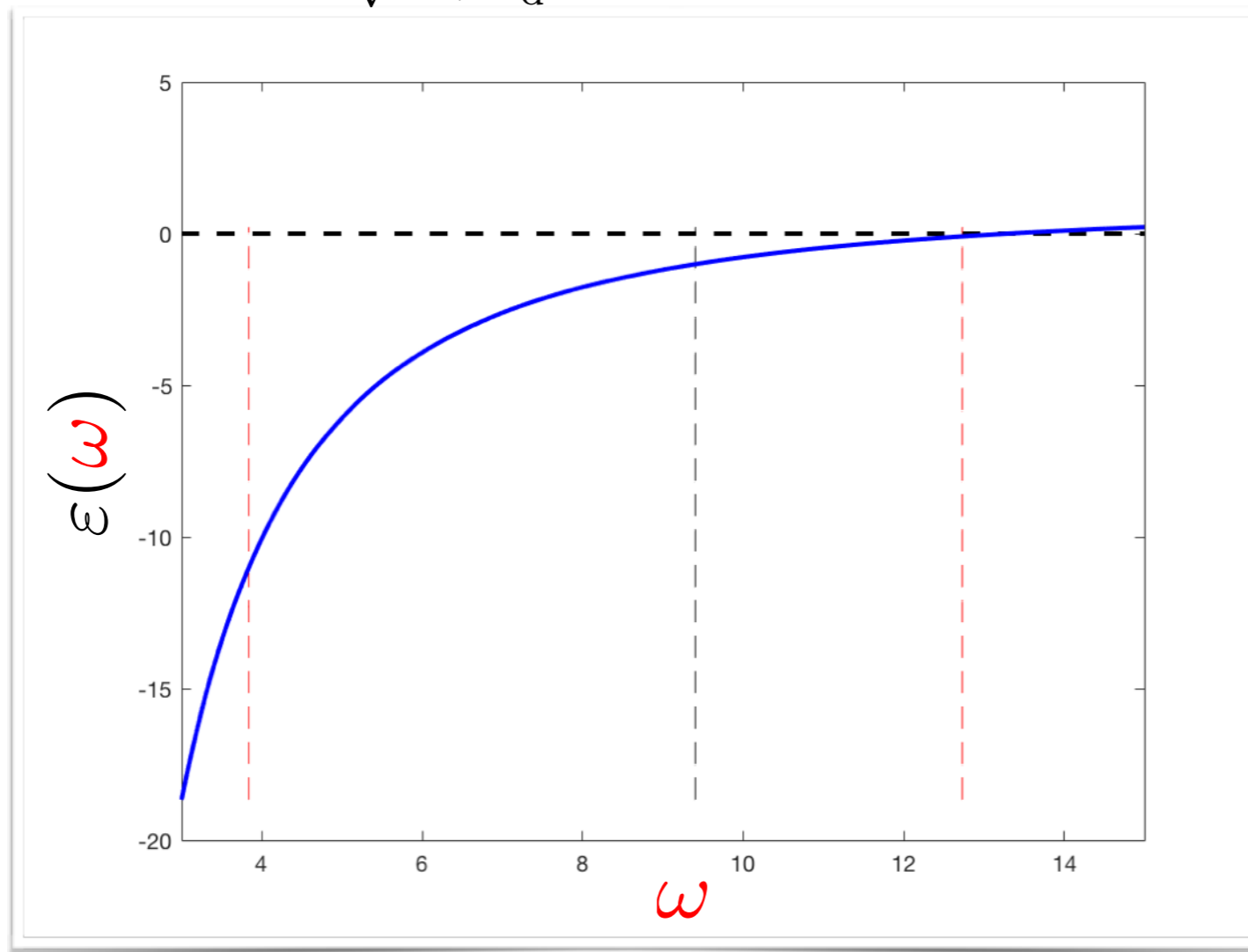
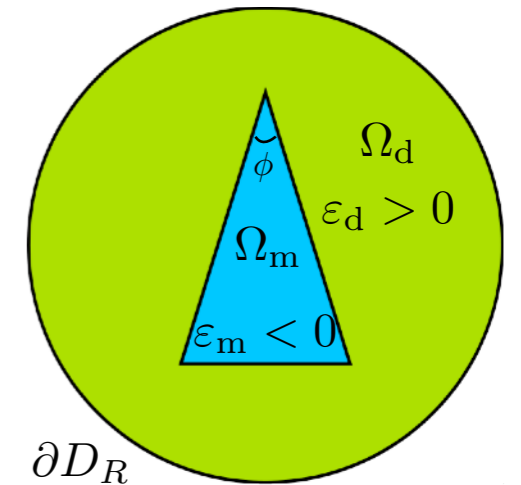
Critical interval and critical frequencies

The critical interval is related to **critical frequencies**:
for dissipationless Drude's we have

$$\kappa_{\varepsilon} \in \left[\frac{\phi - 2\pi}{\phi}; \frac{\phi}{2\pi - \phi} \right] \iff \omega \in \left[\frac{\omega_p}{\sqrt{1 + \frac{\phi}{\varepsilon_d(2\pi - \phi)}}}; \frac{\omega_p}{\sqrt{1 + \frac{\varepsilon_d \phi}{2\pi - \phi}}} \right]$$

$$\kappa_{\varepsilon} = -1 \iff \omega = \omega_{sp} := \frac{\omega_p}{\sqrt{1 + \varepsilon_d}} \text{ Surface plasmons frequency}$$

$$I_c = \left[\frac{\phi - 2\pi}{\phi}; \frac{\phi}{\phi - 2\pi} \right]$$



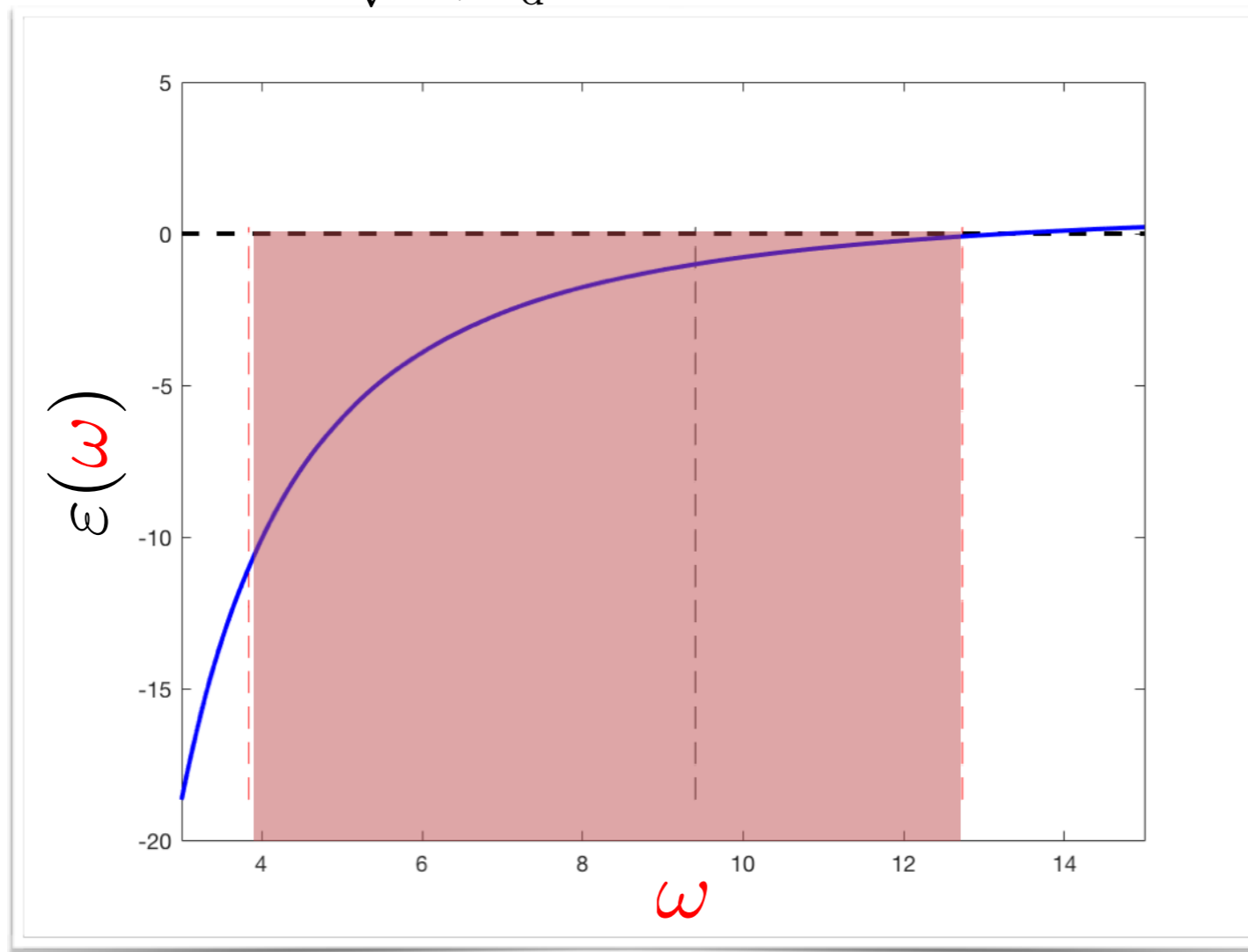
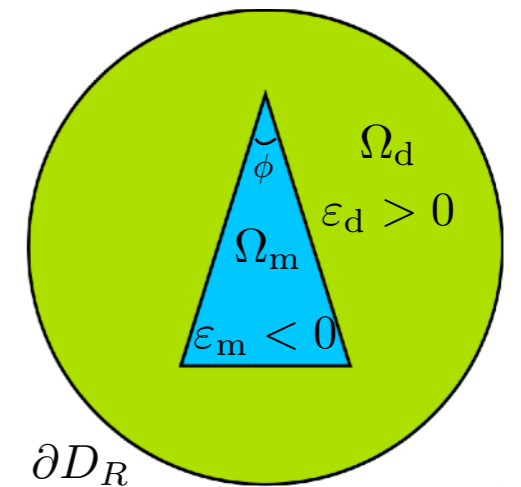
Critical interval and critical frequencies

The critical interval is related to **critical frequencies**:
for dissipationless Drude's we have

$$\kappa_{\varepsilon} \in \left[\frac{\phi - 2\pi}{\phi}; \frac{\phi}{2\pi - \phi} \right] \iff \omega \in \left[\frac{\omega_p}{\sqrt{1 + \frac{\phi}{\varepsilon_d(2\pi - \phi)}}}; \frac{\omega_p}{\sqrt{1 + \frac{\varepsilon_d \phi}{2\pi - \phi}}} \right]$$

$$\kappa_{\varepsilon} = -1 \iff \omega = \omega_{sp} := \frac{\omega_p}{\sqrt{1 + \varepsilon_d}} \text{ Surface plasmons frequency}$$

$$I_c = \left[\frac{\phi - 2\pi}{\phi}; \frac{\phi}{\phi - 2\pi} \right]$$



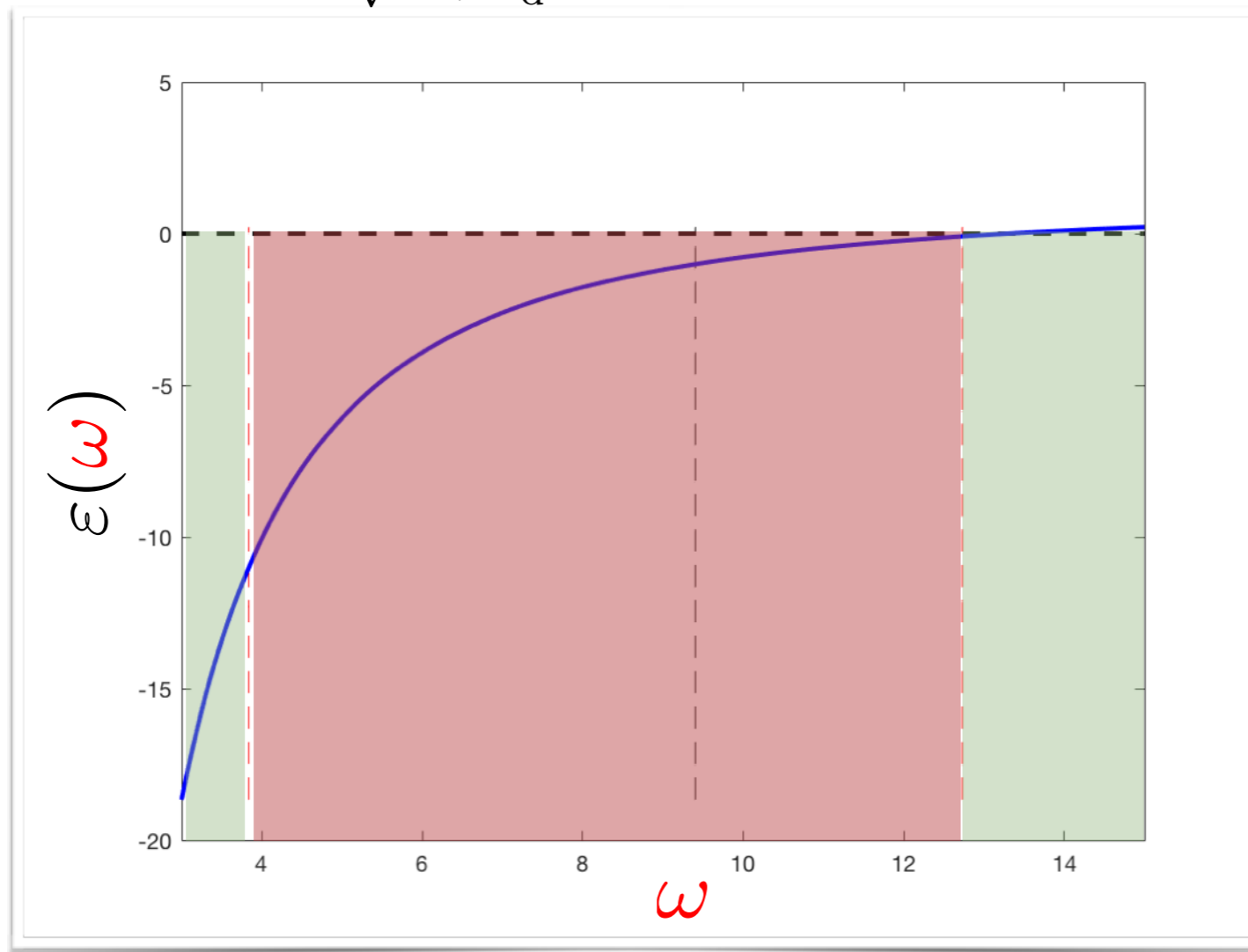
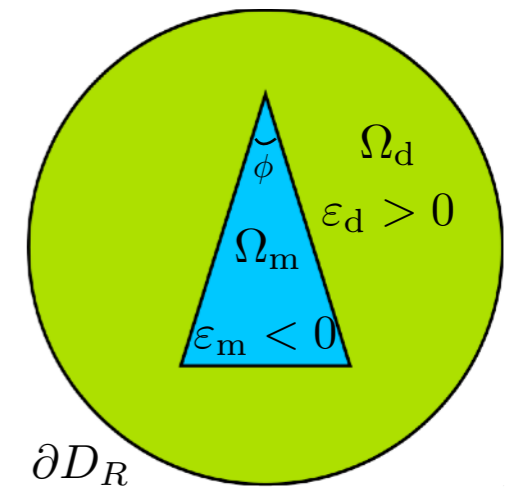
Critical interval and critical frequencies

The critical interval is related to **critical frequencies**:
for dissipationless Drude's we have

$$\kappa_{\varepsilon} \in \left[\frac{\phi - 2\pi}{\phi}; \frac{\phi}{2\pi - \phi} \right] \iff \omega \in \left[\frac{\omega_p}{\sqrt{1 + \frac{\phi}{\varepsilon_d(2\pi - \phi)}}}; \frac{\omega_p}{\sqrt{1 + \frac{\varepsilon_d \phi}{2\pi - \phi}}} \right]$$

$$\kappa_{\varepsilon} = -1 \iff \omega = \omega_{sp} := \frac{\omega_p}{\sqrt{1 + \varepsilon_d}} \text{ Surface plasmons frequency}$$

$$I_c = \left[\frac{\phi - 2\pi}{\phi}; \frac{\phi}{\phi - 2\pi} \right]$$

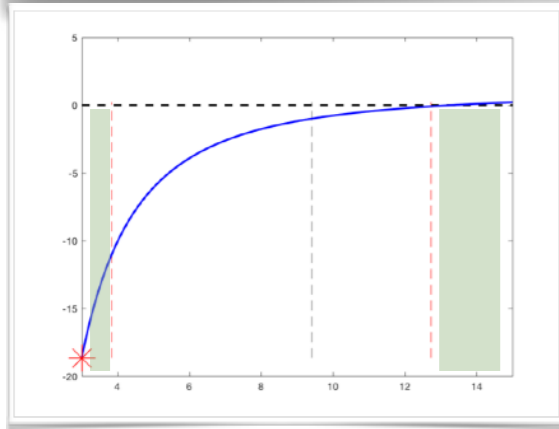


Two configurations (1)

Outside I_c
(YES)

The scattering problem has a **unique solution** $u \in H^1(D_R)$

Finite Elements converge (under some condition on the mesh):
design symmetric meshes near the interface to ensure optimal
FE convergence



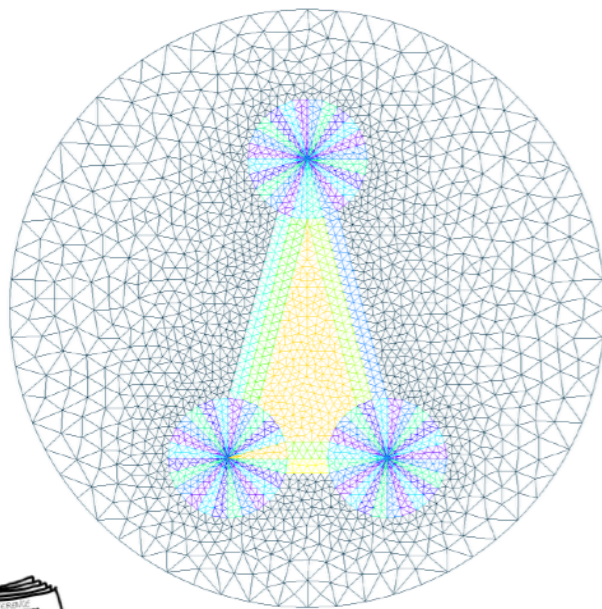
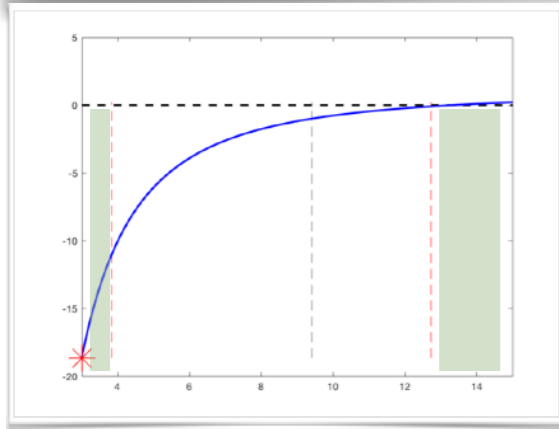
Chesnel, Ciarlet (2013), Carvalho, Chesnel, Ciarlet (2017), Bonnet-Ben Dhia, Carvalho, Ciarlet (2018).

Two configurations (1)

Outside I_c
(YES)

The scattering problem has a **unique solution** $u \in H^1(D_R)$

Finite Elements converge (under some condition on the mesh):
design symmetric meshes near the interface to ensure optimal
FE convergence



Chesnel, Ciarlet (2013), Carvalho, Chesnel, Ciarlet (2017), Bonnet-Ben Dhia, Carvalho, Ciarlet (2018).

Two configurations (1)

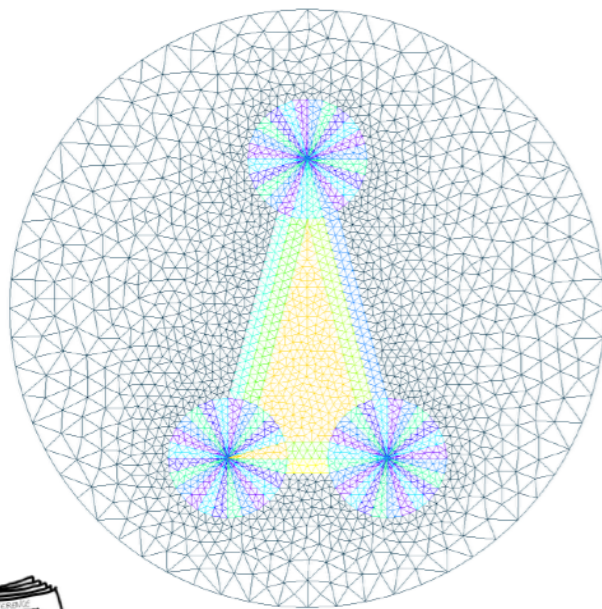
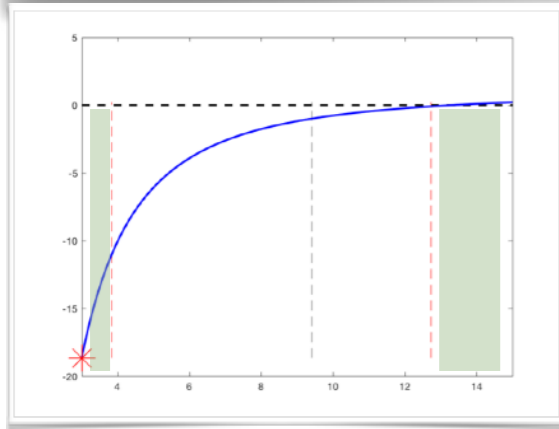
Outside I_c
(YES)

The scattering problem has a **unique solution** $u \in H^1(D_R)$

Finite Elements converge (under some condition on the mesh):
design symmetric meshes near the interface to ensure optimal
FE convergence

For silver: $\kappa_\varepsilon \in I_c \iff \omega \in [3.839 \text{ PHz}; 12.733 \text{ PHz}]$.

Results for $\omega = 3.7 \text{ PHz}$



Chesnel, Ciarlet (2013), Carvalho, Chesnel, Ciarlet (2017), Bonnet-Ben Dhia, Carvalho, Ciarlet (2018).

Two configurations (1)

Outside I_c
(YES)

The scattering problem has a **unique solution** $u \in H^1(D_R)$

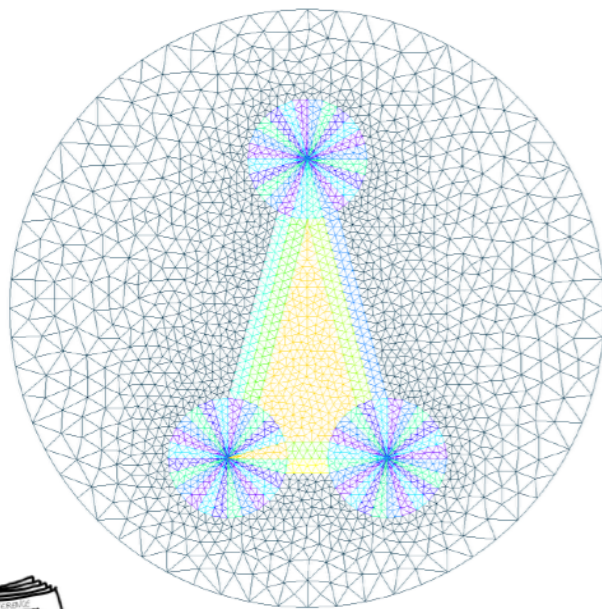
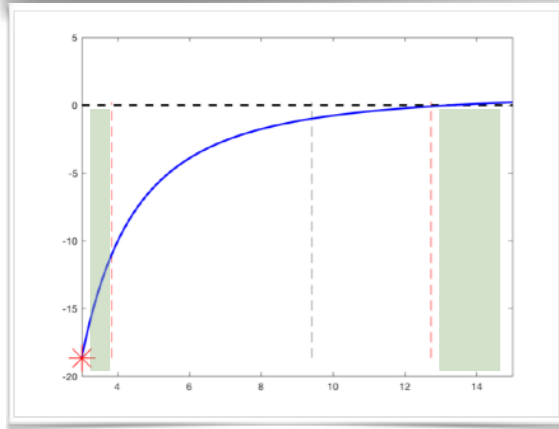
Finite Elements converge (under some condition on the mesh):
design symmetric meshes near the interface to ensure optimal
FE convergence

For silver: $\kappa_\varepsilon \in I_c \iff \omega \in [3.839 \text{ PHz}; 12.733 \text{ PHz}]$.

Results for $\omega = 3.7 \text{ PHz}$

Standard Meshes

T conform Meshes



Chesnel, Ciarlet (2013), Carvalho, Chesnel, Ciarlet (2017), Bonnet-Ben Dhia, Carvalho, Ciarlet (2018).

Two configurations (1)

Outside I_c
(YES)

The scattering problem has a **unique solution** $u \in H^1(D_R)$

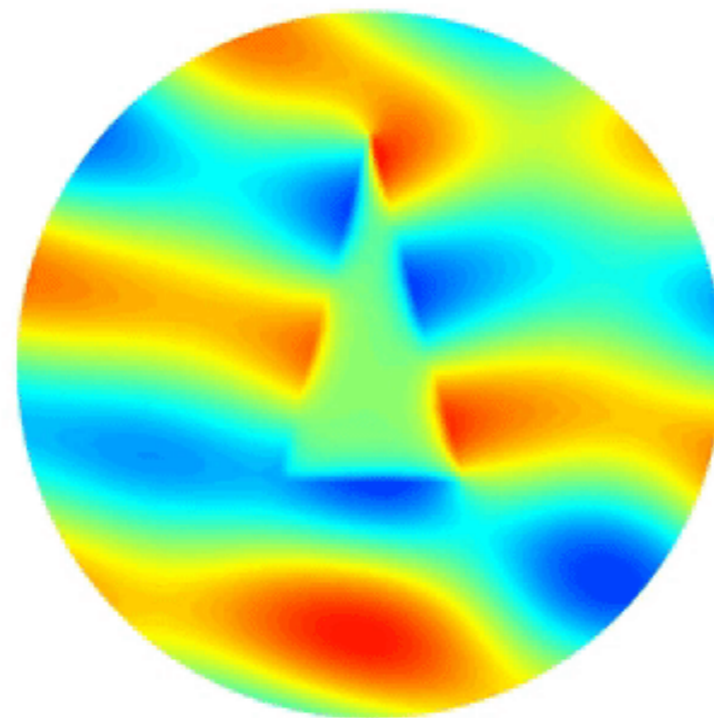
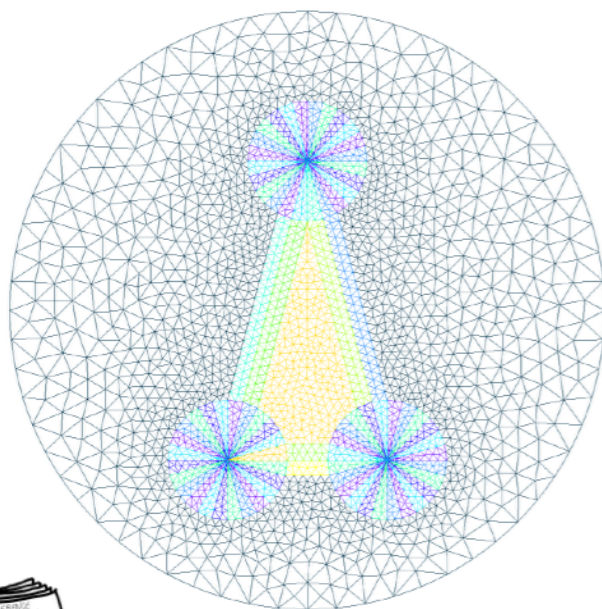
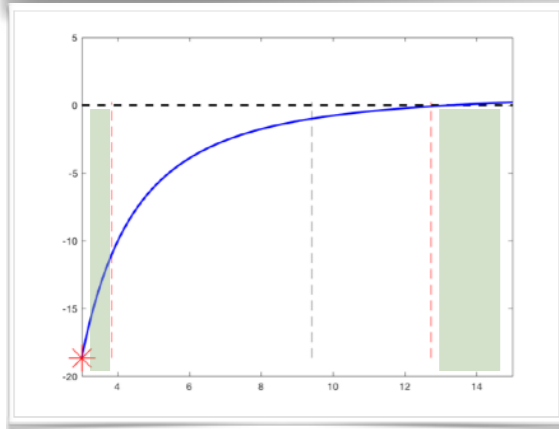
Finite Elements converge (under some condition on the mesh):
design symmetric meshes near the interface to ensure optimal
FE convergence

For silver: $\kappa_\varepsilon \in I_c \iff \omega \in [3.839 \text{ PHz}; 12.733 \text{ PHz}]$.

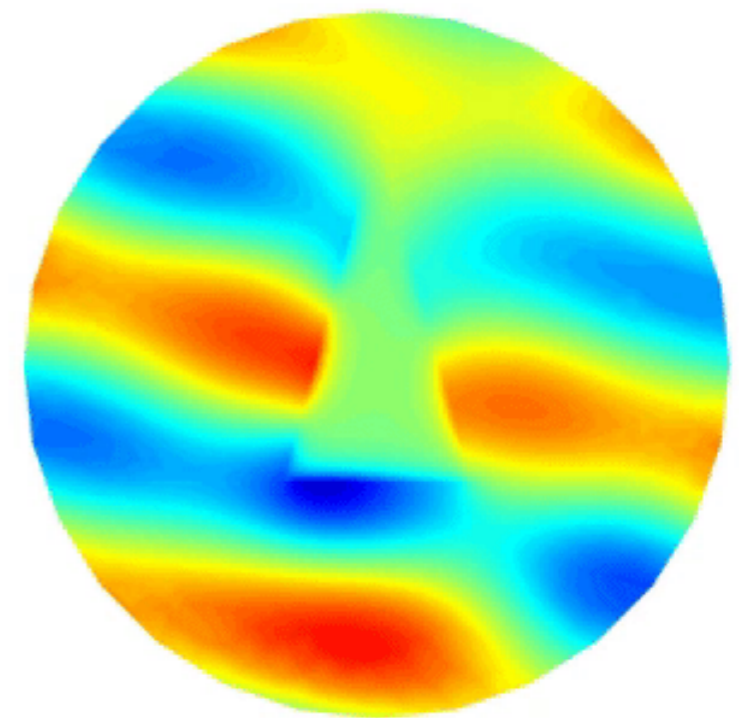
Results for $\omega = 3.7 \text{ PHz}$

Standard Meshes

T conform Meshes



$h = 0.5$



$h = 0.5$

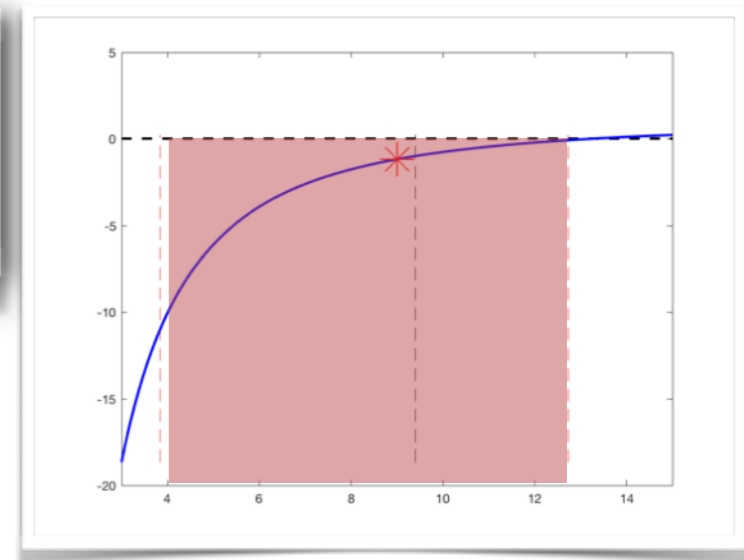
Chesnel, Ciarlet (2013), Carvalho, Chesnel, Ciarlet (2017), Bonnet-Ben Dhia, Carvalho, Ciarlet (2018).



Two configurations (2)

Inside I_c
(NO)

The scattering problem is **ill-posed** in $H^1(D_R)$
No FEM convergence



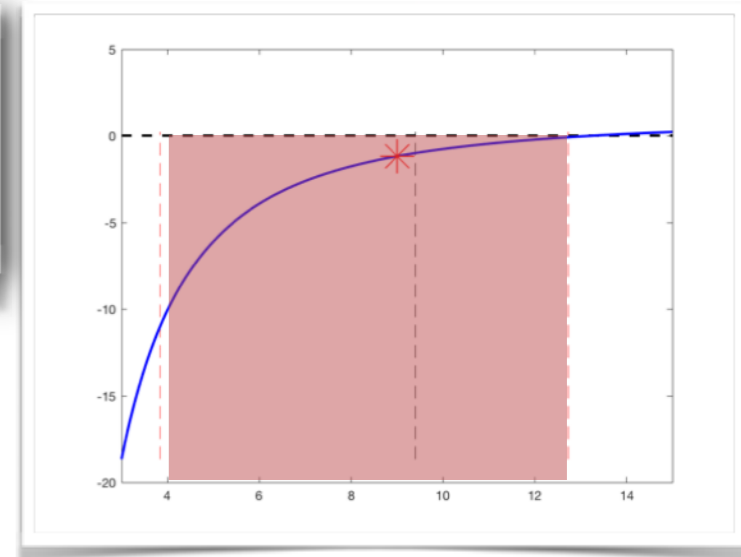
Two configurations (2)

Inside I_c (NO) The scattering problem is **ill-posed** in $H^1(D_R)$
No FEM convergence

Numerical results for triangular silver inclusion in vacuum for $\kappa_\varepsilon \in I_c$

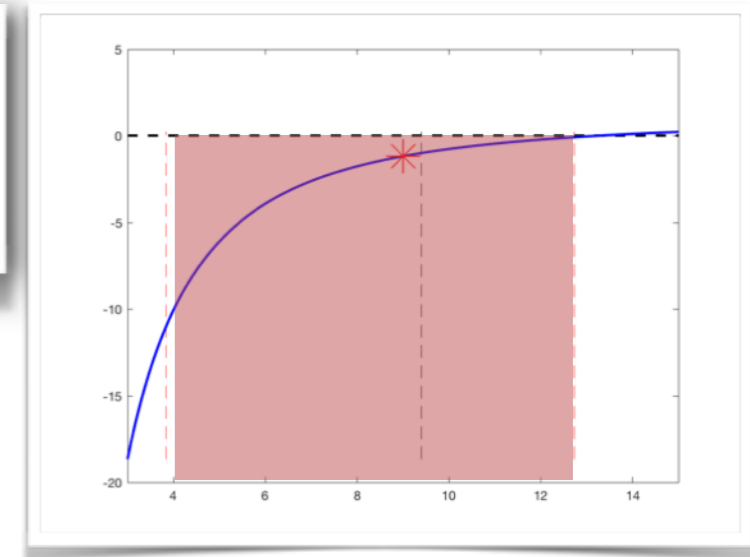
$$\kappa_\varepsilon \in I_c \iff \omega \in [3.839 \text{ PHz}; 12.733 \text{ PHz}].$$

Results for $\omega = 9 \text{ PHz}$.



Two configurations (2)

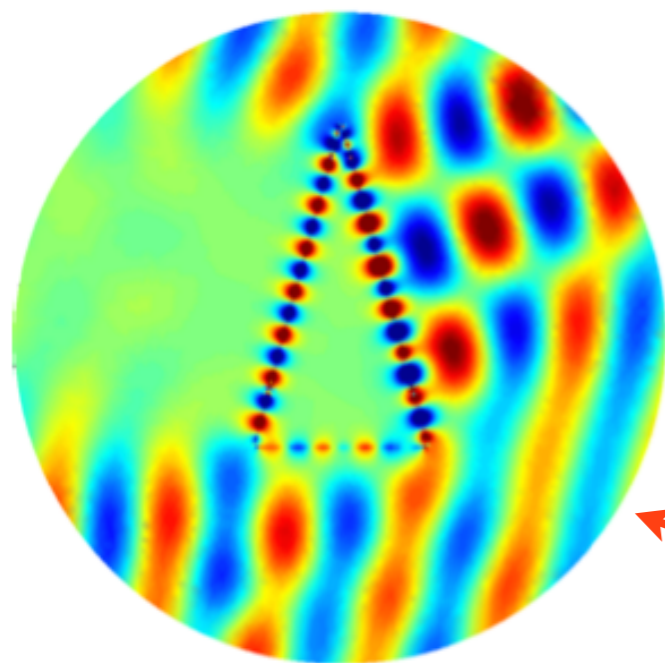
Inside I_c (NO) The scattering problem is ill-posed in $H^1(D_R)$
No FEM convergence



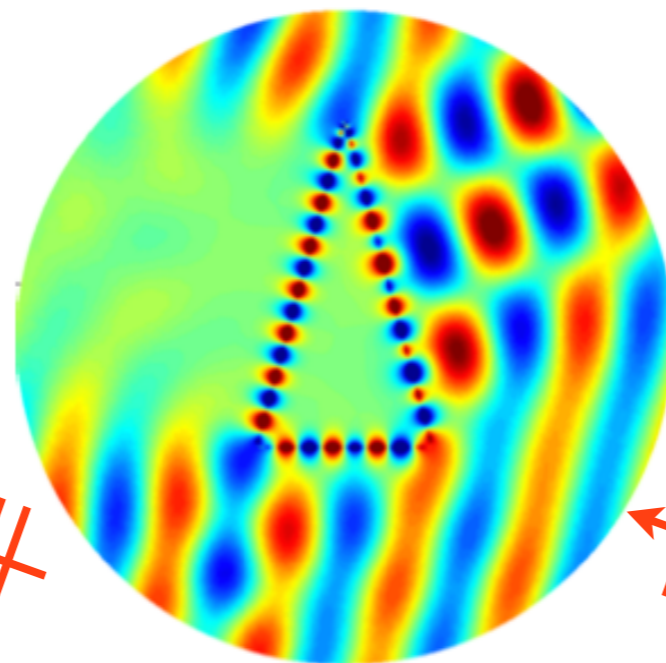
Numerical results for triangular silver inclusion in vacuum for $\kappa_\varepsilon \in I_c$

$$\kappa_\varepsilon \in I_c \iff \omega \in [3.839 \text{ PHz}; 12.733 \text{ PHz}].$$

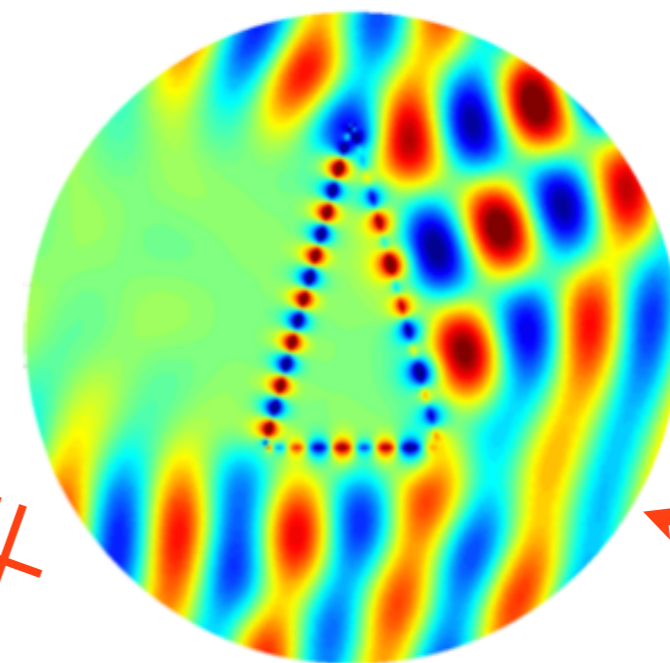
Results for $\omega = 9 \text{ PHz}$.



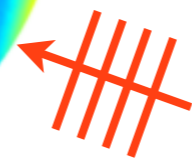
coarse mesh



intermediate mesh

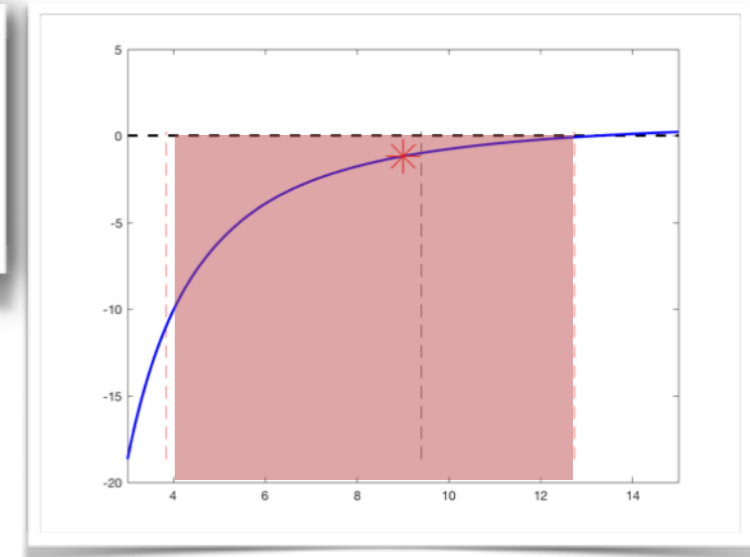


refined mesh



Two configurations (2)

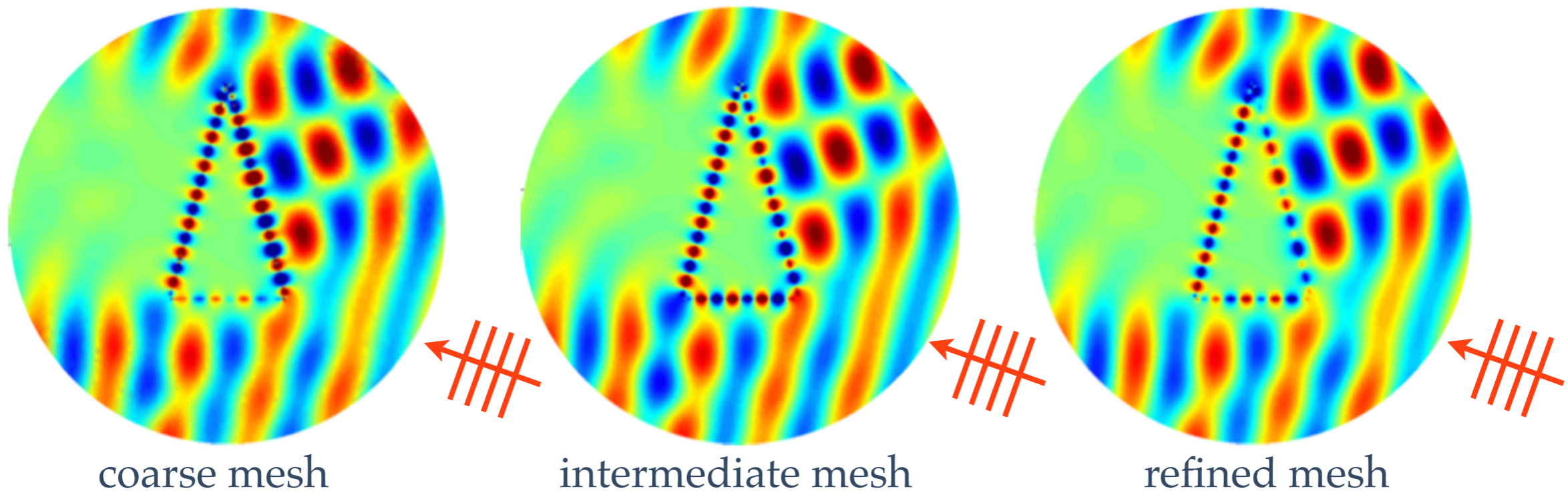
Inside I_c (NO) The scattering problem is **ill-posed** in $H^1(D_R)$
No FEM convergence



Numerical results for triangular silver inclusion in vacuum for $\kappa_\varepsilon \in I_c$

$$\kappa_\varepsilon \in I_c \iff \omega \in [3.839 \text{ PHz}; 12.733 \text{ PHz}].$$

Results for $\omega = 9 \text{ PHz}$.



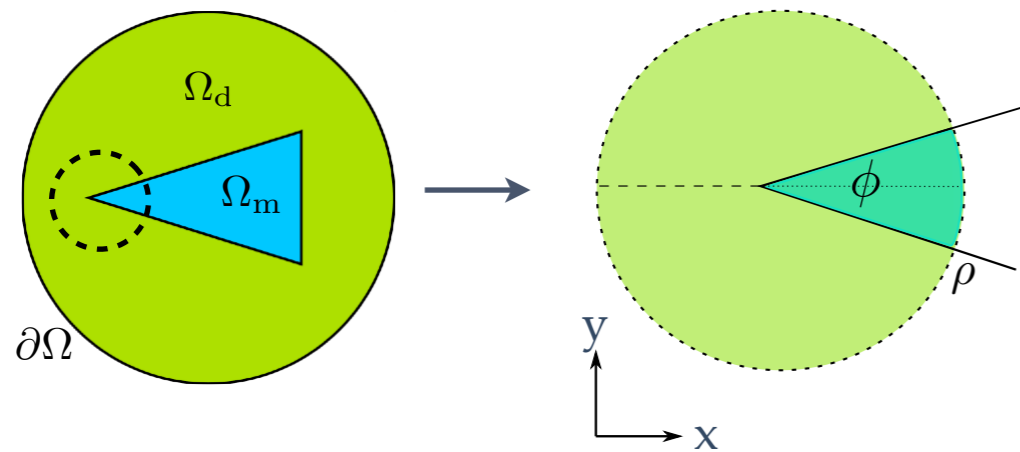
Singular behavior to near the corners to understand

Outline

- ❖ Introduction
- ❖ The limit problem
- ❖ Analysis at the corners
- ❖ Multiscale-FEM approach
- ❖ Extensions

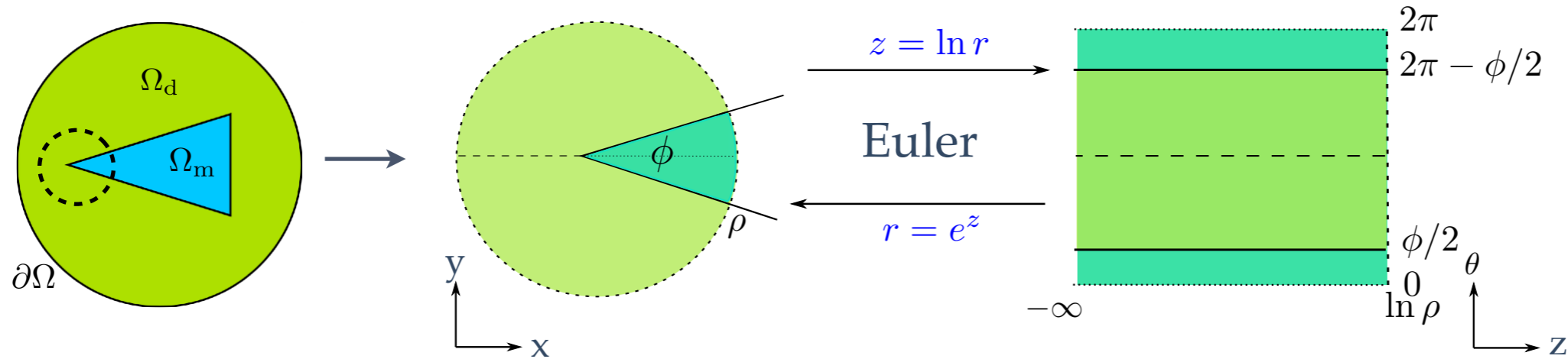
Analysis and scaling at the corners

For simplicity, we consider only one corner.



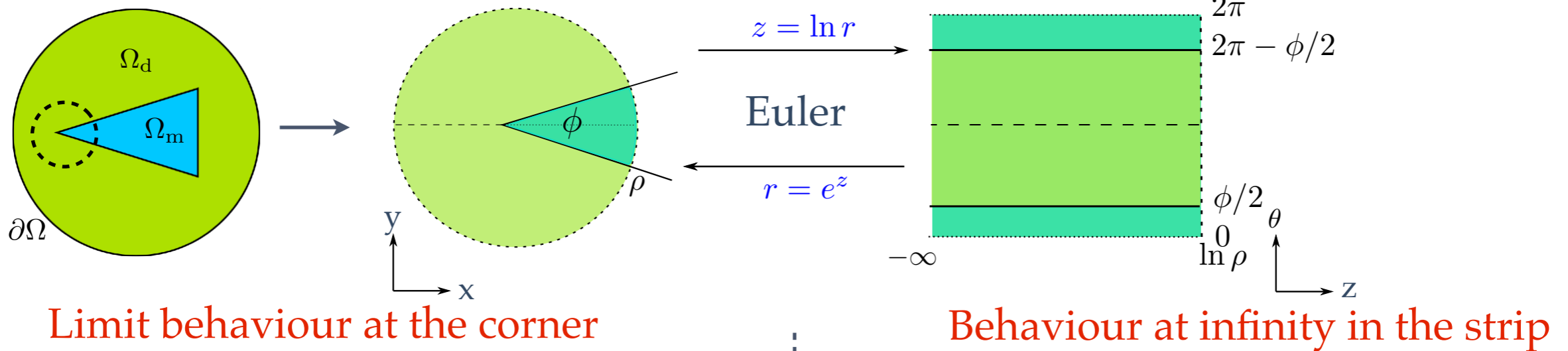
Analysis and scaling at the corners

For simplicity, we consider only one corner.



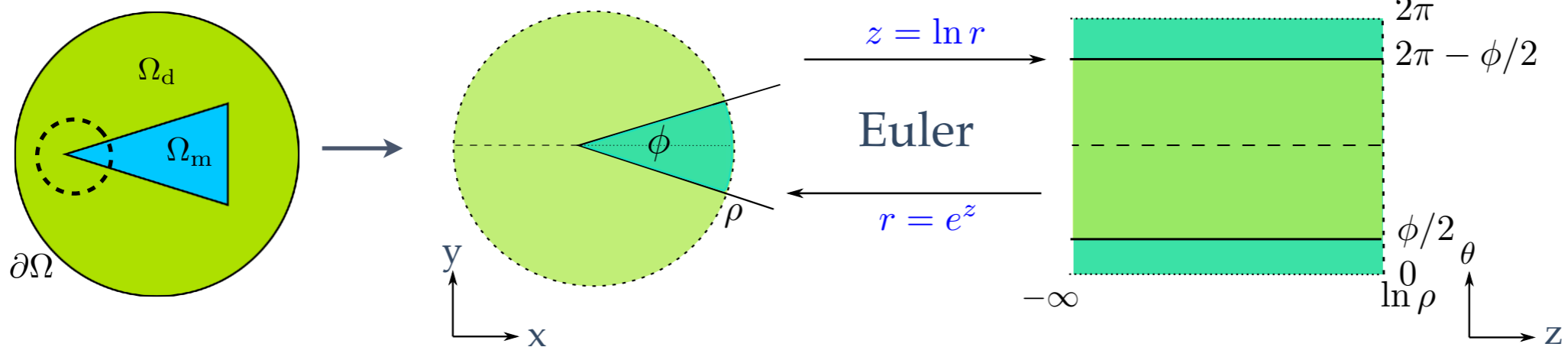
Analysis and scaling at the corners

For simplicity, we consider only one corner.



Analysis and scaling at the corners

For simplicity, we consider only one corner.



Limit behaviour at the corner

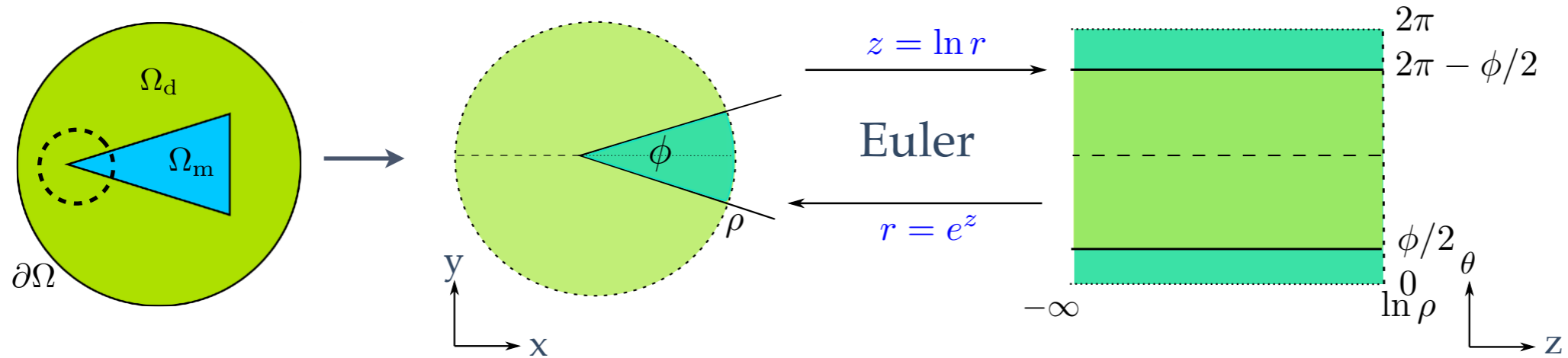
Behaviour at infinity in the strip

$$-\varepsilon^{-1} r \partial_r (r \partial_r u) - \partial_\theta (\varepsilon^{-1} \partial_\theta u) + \omega^2 \mu r^2 u = 0$$

$$-\operatorname{div} (\varepsilon^{-1} \nabla u) + \omega^2 \mu e^{2z} u = 0$$

Analysis and scaling at the corners

For simplicity, we consider only one corner.



Limit behaviour at the corner

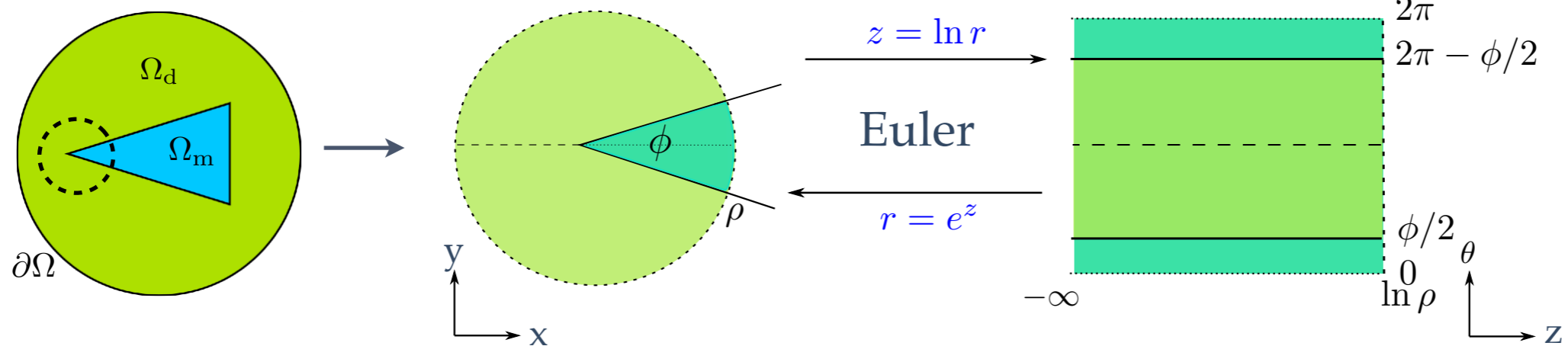
Behaviour at infinity in the strip

$$-\varepsilon^{-1} r \partial_r (r \partial_r u) - \partial_\theta (\varepsilon^{-1} \partial_\theta u) + \omega^2 \mu r^2 u = 0$$

$$-\operatorname{div} (\varepsilon^{-1} \nabla u) + \omega^2 \mu e^{2z} u = 0$$

Analysis and scaling at the corners

For simplicity, we consider only one corner.



Limit behaviour at the corner

Behaviour at infinity in the strip

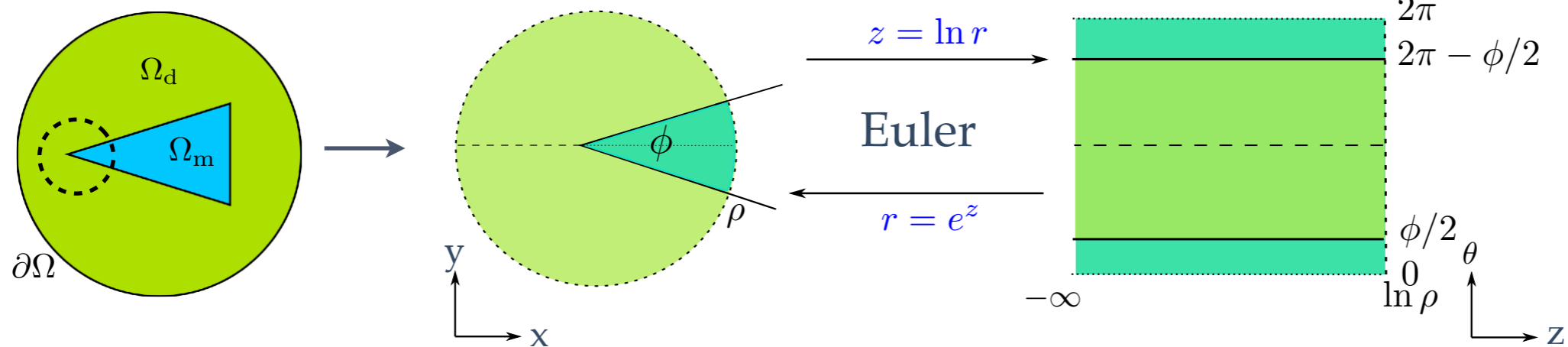
$$-\varepsilon^{-1} r \partial_r (r \partial_r u) - \partial_\theta (\varepsilon^{-1} \partial_\theta u) + \omega^2 \mu r^2 u = 0$$

$$-\operatorname{div} (\varepsilon^{-1} \nabla u) + \omega^2 \mu e^{2z} u = 0$$

We look for solutions $u(z, \theta) = e^{\lambda z} \phi(\theta)$
 λ are called singular exponents.

Analysis and scaling at the corners

For simplicity, we consider only one corner.



Limit behaviour at the corner

Behaviour at infinity in the strip

$$-\varepsilon^{-1} r \partial_r (r \partial_r u) - \partial_\theta (\varepsilon^{-1} \partial_\theta u) + \omega^2 \mu r^2 u = 0$$

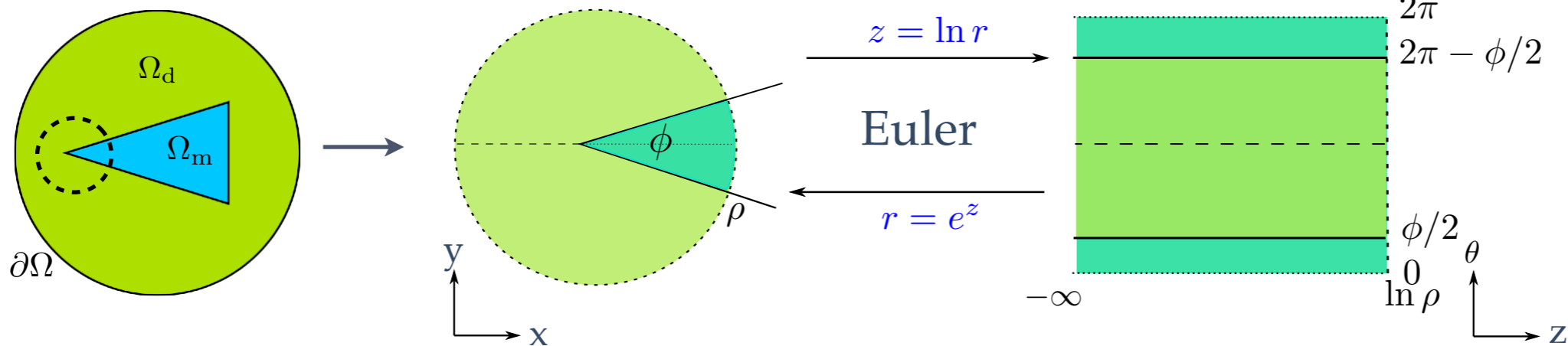
In the physical domain, the solutions are
 $u(r, \theta) = r^\lambda \phi(\theta)$

$$-\operatorname{div} (\varepsilon^{-1} \nabla u) + \omega^2 \mu e^{2z} u = 0$$

We look for solutions $u(z, \theta) = e^{\lambda z} \phi(\theta)$
 λ are called singular exponents.

Analysis and scaling at the corners

For simplicity, we consider only one corner.



Limit behaviour at the corner

Behaviour at infinity in the strip

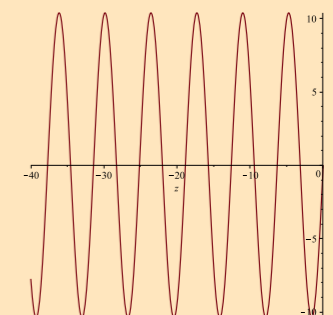
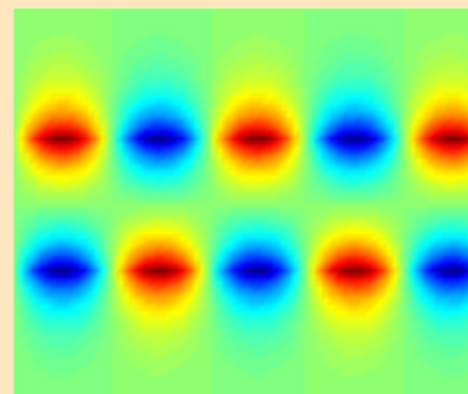
$$-\varepsilon^{-1} r \partial_r (r \partial_r u) - \partial_\theta (\varepsilon^{-1} \partial_\theta u) + \omega^2 \mu r^2 u = 0$$

$$-\operatorname{div} (\varepsilon^{-1} \nabla u) + \omega^2 \mu e^{2z} u = 0$$

In the physical domain, the solutions are
 $u(r, \theta) = r^\lambda \phi(\theta)$

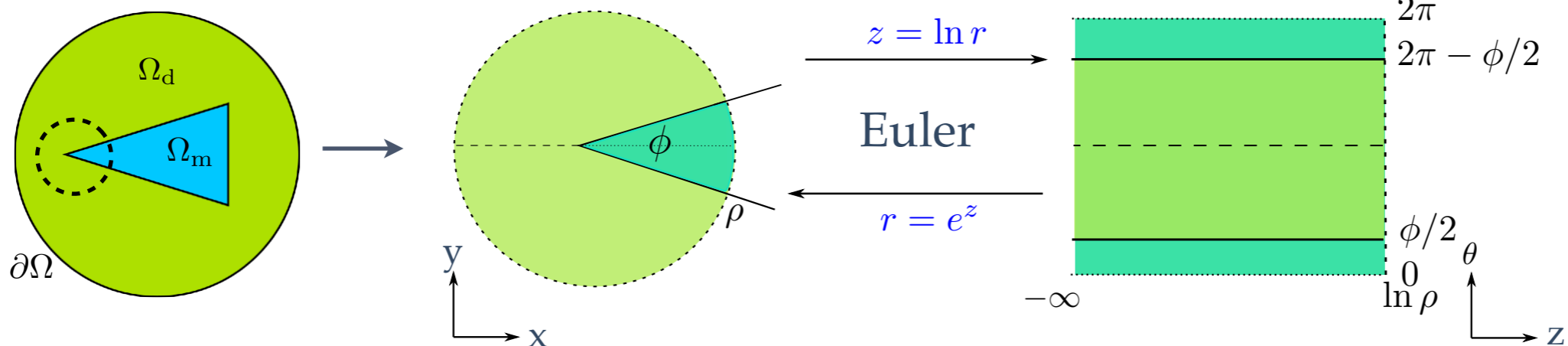
We look for solutions $u(z, \theta) = e^{\lambda z} \phi(\theta)$
 λ are called singular exponents.

$\kappa_\varepsilon \in I_c$ appearance of a **propagative mode**
 $s(z, \theta) = e^{i\eta z} \phi(\theta) \notin H^1$



Analysis and scaling at the corners

For simplicity, we consider only one corner.



Limit behaviour at the corner

Behaviour at infinity in the strip

$$-\varepsilon^{-1} r \partial_r (r \partial_r u) - \partial_\theta (\varepsilon^{-1} \partial_\theta u) + \omega^2 \mu r^2 u = 0$$

$$-\operatorname{div} (\varepsilon^{-1} \nabla u) + \omega^2 \mu e^{2z} u = 0$$

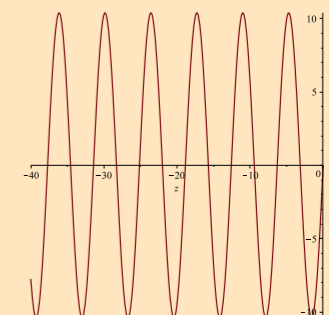
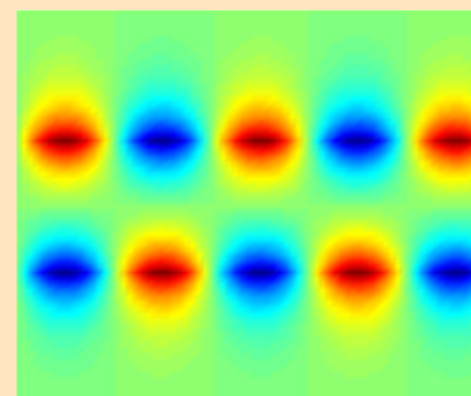
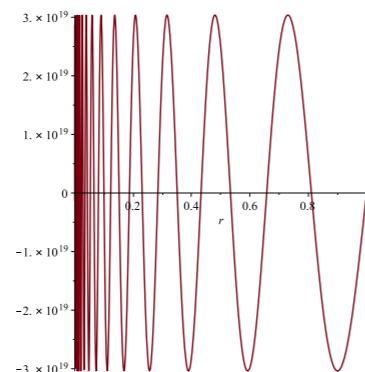
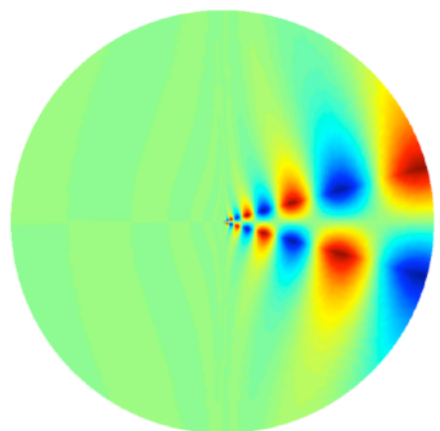
In the physical domain, the solutions are

$$u(r, \theta) = r^\lambda \phi(\theta)$$

We look for solutions $u(z, \theta) = e^{\lambda z} \phi(\theta)$
 λ are called singular exponents.

Appearance of an **oscillating hypersingularity** $s(r, \theta) = e^{i\eta \ln r} \phi(\theta) \notin H^1$

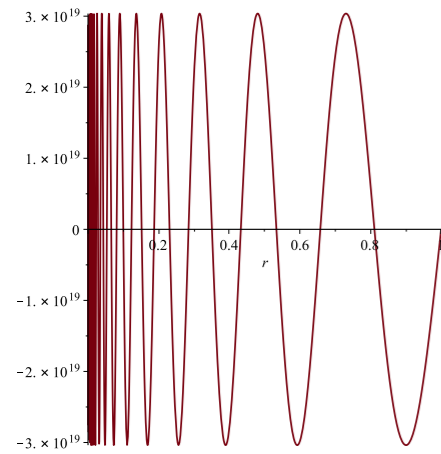
$\kappa_\varepsilon \in I_c$ appearance of a **propagative mode**
 $s(z, \theta) = e^{i\eta z} \phi(\theta) \notin H^1$



Black-hole wave.

Taking into account the black-hole waves

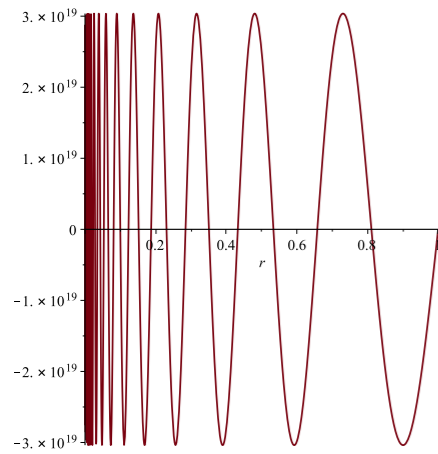
$$s^{\pm}(r, \theta) = e^{i(\pm\eta \ln r - \omega t)} \Phi(\theta)$$



Taking into account the black-hole waves

$$s^{\pm}(r, \theta) = e^{i(\pm\eta \ln r - \omega t)} \Phi(\theta)$$

These black-hole waves are of **infinite energy** and strongly oscillating at the corners.

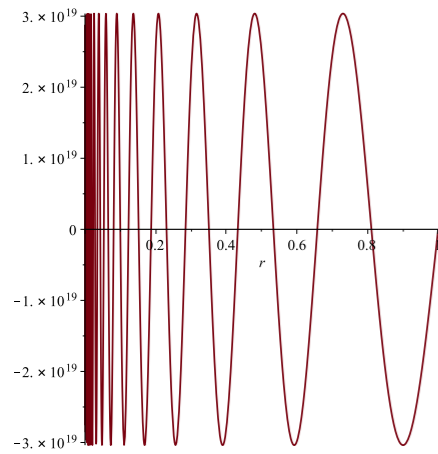


Taking into account the black-hole waves

$$s^\pm(r, \theta) = e^{i(\pm\eta \ln r - \omega t)} \Phi(\theta)$$

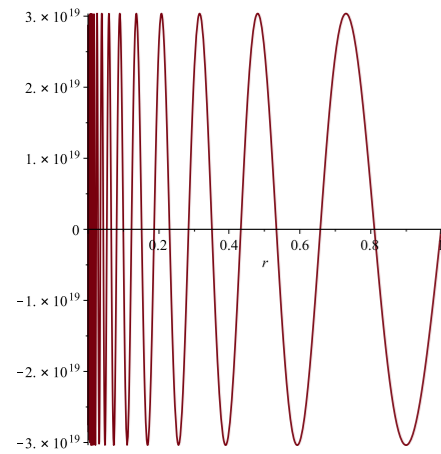
These black-hole waves are of **infinite energy** and strongly oscillating at the corners.

This is why standard FEM fail to approximate the solution: spurious reflexions appear.



Taking into account the black-hole waves

$$s^\pm(r, \theta) = e^{i(\pm\eta \ln r - \omega t)} \Phi(\theta)$$



These black-hole waves are of **infinite energy** and strongly oscillating at the corners.

This is why standard FEM fail to approximate the solution: spurious reflexions appear.

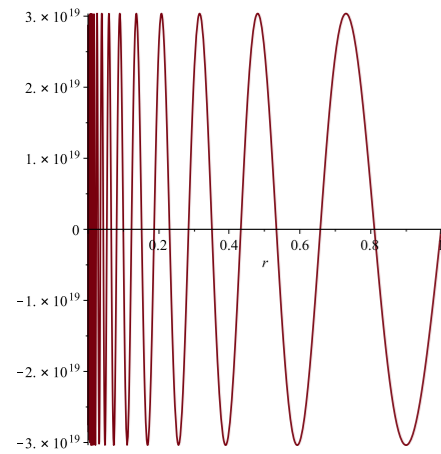
However we **need to take them into account** to recover a **well-posed formulation**.



Bonnet-Ben Dhia, Chesnel, Claeys (2013) , Bonnet-Ben Dhia, Carvalho, Chesnel, Ciarlet (2016).

Taking into account the black-hole waves

$$s^\pm(r, \theta) = e^{i(\pm\eta \ln r - \omega t)} \Phi(\theta)$$



These black-hole waves are of **infinite energy** and strongly oscillating at the corners.

This is why standard FEM fail to approximate the solution: spurious reflexions appear.

However we **need to take them into account** to recover a **well-posed formulation**.

Near the corners the solution decomposes as

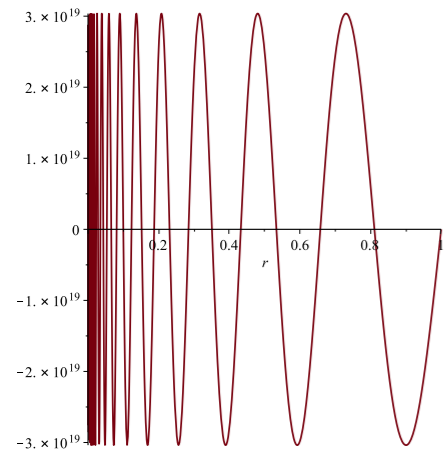
$$u = b^+ s^+ + b^- s^- + \tilde{u}, \quad \tilde{u} \in H^1(D_R), \quad s^\pm \notin H^1(D_R), \quad b^\pm \in \mathbb{C}$$



Bonnet-Ben Dhia, Chesnel, Claeys (2013), Bonnet-Ben Dhia, Carvalho, Chesnel, Ciarlet (2016).

Taking into account the black-hole waves

$$s^\pm(r, \theta) = e^{i(\pm\eta \ln r - \omega t)} \Phi(\theta)$$



These black-hole waves are of **infinite energy** and strongly oscillating at the corners.

This is why standard FEM fail to approximate the solution: spurious reflexions appear.

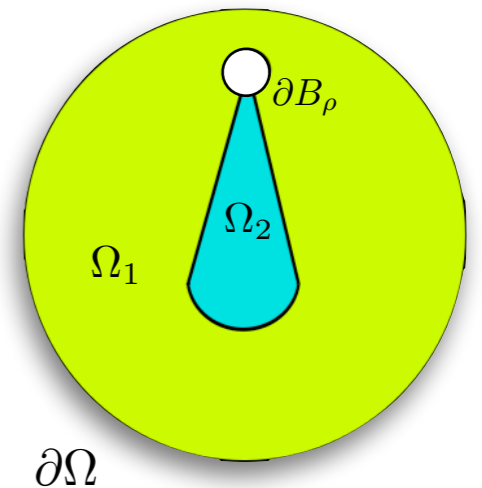
However we **need to take them into account** to recover a **well-posed formulation**.

Near the corners the solution decomposes as

$$u = b^+ s^+ + b^- s^- + \tilde{u}, \quad \tilde{u} \in H^1(D_R), \quad s^\pm \notin H^1(D_R), \quad b^\pm \in \mathbb{C}$$

To get a **unique solution**, one needs to enforce a condition on b^\pm . **How to proceed ?**

By energy flux:



Bonnet-Ben Dhia, Chesnel, Claeys (2013), Bonnet-Ben Dhia, Carvalho, Chesnel, Ciarlet (2016).

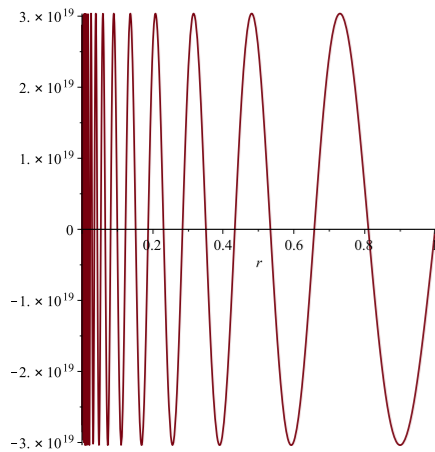
Taking into account the black-hole waves

$$s^\pm(r, \theta) = e^{i(\pm\eta \ln r - \omega t)} \Phi(\theta)$$

These black-hole waves are of **infinite energy** and strongly oscillating at the corners.

This is why standard FEM fail to approximate the solution: spurious reflexions appear.

However we **need to take them into account** to recover a **well-posed formulation**.



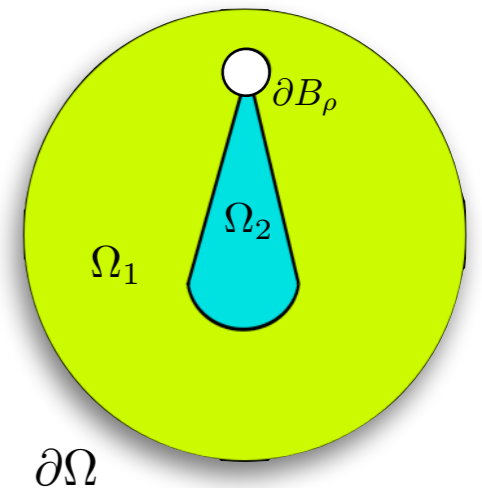
Near the corners the solution decomposes as

$$u = b^+ s^+ + b^- s^- + \tilde{u}, \quad \tilde{u} \in H^1(D_R), \quad s^\pm \notin H^1(D_R), \quad b^\pm \in \mathbb{C}$$

To get a **unique solution**, one needs to enforce a condition on b^\pm . **How to proceed ?**

By energy flux:

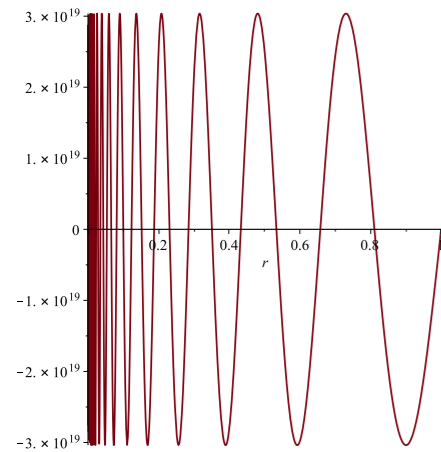
- one singularity carries **energy absorbed** by the corner
- the other **brings energy** emitted from the corner



Bonnet-Ben Dhia, Chesnel, Claeys (2013) , Bonnet-Ben Dhia, Carvalho, Chesnel, Ciarlet (2016).

Taking into account the black-hole waves

$$s^\pm(r, \theta) = e^{i(\pm\eta \ln r - \omega t)} \Phi(\theta)$$



These black-hole waves are of **infinite energy** and strongly oscillating at the corners.

This is why standard FEM fail to approximate the solution: spurious reflexions appear.

However we **need to take them into account** to recover a **well-posed formulation**.

Near the corners the solution decomposes as

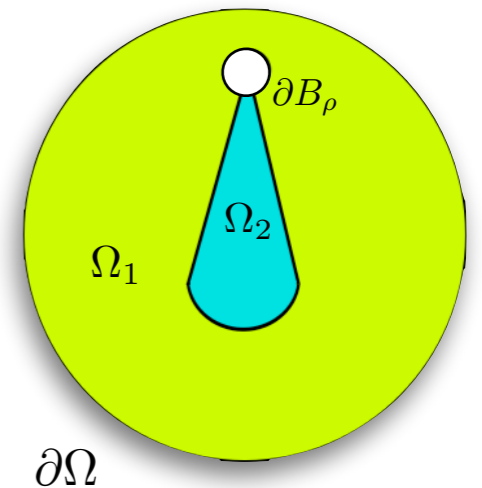
$$u = b^+ s^+ + b^- s^- + \tilde{u}, \quad \tilde{u} \in H^1(D_R), \quad s^\pm \notin H^1(D_R), \quad b^\pm \in \mathbb{C}$$

To get a **unique solution**, one needs to enforce a condition on b^\pm . **How to proceed ?**

By energy flux:

- one singularity carries **energy absorbed** by the corner
- the other **brings energy** emitted from the corner

The **physical** solution takes into account the one that **does not add energy** into the system, the **outgoing** solution in the waveguide setting.



Bonnet-Ben Dhia, Chesnel, Claeys (2013) , Bonnet-Ben Dhia, Carvalho, Chesnel, Ciarlet (2016).

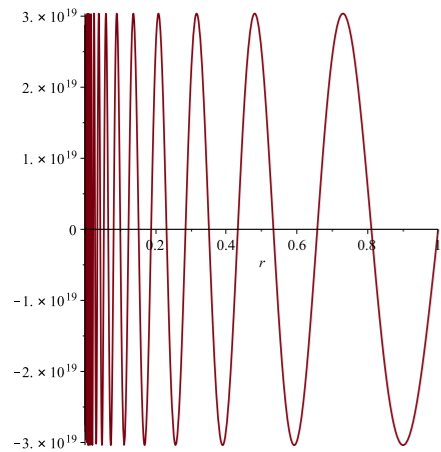
Taking into account the black-hole waves

$$s^\pm(r, \theta) = e^{i(\pm\eta \ln r - \omega t)} \Phi(\theta)$$

These black-hole waves are of **infinite energy** and strongly oscillating at the corners.

This is why standard FEM fail to approximate the solution: spurious reflexions appear.

However we **need to take them into account** to recover a **well-posed formulation**.



Near the corners the solution decomposes as

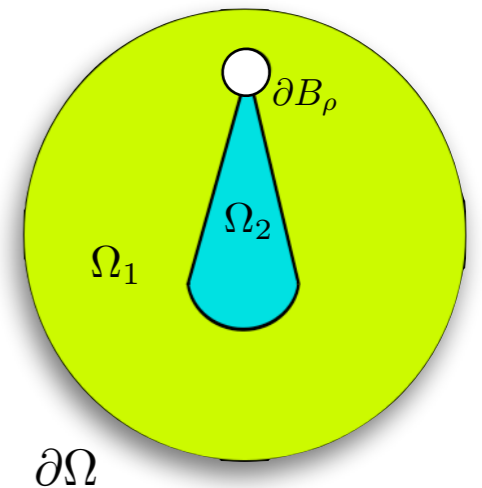
$$u = b^+ s^+ + b^- s^- + \tilde{u}, \quad \tilde{u} \in H^1(D_R), \quad s^\pm \notin H^1(D_R), \quad b^\pm \in \mathbb{C}$$

To get a **unique solution**, one needs to enforce a condition on b^\pm . **How to proceed ?**

By energy flux:

- one singularity carries **energy absorbed** by the corner
- the other **brings energy** emitted from the corner

The **physical** solution takes into account the one that **does not add energy** into the system, the **outgoing** solution in the waveguide setting.



How to proceed numerically to select the good singularity ?

Outline

- ❖ Introduction
- ❖ The limit problem
- ❖ Analysis at the corners
- ❖ Multiscale-FEM approach
- ❖ Extensions

Perfectly Matched Layers (PMLs)

PMLs enable to **artificially bound** the strip while making the propagative modes become **evanescent**.

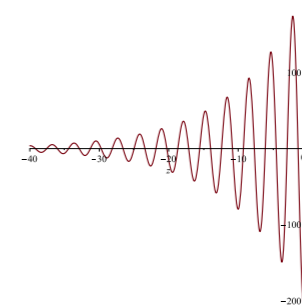
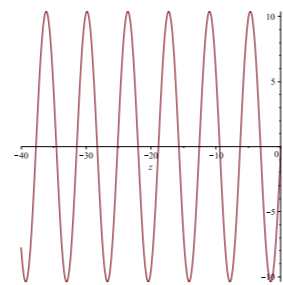
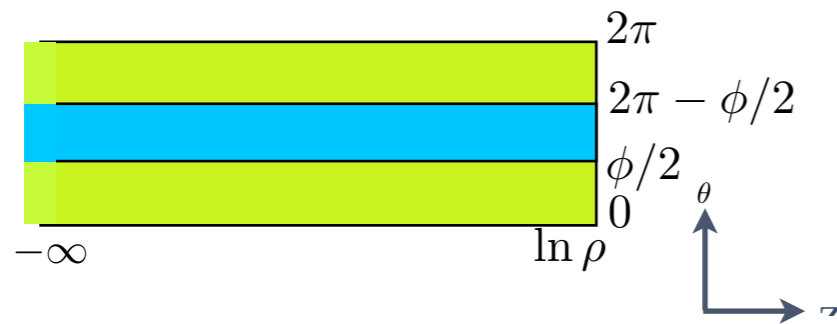
$$\frac{\partial}{\partial z} \mapsto \alpha \frac{\partial}{\partial z} \quad \alpha \in \mathbb{C}$$

Perfectly Matched Layers (PMLs)

PMLs enable to **artificially bound** the strip while making the propagative modes become **evanescent**.

$$\frac{\partial}{\partial z} \mapsto \alpha \frac{\partial}{\partial z} \quad \alpha \in \mathbb{C}$$

$$u(z, \theta) = e^{\lambda z} \phi(\theta) \quad \longrightarrow \quad u(z, \theta) = e^{\frac{\lambda}{\alpha} z} \phi(\theta)$$

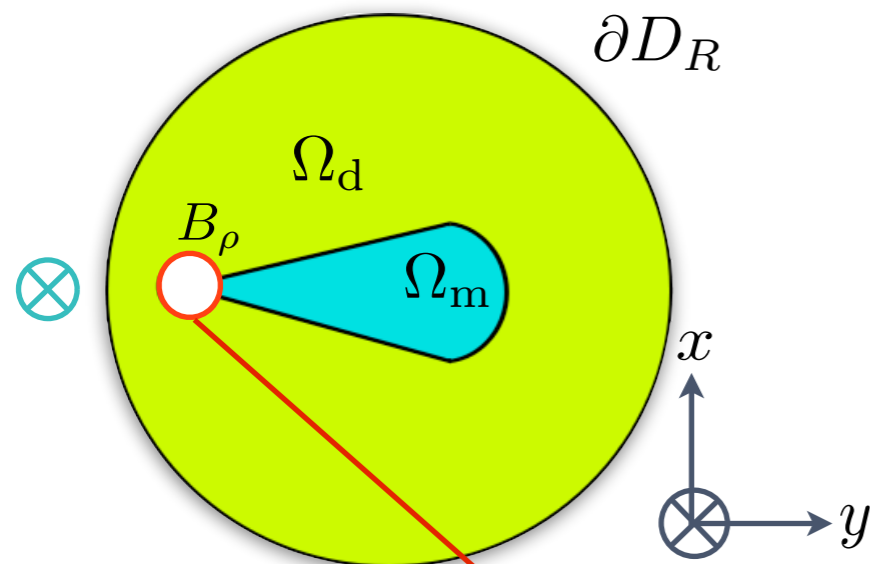
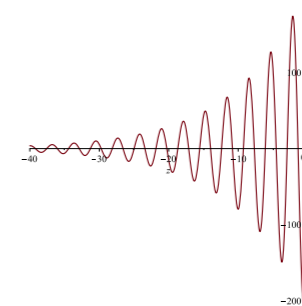
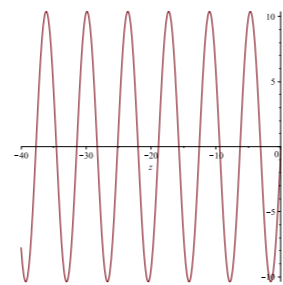
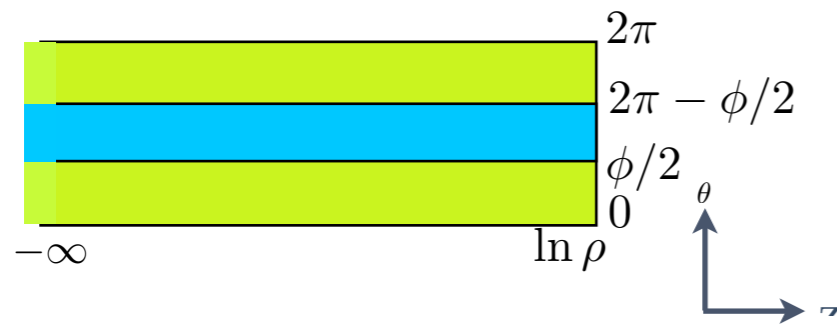


Perfectly Matched Layers (PMLs)

PMLs enable to **artificially bound** the strip while making the propagative modes become **evanescent**.

$$\frac{\partial}{\partial z} \mapsto \alpha \frac{\partial}{\partial z} \quad \alpha \in \mathbb{C}$$

$$u(z, \theta) = e^{\lambda z} \phi(\theta) \quad \longrightarrow \quad u(z, \theta) = e^{\frac{\lambda}{\alpha} z} \phi(\theta)$$

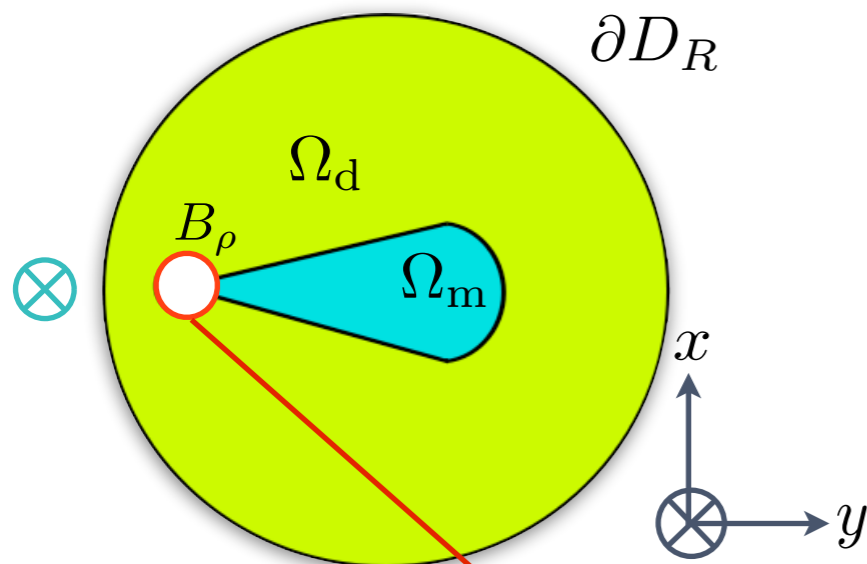
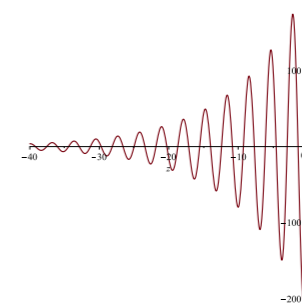
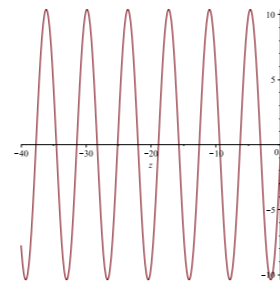
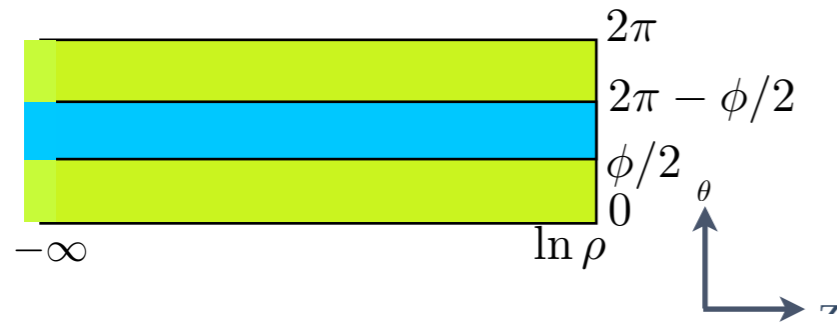


Perfectly Matched Layers (PMLs)

PMLs enable to **artificially bound** the strip while making the propagative modes become **evanescent**.

$$\frac{\partial}{\partial z} \mapsto \alpha \frac{\partial}{\partial z} \quad \alpha \in \mathbb{C}$$

$$u(z, \theta) = e^{\lambda z} \phi(\theta) \quad \longrightarrow \quad u(z, \theta) = e^{\frac{\lambda}{\alpha} z} \phi(\theta)$$



$$-\operatorname{div}(\varepsilon^{-1} \nabla u) + \omega^2 \mu u = 0 \quad D_R \setminus \overline{B_\rho}$$

$$\partial_r u - iku = \partial_r u^{\text{inc}} - iku^{\text{inc}} \quad \partial D_R$$

+ matching between the PML and the strip +

$$-\alpha \varepsilon^{-1} \partial_{zz} u - \frac{1}{\alpha} \partial_\theta \varepsilon^{-1} \partial_\theta u + \frac{\omega^2}{\alpha} \mu e^{\frac{2z}{\alpha}} u = 0 \quad S_\rho$$

+ periodic conditions

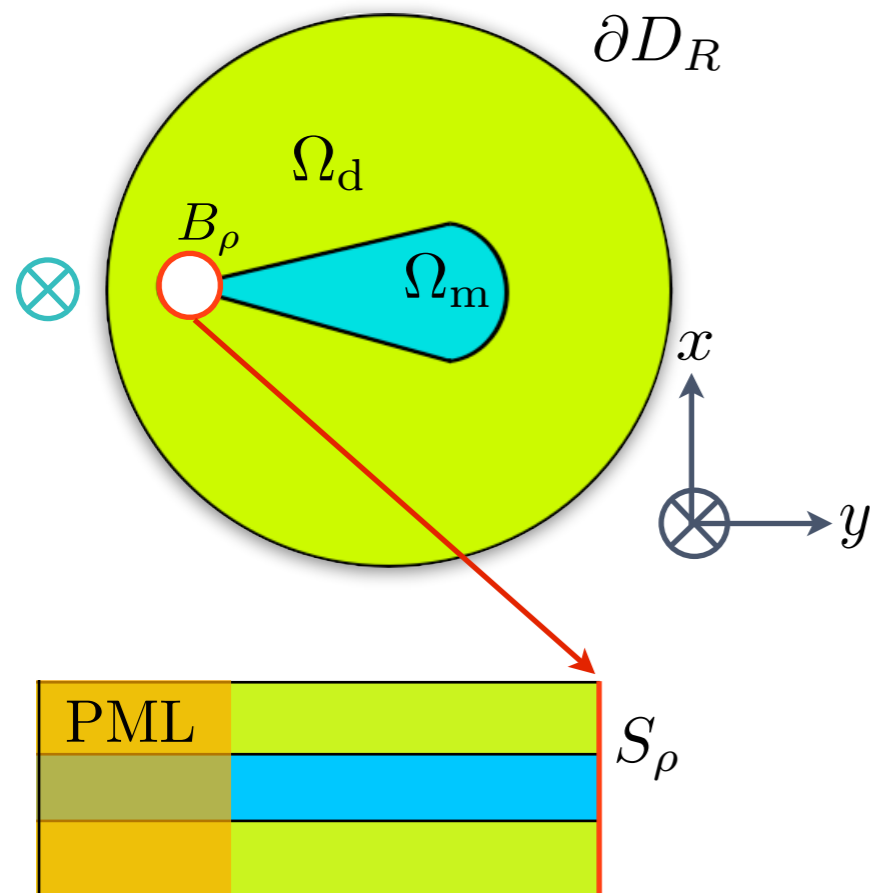
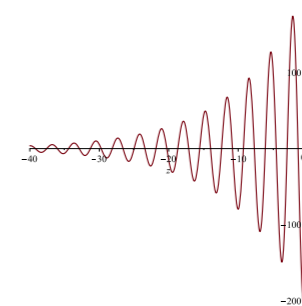
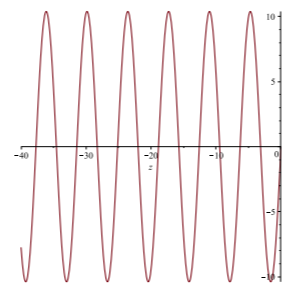
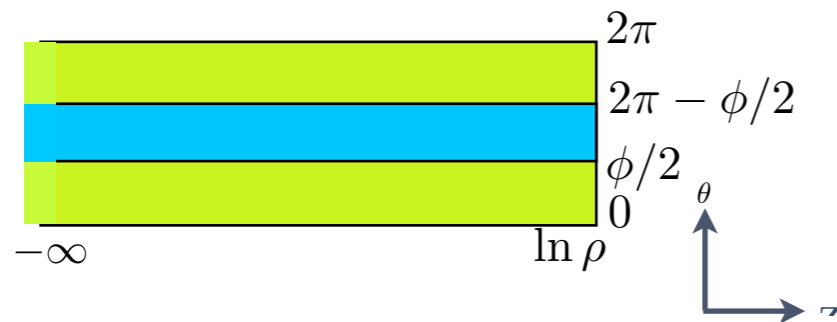


Perfectly Matched Layers (PMLs)

PMLs enable to **artificially bound** the strip while making the propagative modes become **evanescent**.

$$\frac{\partial}{\partial z} \mapsto \alpha \frac{\partial}{\partial z} \quad \alpha \in \mathbb{C}$$

$$u(z, \theta) = e^{\lambda z} \phi(\theta) \quad \longrightarrow \quad u(z, \theta) = e^{\frac{\lambda}{\alpha} z} \phi(\theta)$$



$$-\operatorname{div}(\varepsilon^{-1} \nabla u) + \omega^2 \mu u = 0 \quad D_R \setminus \overline{B_\rho}$$

$$\partial_r u - iku = \partial_r u^{\text{inc}} - iku^{\text{inc}} \quad \partial D_R$$

+ matching between the PML and the strip +

$$-\alpha \varepsilon^{-1} \partial_{zz} u - \frac{1}{\alpha} \partial_\theta \varepsilon^{-1} \partial_\theta u + \frac{\omega^2}{\alpha} \mu e^{\frac{2z}{\alpha}} u = 0 \quad S_\rho$$

$$\partial_z u(-L, \cdot) = 0$$

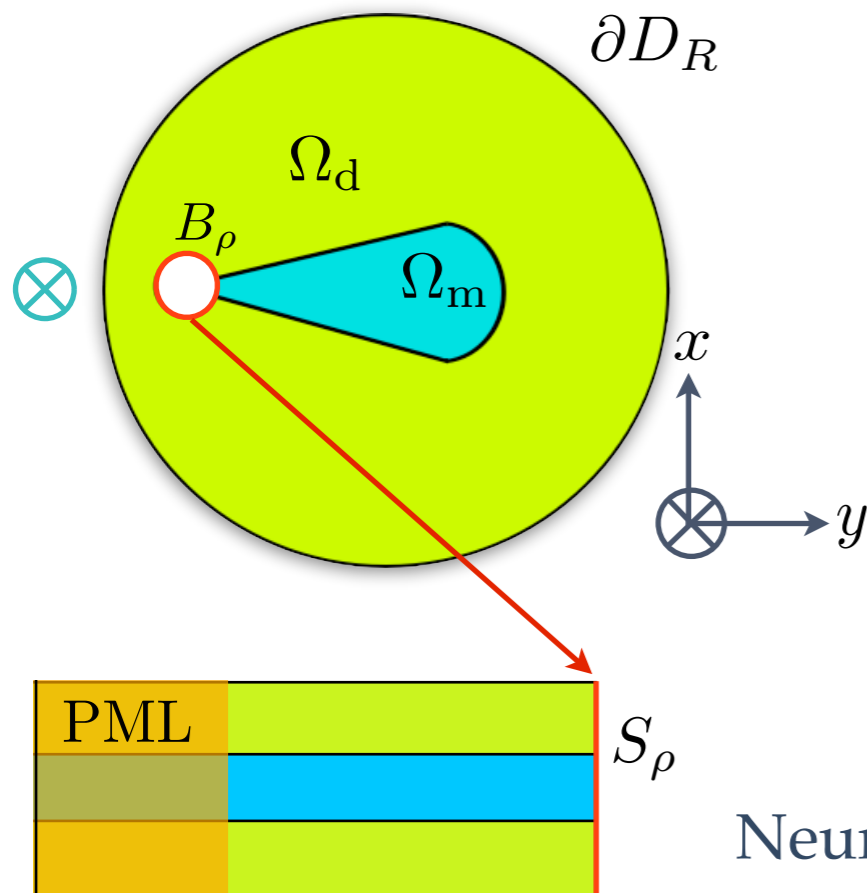
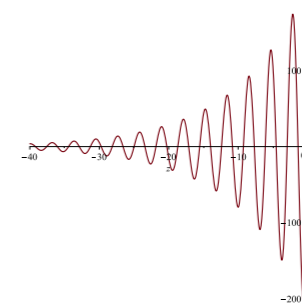
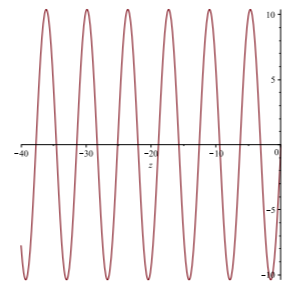
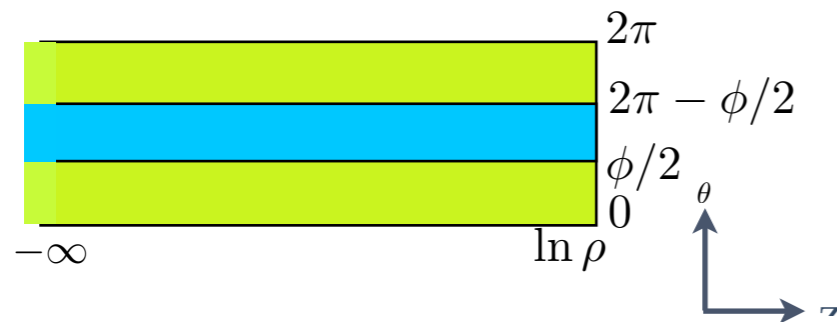
+ periodic conditions

Perfectly Matched Layers (PMLs)

PMLs enable to **artificially bound** the strip while making the propagative modes become **evanescent**.

$$\frac{\partial}{\partial z} \mapsto \alpha \frac{\partial}{\partial z} \quad \alpha \in \mathbb{C}$$

$$u(z, \theta) = e^{\lambda z} \phi(\theta) \quad \longrightarrow \quad u(z, \theta) = e^{\frac{\lambda}{\alpha} z} \phi(\theta)$$



$$-\operatorname{div}(\varepsilon^{-1} \nabla u) + \omega^2 \mu u = 0 \quad D_R \setminus \overline{B_\rho}$$

$$\partial_r u - iku = \partial_r u^{\text{inc}} - iku^{\text{inc}} \quad \partial D_R$$

+ matching between the PML and the strip +

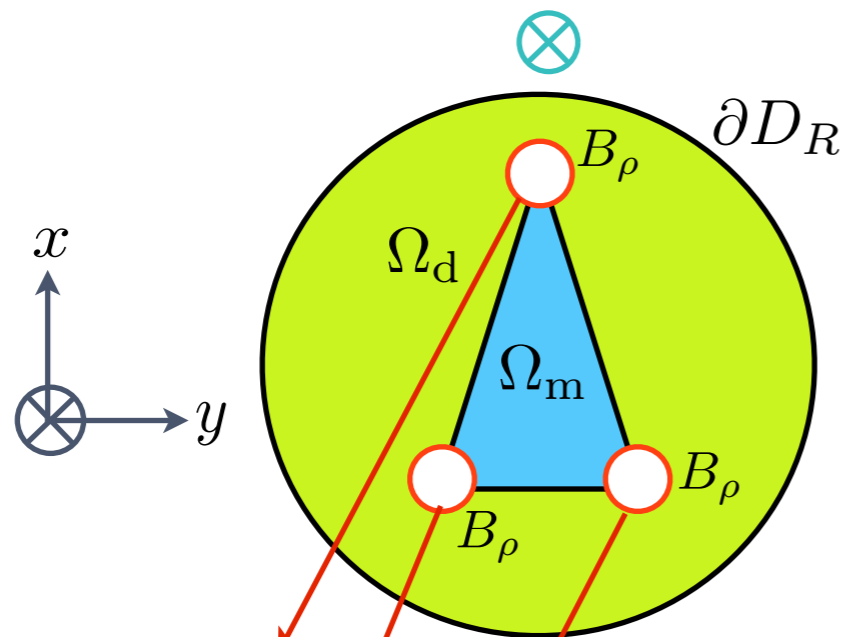
$$-\alpha \varepsilon^{-1} \partial_{zz} u - \frac{1}{\alpha} \partial_\theta \varepsilon^{-1} \partial_\theta u + \frac{\omega^2}{\alpha} \mu e^{\frac{2z}{\alpha}} u = 0 \quad S_\rho$$

$$\partial_z u(-L, \cdot) = 0$$

+ periodic conditions

Neumann condition due to the constant mode

With several corners



$$-\operatorname{div}(\varepsilon^{-1} \nabla u) + \omega^2 \mu u = 0 \quad D_R \setminus \cup \overline{B_\rho}$$

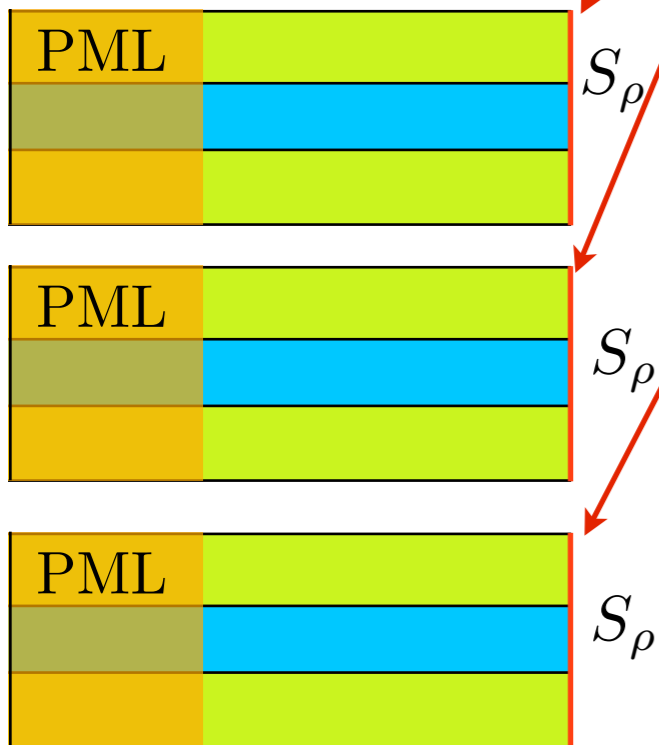
$$\partial_r u - iku = \partial_r u^{\text{inc}} - iku^{\text{inc}} \quad \partial D_R$$

+ matching between the PML and the strip +

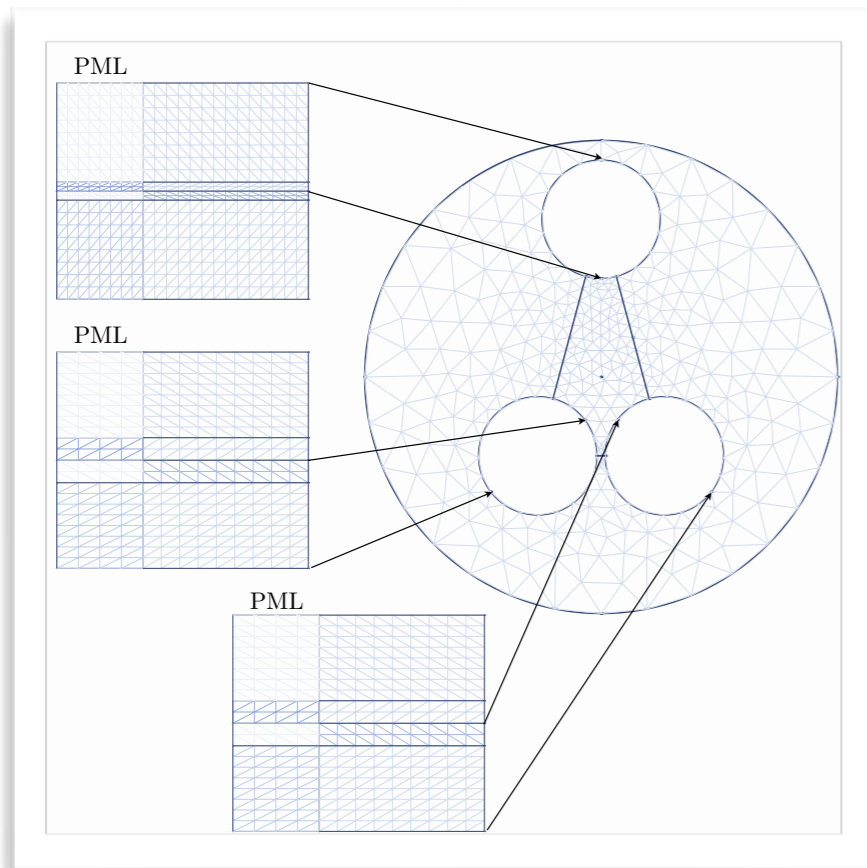
$$-\alpha \varepsilon^{-1} \partial_{zz} u - \frac{1}{\alpha} \partial_\theta \varepsilon^{-1} \partial_\theta u + \frac{\omega^2}{\alpha} \mu e^{\frac{2z}{\alpha}} u = 0 \quad S_\rho$$

$$\partial_z u(-L, \cdot) = 0$$

+ periodic conditions



With several corners



$$-\operatorname{div}(\varepsilon^{-1} \nabla u) + \omega^2 \mu u = 0 \quad D_R \setminus \cup \overline{B_\rho}$$

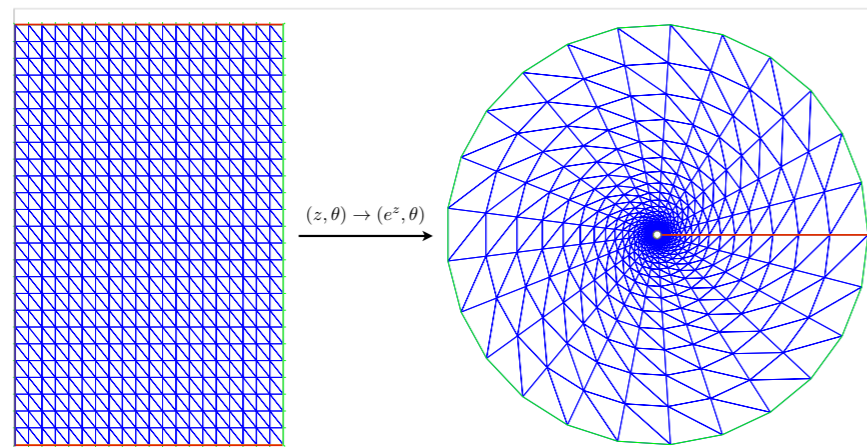
$$\partial_r u - iku = \partial_r u^{\text{inc}} - iku^{\text{inc}} \quad \partial D_R$$

+ matching between the PML and the strip +

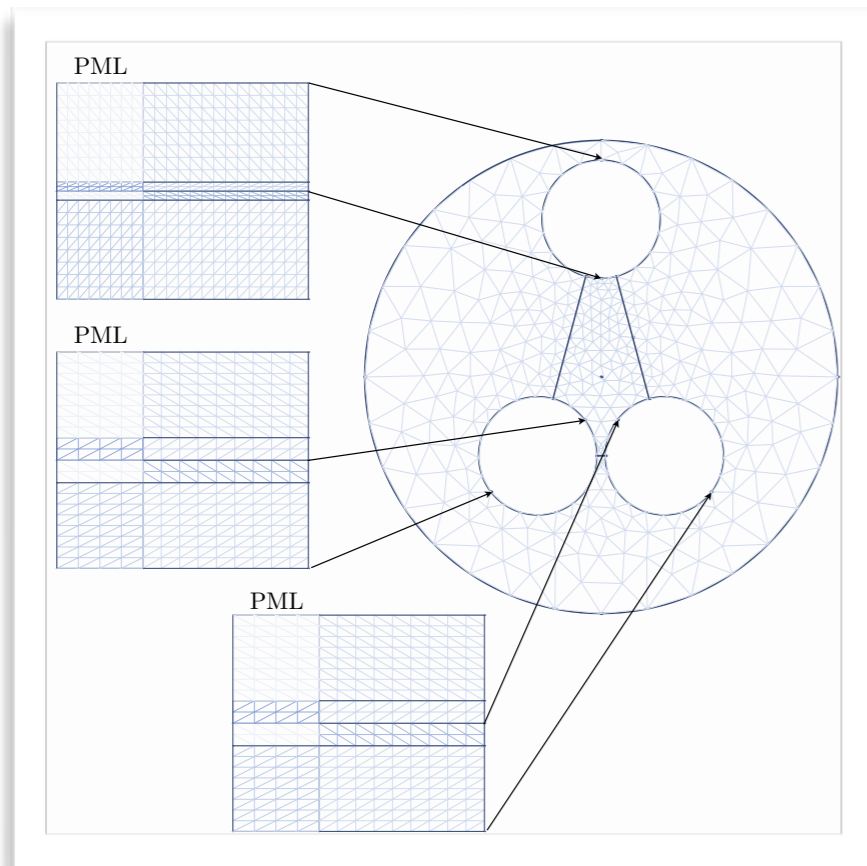
$$-\alpha \varepsilon^{-1} \partial_{zz} u - \frac{1}{\alpha} \partial_\theta \varepsilon^{-1} \partial_\theta u + \frac{\omega^2}{\alpha} \mu e^{\frac{2z}{\alpha}} u = 0 \quad S_\rho$$

$$\partial_z u(-L, \cdot) = 0$$

+ periodic conditions



With several corners



$$-\operatorname{div}(\varepsilon^{-1}\nabla u) + \omega^2 \mu u = 0 \quad D_R \setminus \cup \overline{B_\rho}$$

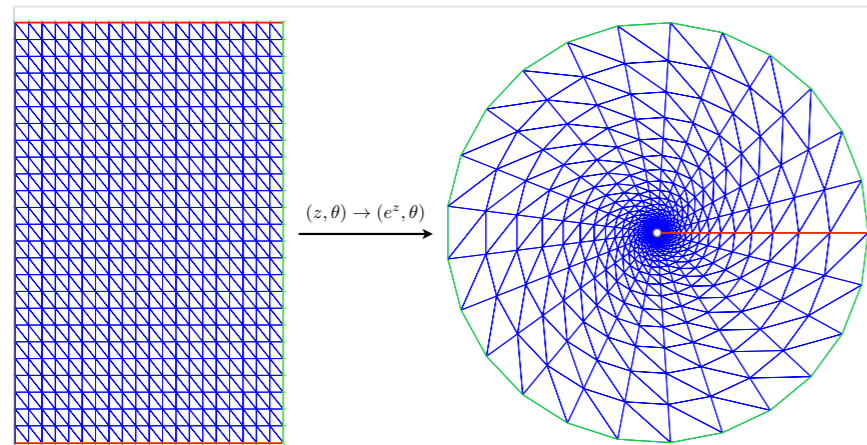
$$\partial_r u - iku = \partial_r u^{\text{inc}} - iku^{\text{inc}} \quad \partial D_R$$

+ matching between the PML and the strip +

$$-\alpha \varepsilon^{-1} \partial_{zz} u - \frac{1}{\alpha} \partial_\theta \varepsilon^{-1} \partial_\theta u + \frac{\omega^2}{\alpha} \mu e^{\frac{2z}{\alpha}} u = 0 \quad S_\rho$$

$$\partial_z u(-L, \cdot) = 0$$

+ periodic conditions



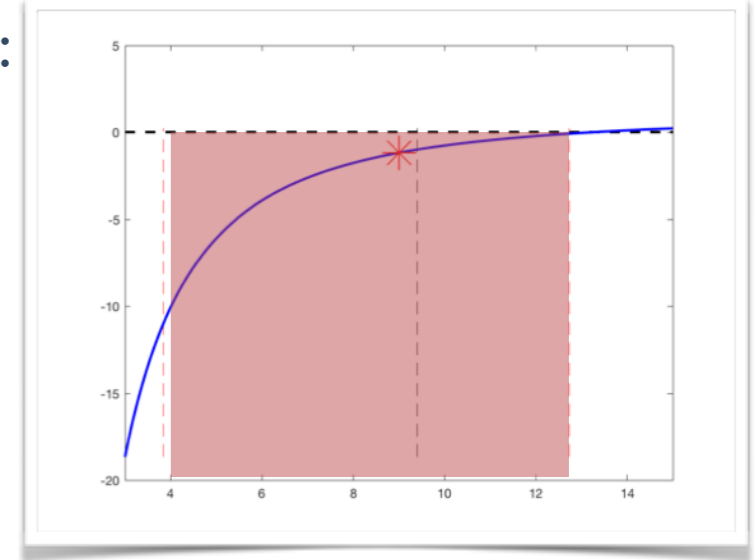
Computation with Lagrange FE of order 2 with a Matlab code

Numerical results with the multiscale-FEM

Numerical illustrations for triangular silver inclusion in vacuum:

$$\kappa_\varepsilon \in I_c \iff \omega \in [3.839 \text{ PHz}; 12.733 \text{ PHz}].$$

Results for $\omega = 9 \text{ PHz}$.

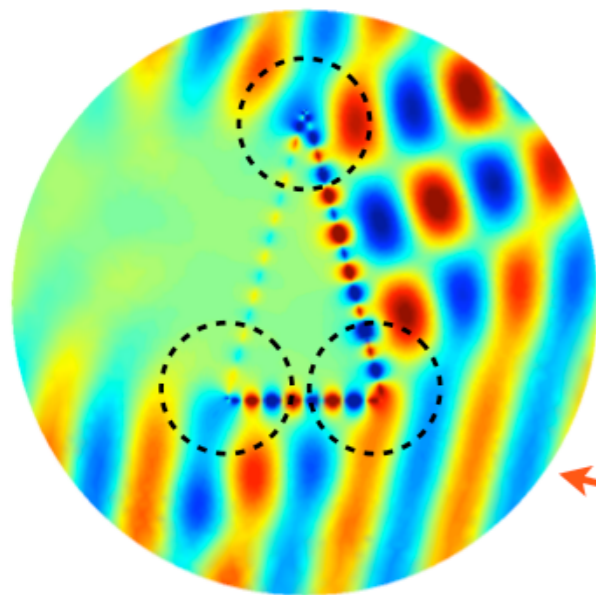
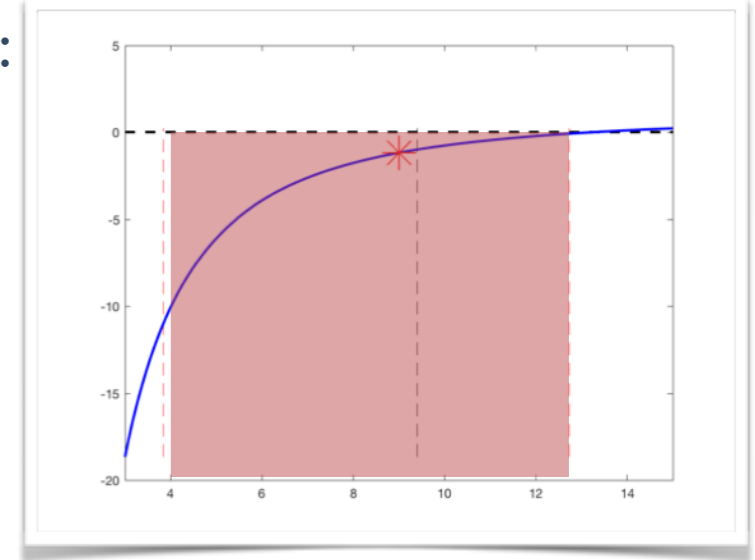


Numerical results with the multiscale-FEM

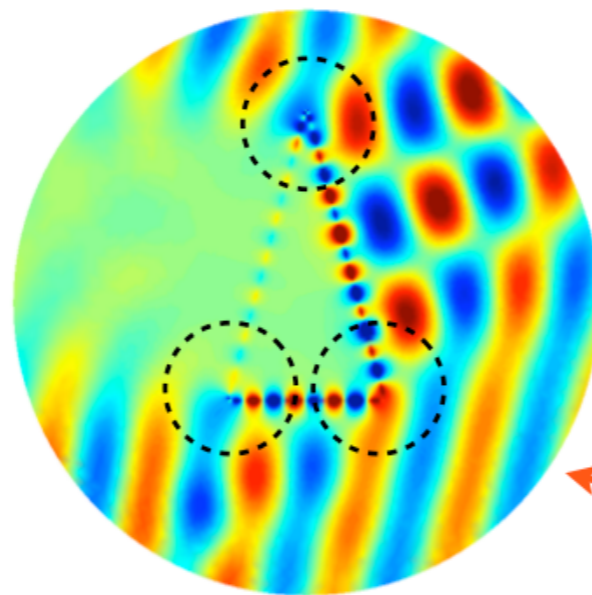
Numerical illustrations for triangular silver inclusion in vacuum:

$$\kappa_{\varepsilon} \in I_c \iff \omega \in [3.839 \text{ PHz}; 12.733 \text{ PHz}].$$

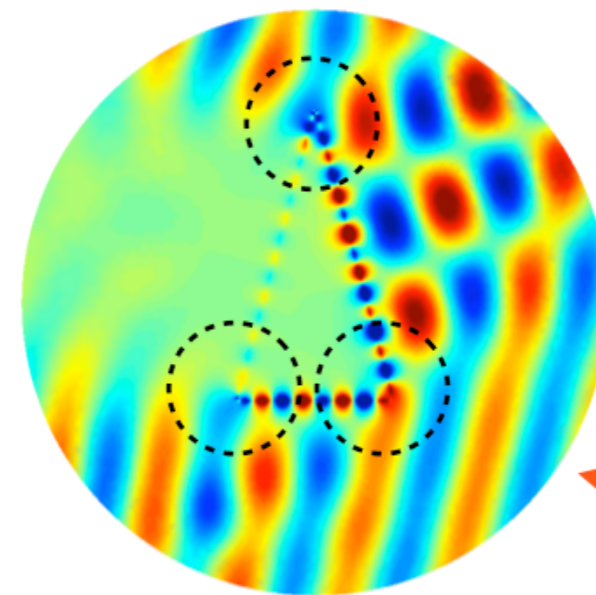
Results for $\omega = 9 \text{ PHz}$.



coarse mesh



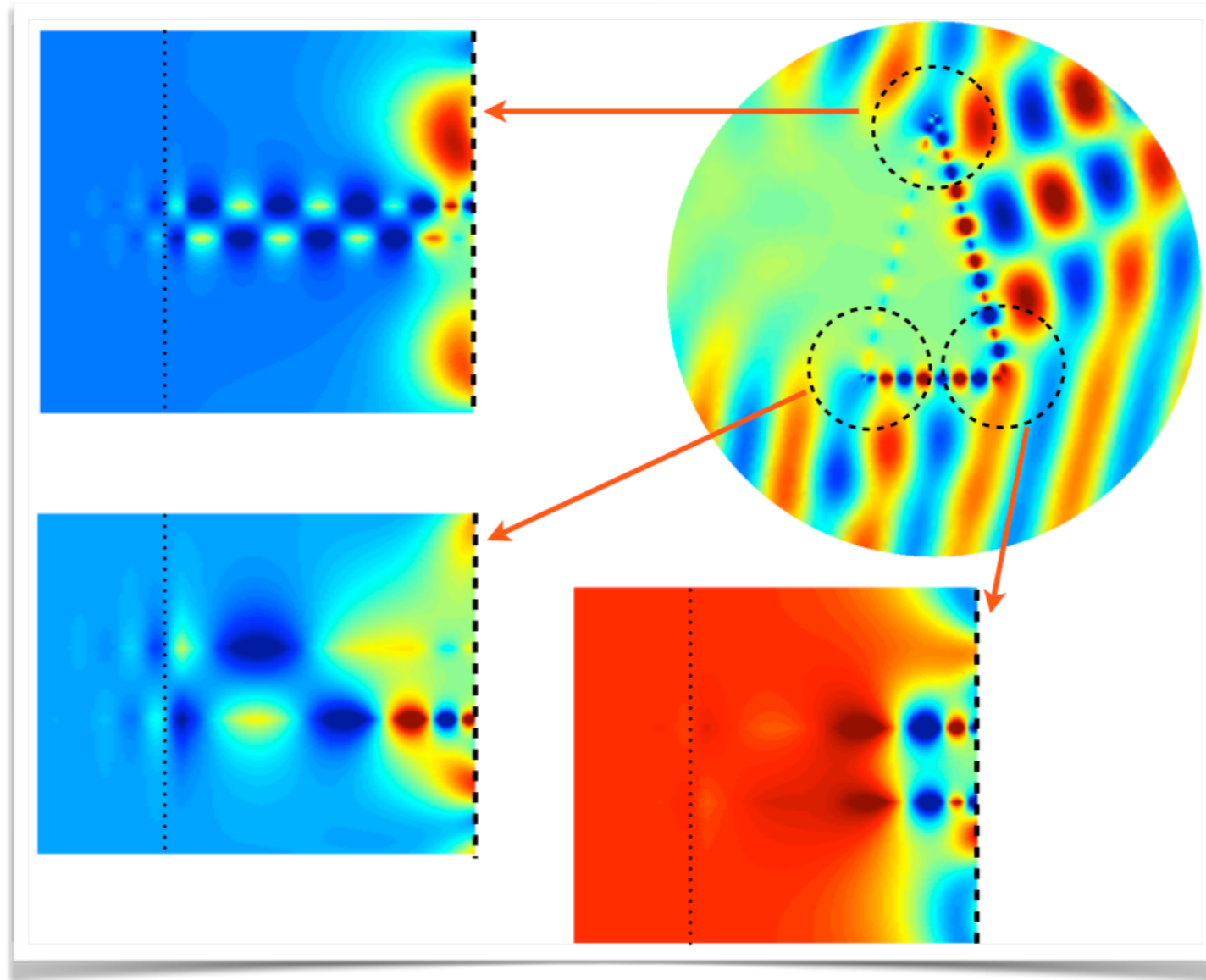
intermediate mesh



refined mesh

Numerical results with the multiscale-FEM

Numerical illustrations for triangular silver inclusion in vacuum: $\kappa_\varepsilon \in I_c$



Back to dissipative medium

Back to dissipative medium

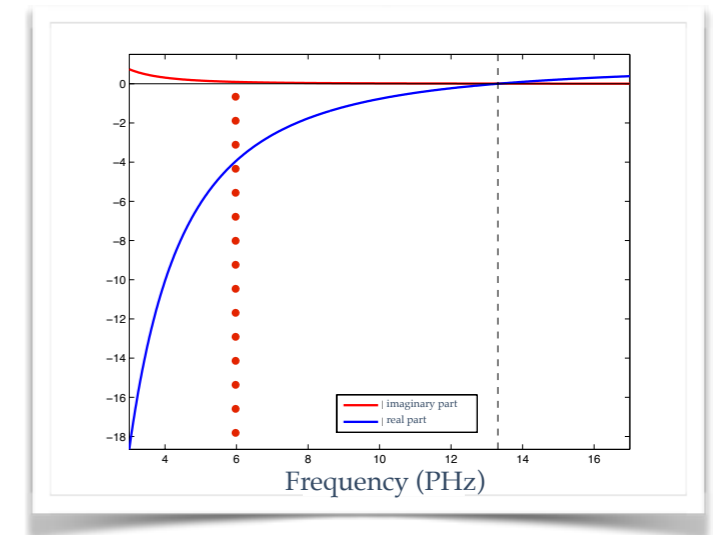
Considering losses in the metal, then the problem is well-posed. **The black-hole waves becomes of finite energy.** If dissipation is small, it requires **meshes sufficiently refined** at the corners to capture the oscillations.

Back to dissipative medium

Considering losses in the metal, then the problem is well-posed. **The black-hole waves becomes of finite energy.** If dissipation is small, it requires **meshes sufficiently refined** at the corners to capture the oscillations.

$$\kappa_\varepsilon \in I_c \iff \omega \in [3.839 \text{ PHz}; 12.733 \text{ PHz}].$$

$$\begin{aligned} \omega_p &= 13.3 \text{ PHz} & \omega &= 6 \text{ PHz} & \gamma &= 0.113 \text{ PHz} \\ \varepsilon_m(\omega) &= -3.9193 + 0.0926i & \varepsilon_d &= \mu_d = \mu_m = 1 \end{aligned}$$

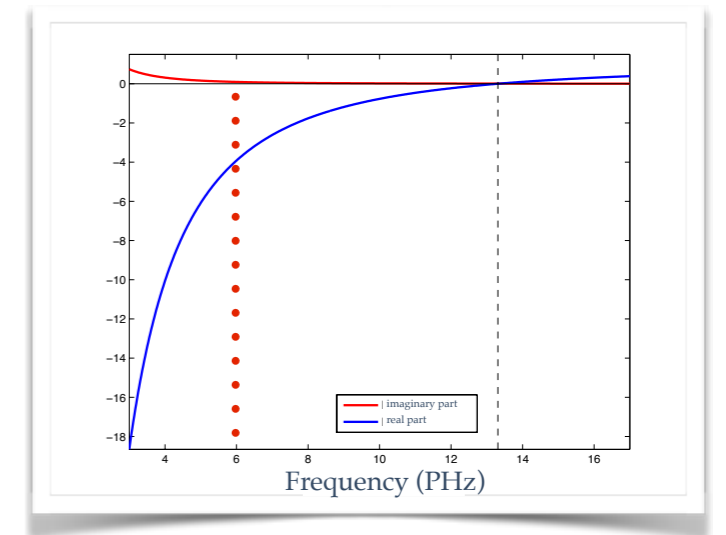


Back to dissipative medium

Considering losses in the metal, then the problem is well-posed. **The black-hole waves becomes of finite energy.** If dissipation is small, it requires **meshes sufficiently refined** at the corners to capture the oscillations.

$$\kappa_\varepsilon \in I_c \iff \omega \in [3.839 \text{ PHz}; 12.733 \text{ PHz}].$$

$$\begin{aligned} \omega_p &= 13.3 \text{ PHz} & \omega &= 6 \text{ PHz} & \gamma &= 0.113 \text{ PHz} \\ \varepsilon_m(\omega) &= -3.9193 + 0.0926i & \varepsilon_d &= \mu_d = \mu_m = 1 \end{aligned}$$



Without PMLs

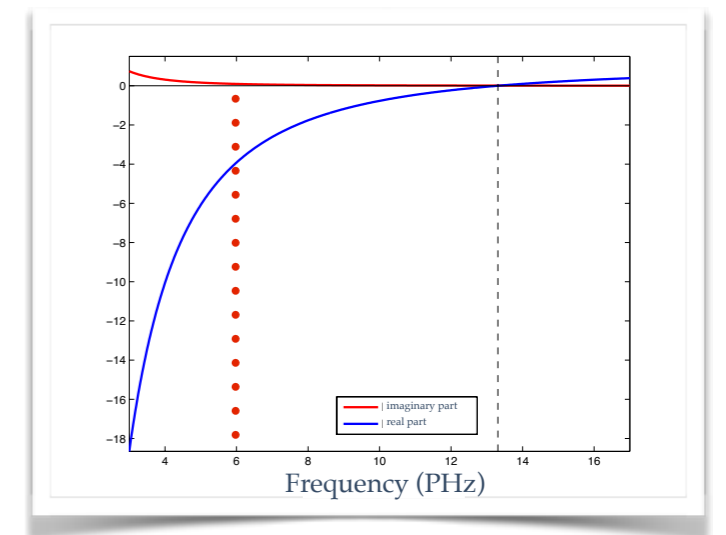
With PMLs

Back to dissipative medium

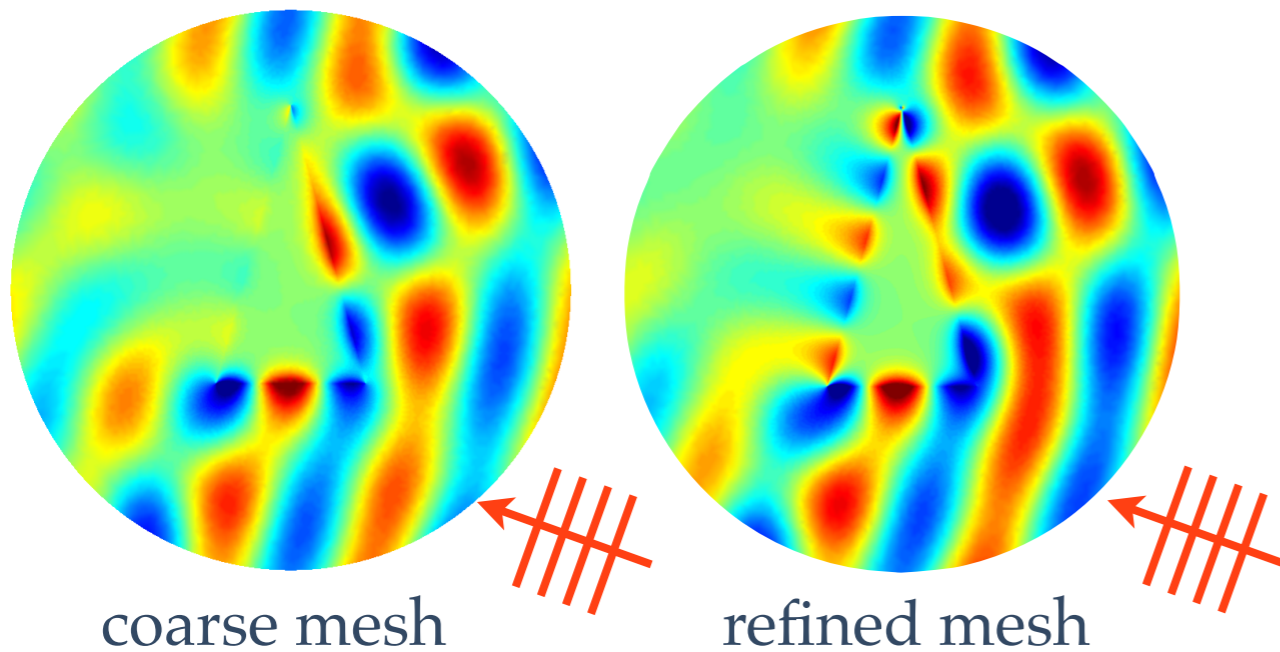
Considering losses in the metal, then the problem is well-posed. **The black-hole waves becomes of finite energy.** If dissipation is small, it requires **meshes sufficiently refined** at the corners to capture the oscillations.

$$\kappa_\varepsilon \in I_c \iff \omega \in [3.839 \text{ PHz}; 12.733 \text{ PHz}].$$

$$\begin{aligned} \omega_p &= 13.3 \text{ PHz} & \omega &= 6 \text{ PHz} & \gamma &= 0.113 \text{ PHz} \\ \varepsilon_m(\omega) &= -3.9193 + 0.0926i & \varepsilon_d &= \mu_d = \mu_m = 1 \end{aligned}$$



Without PMLs



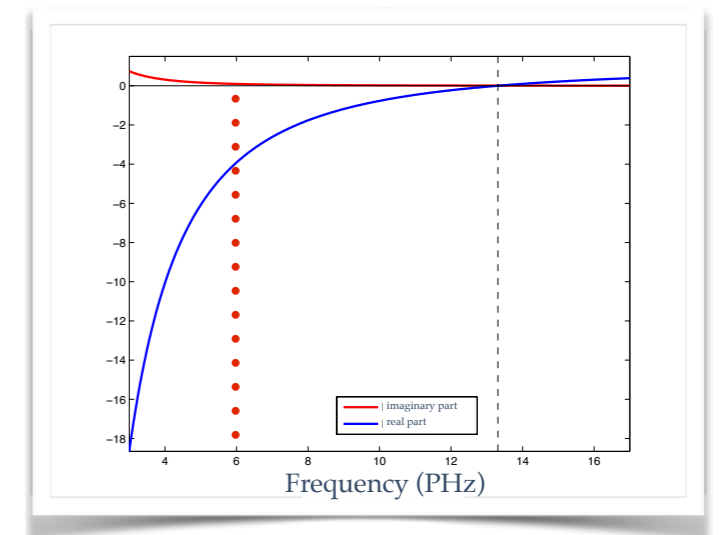
With PMLs

Back to dissipative medium

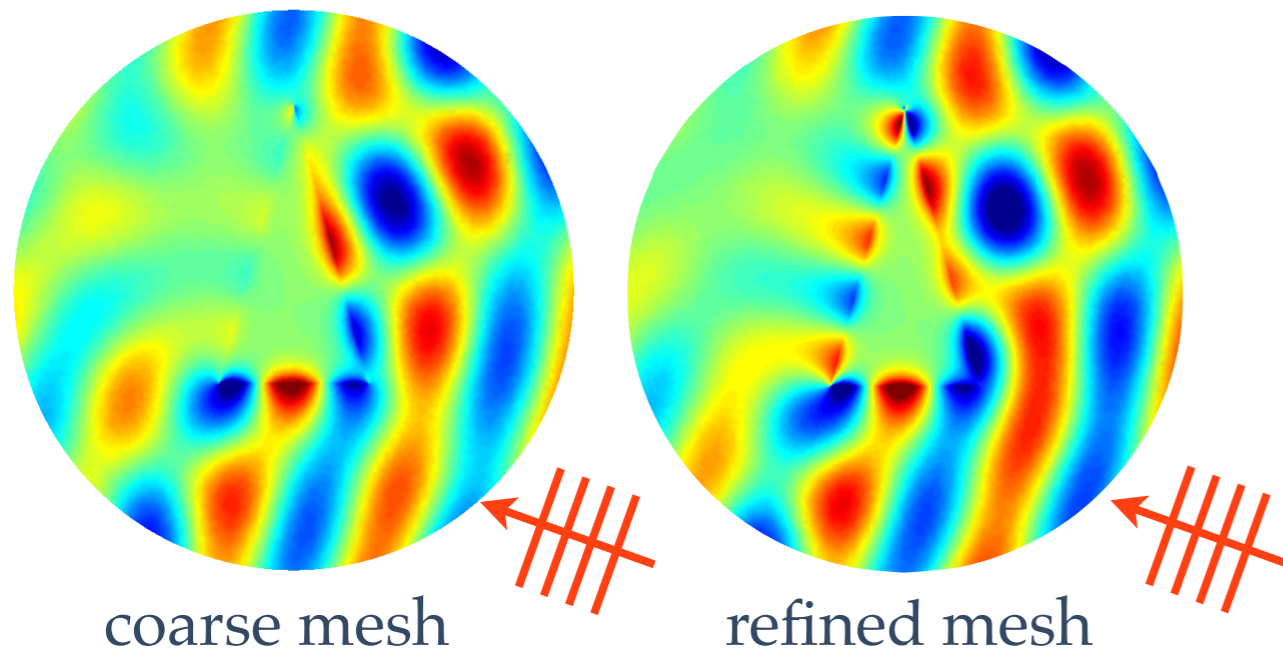
Considering losses in the metal, then the problem is well-posed. **The black-hole waves becomes of finite energy.** If dissipation is small, it requires **meshes sufficiently refined** at the corners to capture the oscillations.

$$\kappa_\varepsilon \in I_c \iff \omega \in [3.839 \text{ PHz}; 12.733 \text{ PHz}].$$

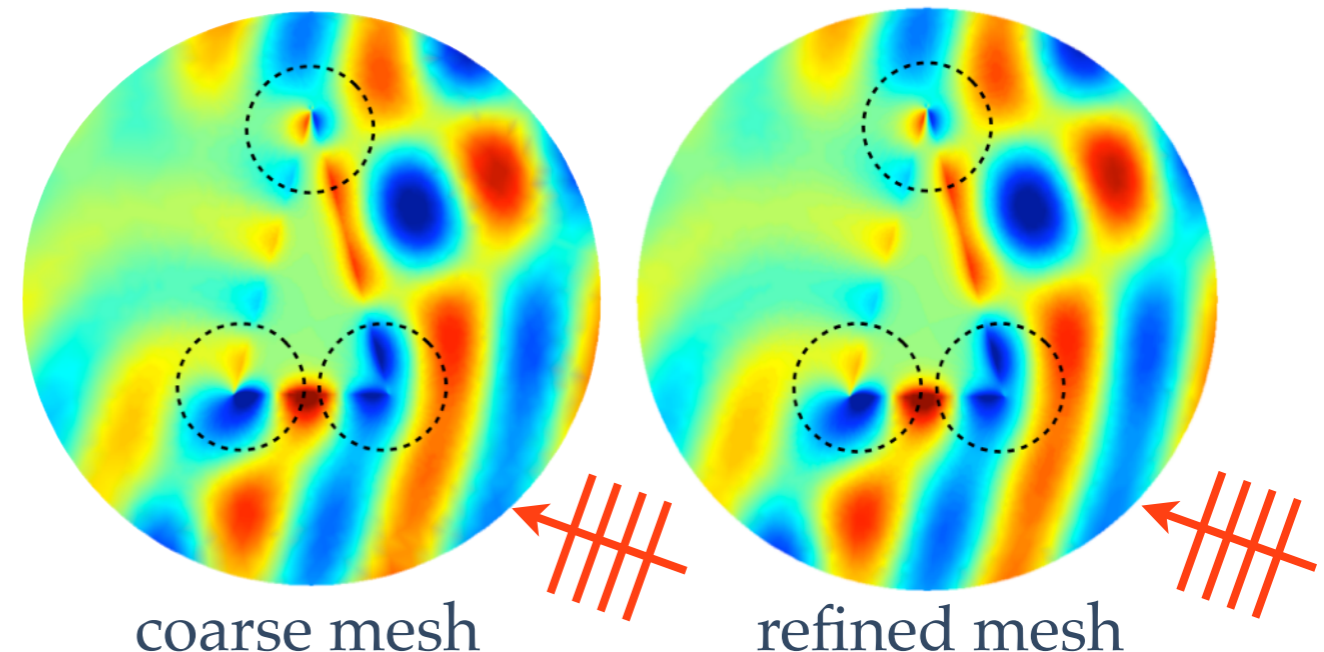
$$\begin{aligned} \omega_p &= 13.3 \text{ PHz} & \omega &= 6 \text{ PHz} & \gamma &= 0.113 \text{ PHz} \\ \varepsilon_m(\omega) &= -3.9193 + 0.0926i & \varepsilon_d &= \mu_d = \mu_m = 1 \end{aligned}$$



Without PMLs



With PMLs

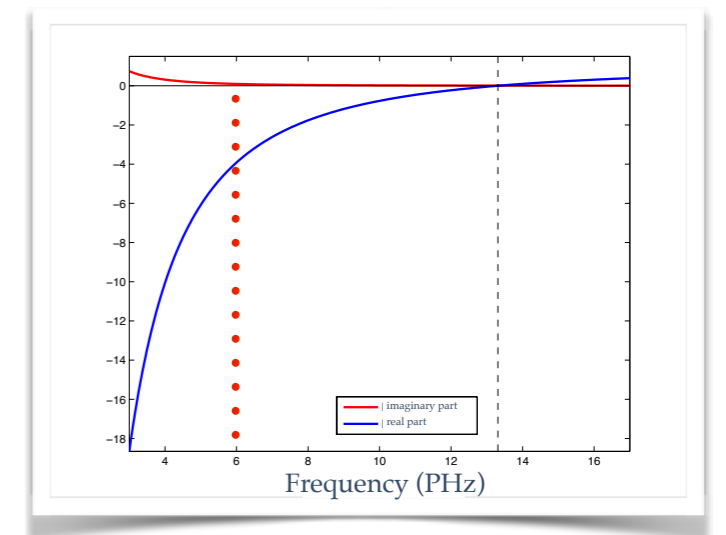


Back to dissipative medium

Considering losses in the metal, then the problem is well-posed. **The black-hole waves becomes of finite energy.** If dissipation is small, it requires **meshes sufficiently refined** at the corners to capture the oscillations.

$$\kappa_\varepsilon \in I_c \iff \omega \in [3.839 \text{ PHz}; 12.733 \text{ PHz}].$$

$$\begin{aligned} \omega_p &= 13.3 \text{ PHz} & \omega &= 6 \text{ PHz} & \gamma &= 0.113 \text{ PHz} \\ \varepsilon_m(\omega) &= -3.9193 + 0.0926i & \varepsilon_d &= \mu_d = \mu_m = 1 \end{aligned}$$



Without PMLs

With PMLs

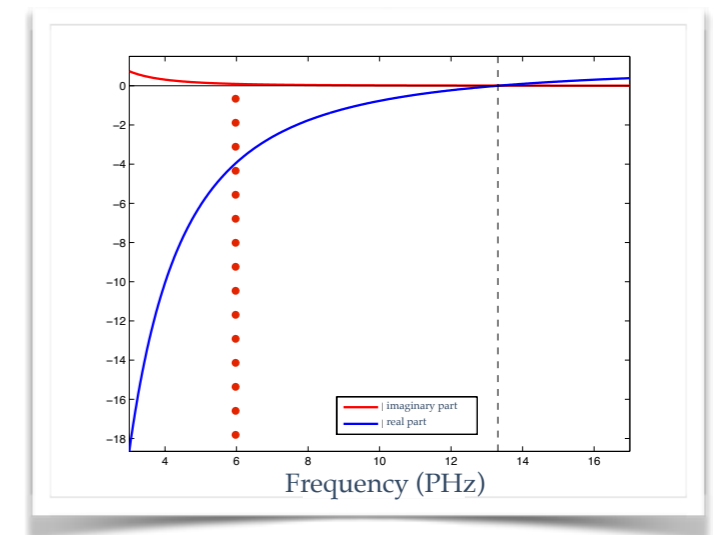
Animation in time $\Re(u e^{-i\omega t})$

Back to dissipative medium

Considering losses in the metal, then the problem is well-posed. **The black-hole waves becomes of finite energy.** If dissipation is small, it requires **meshes sufficiently refined** at the corners to capture the oscillations.

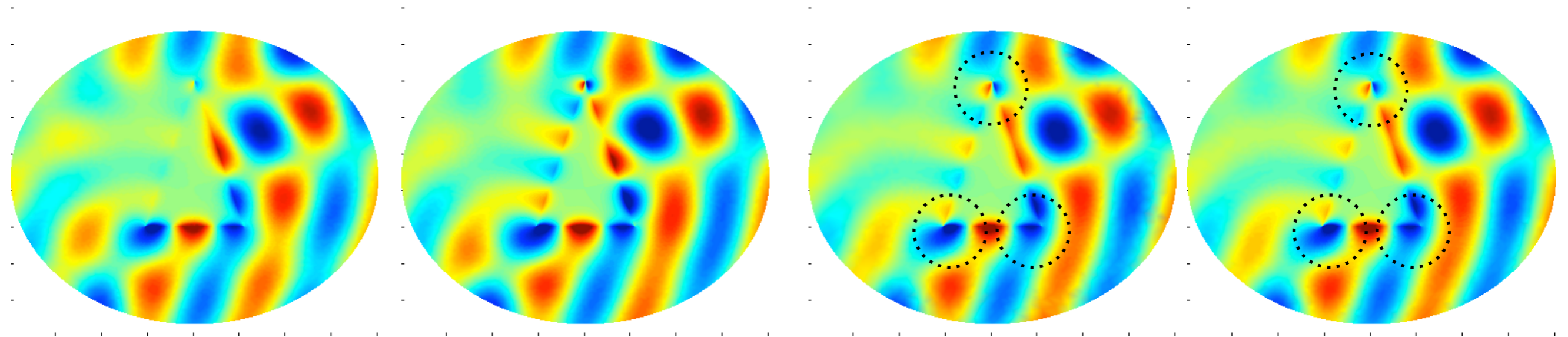
$$\kappa_\varepsilon \in I_c \iff \omega \in [3.839 \text{ PHz}; 12.733 \text{ PHz}].$$

$$\begin{aligned} \omega_p &= 13.3 \text{ PHz} & \omega &= 6 \text{ PHz} & \gamma &= 0.113 \text{ PHz} \\ \varepsilon_m(\omega) &= -3.9193 + 0.0926i & \varepsilon_d &= \mu_d = \mu_m = 1 \end{aligned}$$



Without PMLs

With PMLs



Animation in time $\Re(u e^{-i\omega t})$

Outline

- ❖ Introduction
- ❖ The limit problem
- ❖ Analysis at the corners
- ❖ Multiscale-FEM approach
- ❖ Extensions

Summary

Summary

Studying the **limit problem** (no dissipation) enabled us to figure out why standard FEM fails to well approximate the near field.

Summary

Studying the **limit problem** (no dissipation) enabled us to figure out why standard FEM fails to well approximate the near field.

T-conforming meshes and taking into account the **black-hole waves** is essential to accurately predict the field.

Summary

Studying the **limit problem** (no dissipation) enabled us to figure out why standard FEM fails to well approximate the near field.

T-conforming meshes and taking into account the **black-hole waves** is essential to accurately predict the field.

The use of **PMLs at the corners** is an original way to capture the black-hole waves.

Summary

Studying the **limit problem** (no dissipation) enabled us to figure out why standard FEM fails to well approximate the near field.

T-conforming meshes and taking into account the **black-hole waves** is essential to accurately predict the field.

The use of **PMLs at the corners** is an original way to capture the black-hole waves.

Extensions:

Summary

Studying the **limit problem** (no dissipation) enabled us to figure out why standard FEM fails to well approximate the near field.

T-conforming meshes and taking into account the **black-hole waves** is essential to accurately predict the field.

The use of **PMLs at the corners** is an original way to capture the black-hole waves.

Extensions:

Other applications: plasmonic waveguides  [Carvalho, Chesnel, Ciarlet \(2017\)](#).

Summary

Studying the **limit problem** (no dissipation) enabled us to figure out why standard FEM fails to well approximate the near field.

T-conforming meshes and taking into account the **black-hole waves** is essential to accurately predict the field.

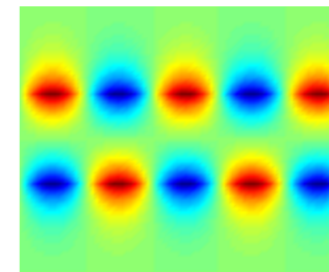
The use of **PMLs at the corners** is an original way to capture the black-hole waves.

Extensions:

Other applications: plasmonic waveguides  [Carvalho, Chesnel, Ciarlet \(2017\)](#).

Consider more relevant models for the metal's permittivity.
(Drude-Lorentz model or hydrodynamic Drude's model)

 [Schmitt, Scheid, Lanteri, Viquerat, Moreau, \(2016\)](#).



Summary

Studying the **limit problem** (no dissipation) enabled us to figure out why standard FEM fails to well approximate the near field.

T-conforming meshes and taking into account the **black-hole waves** is essential to accurately predict the field.

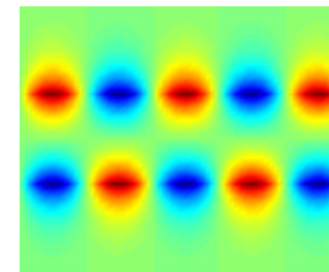
The use of **PMLs at the corners** is an original way to capture the black-hole waves.

Extensions:

Other applications: plasmonic waveguides  [Carvalho, Chesnel, Ciarlet \(2017\)](#).

Consider more relevant models for the metal's permittivity.
(Drude-Lorentz model or hydrodynamic Drude's model)

 [Schmitt, Scheid, Lanteri, Viquerat, Moreau, \(2016\)](#).



Consider Maxwell's equations.  [Bonnet-Ben Dhia, Chesnel, Ciarlet \(2012, 2014\), Carvalho \(2015\)](#).

Summary

Studying the **limit problem** (no dissipation) enabled us to figure out why standard FEM fails to well approximate the near field.

T-conforming meshes and taking into account the **black-hole waves** is essential to accurately predict the field.

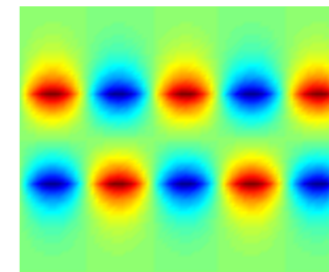
The use of **PMLs at the corners** is an original way to capture the black-hole waves.

Extensions:

Other applications: plasmonic waveguides  [Carvalho, Chesnel, Ciarlet \(2017\)](#).

Consider more relevant models for the metal's permittivity.
(Drude-Lorentz model or hydrodynamic Drude's model)

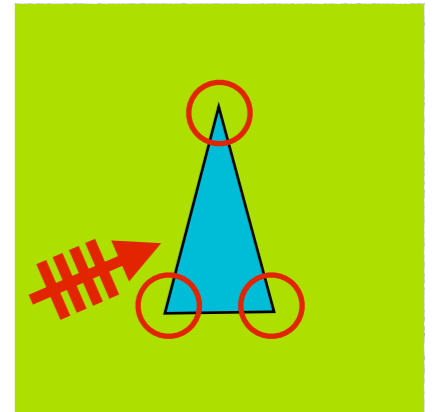
 [Schmitt, Scheid, Lanteri, Viquerat, Moreau, \(2016\)](#).



Consider Maxwell's equations.  [Bonnet-Ben Dhia, Chesnel, Ciarlet \(2012, 2014\), Carvalho \(2015\)](#).

Singular Complement Method

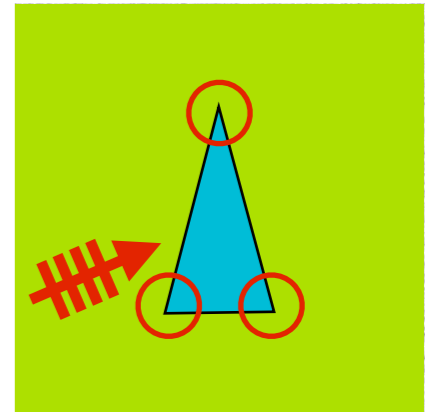
Near the corners, the solution decomposes as $u = bs + \tilde{u}$, $\tilde{u} \in H^1(D_R)$, $b \in \mathbb{C}$



Singular Complement Method

Near the corners, the solution decomposes as $u = bs + \tilde{u}$, $\tilde{u} \in H^1(D_R)$, $b \in \mathbb{C}$

This decomposition incites to use the **singular complement method**: if one knows explicitly bs , solve for \tilde{u}

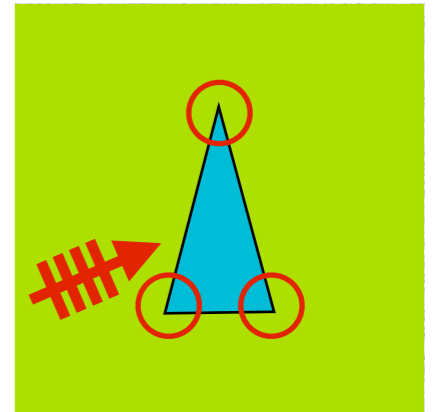


Singular Complement Method

Near the corners, the solution decomposes as $u = bs + \tilde{u}$, $\tilde{u} \in H^1(D_R)$, $b \in \mathbb{C}$

This decomposition incites to use the **singular complement method**: if one knows explicitly bs , solve for \tilde{u}

✓ No mesh constrains



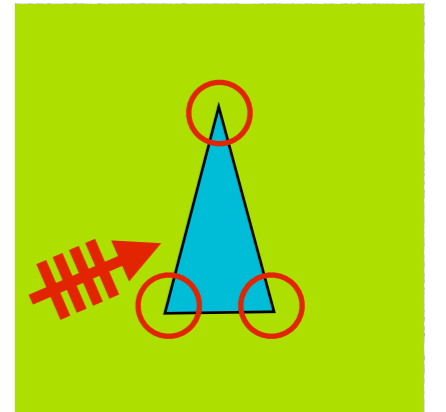
Singular Complement Method

Near the corners, the solution decomposes as $u = bs + \tilde{u}$, $\tilde{u} \in H^1(D_R)$, $b \in \mathbb{C}$

This decomposition incites to use the **singular complement method**: if one knows explicitly bs , solve for \tilde{u}

✓ No mesh constrains

✗ We don't know b



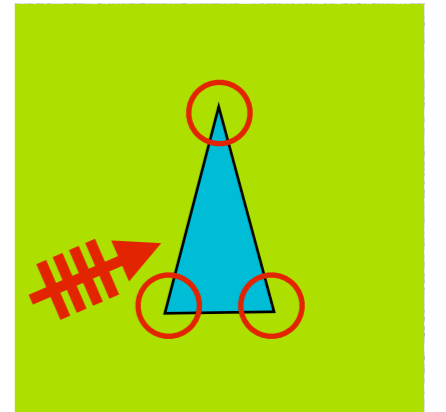
Singular Complement Method

Near the corners, the solution decomposes as $u = bs + \tilde{u}$, $\tilde{u} \in H^1(D_R)$, $b \in \mathbb{C}$

This decomposition incites to use the **singular complement method**: if one knows explicitly bs , solve for \tilde{u}

✓ No mesh constrains

✗ We don't know b



There are techniques to compute this singular coefficient using a **singular complement** (solution of the homogeneous problem, composed of the 2 singularities and a regular part).

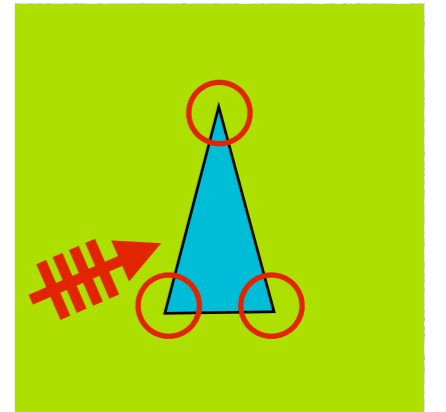
Singular Complement Method

Near the corners, the solution decomposes as $u = bs + \tilde{u}$, $\tilde{u} \in H^1(D_R)$, $b \in \mathbb{C}$

This decomposition incites to use the **singular complement method**: if one knows explicitly bs , solve for \tilde{u}

✓ No mesh constrains

✗ We don't know b



There are techniques to compute this singular coefficient using a **singular complement** (solution of the homogeneous problem, composed of the 2 singularities and a regular part).

Introduce one extra problem to solve (technical) but it has to be solved only once !

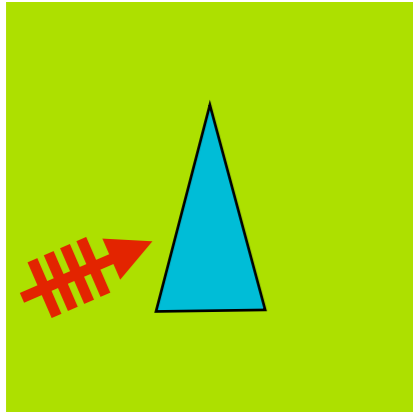


Carvalho, Ciarlet (in preparation).

Future work

Future work

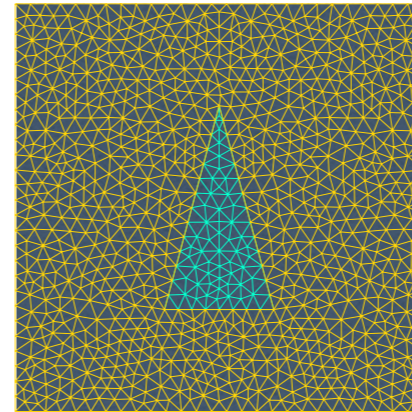
Future work



Variational-based approach

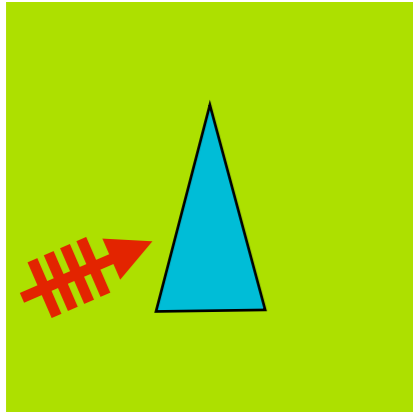


(multiscale- FEM)

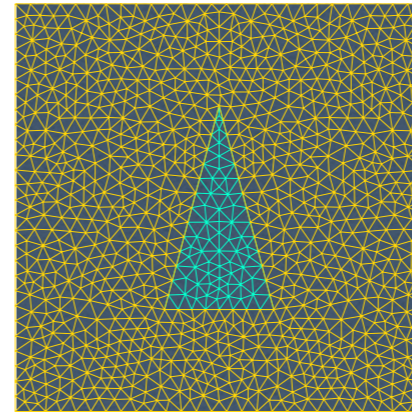


L

Future work

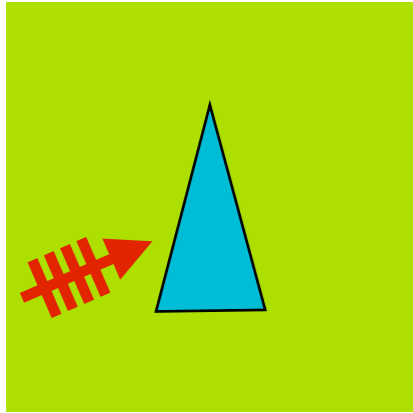


Variational-based approach
→
(multiscale- FEM)

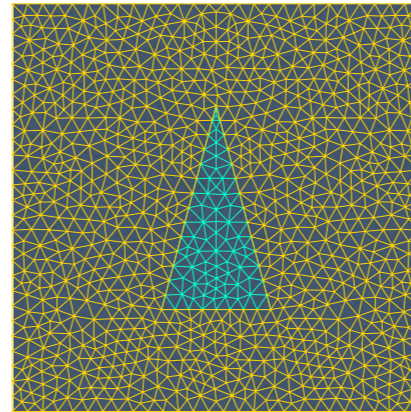


✓ Mathematical challenges solved

Future work

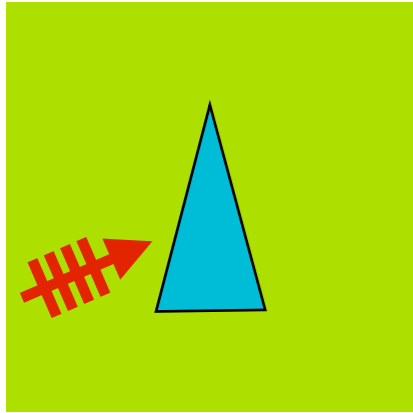


Variational-based approach
→
(multiscale- FEM)

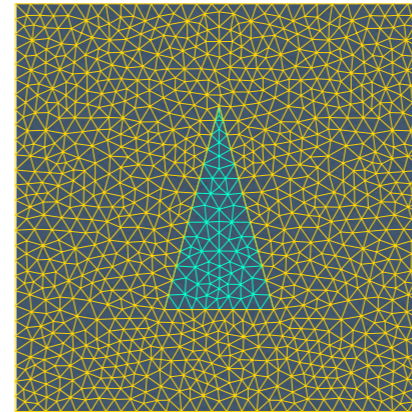


- ✓ Mathematical challenges solved
- ✗ High mesh constraints

Future work

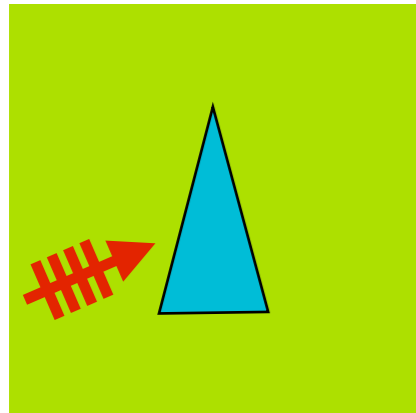


Variational-based approach
→
(multiscale- FEM)

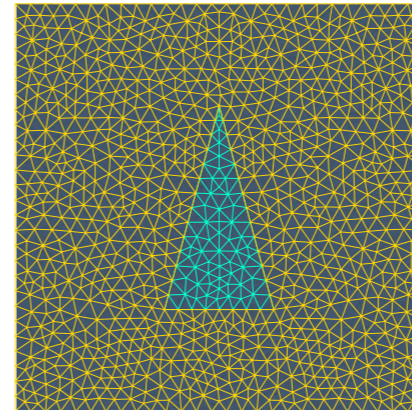


- ✓ Mathematical challenges solved
- ✗ High mesh constraints
- ✓ Use of SCM

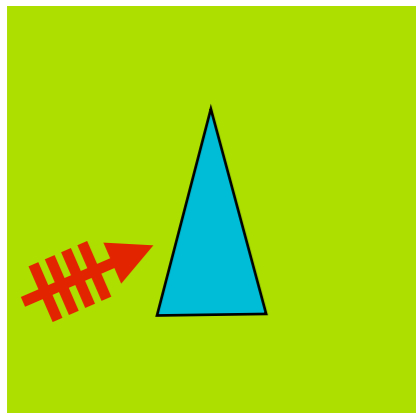
Future work



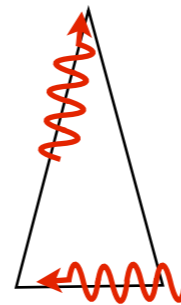
Variational-based approach
→
(multiscale- FEM)



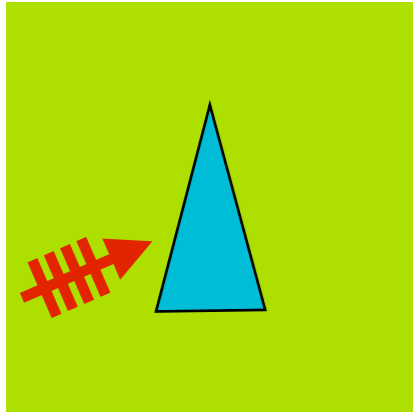
- ✓ Mathematical challenges solved
- ✗ High mesh constraints
- ✓ Use of SCM



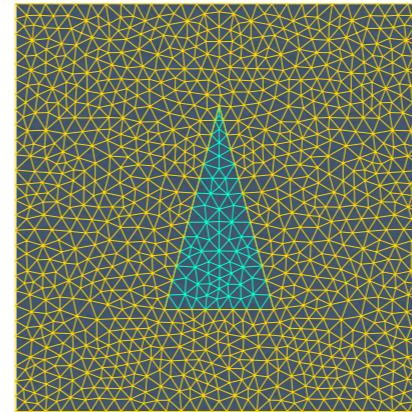
Multiscale asymptotic
boundary integral approach
→



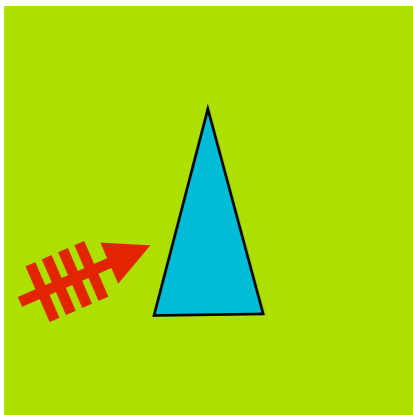
Future work



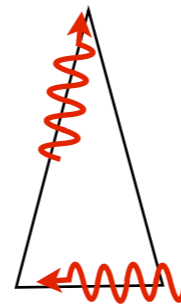
Variational-based approach
→
(multiscale- FEM)



- ✓ Mathematical challenges solved
- ✗ High mesh constraints
- ✓ Use of SCM

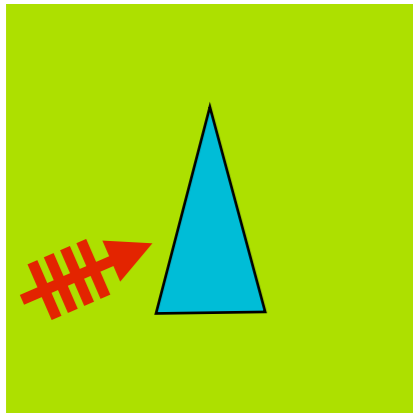


Multiscale asymptotic
boundary integral approach
→

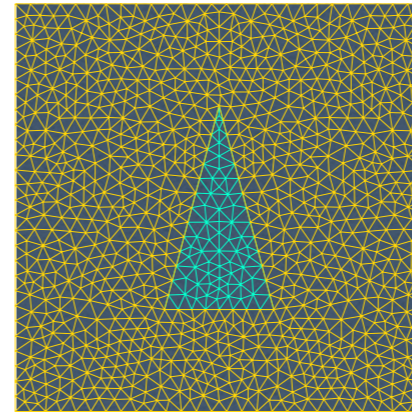


- ✓ No high mesh constraints

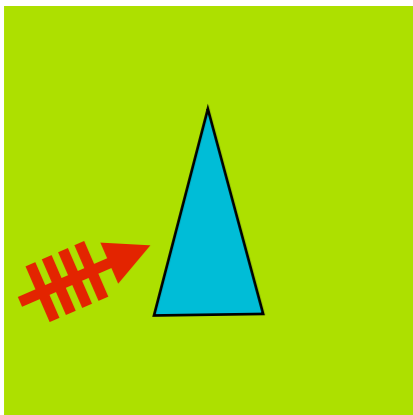
Future work



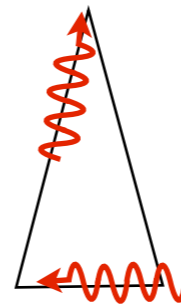
Variational-based approach
→
(multiscale- FEM)



- ✓ Mathematical challenges solved
- ✗ High mesh constraints
- ✓ Use of SCM

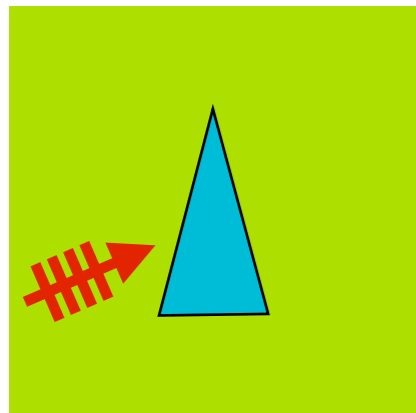


Multiscale asymptotic
boundary integral approach
→

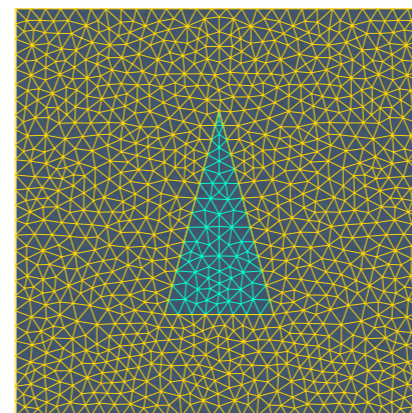


- ✓ No high mesh constraints
- ✗ Adapt the mathematical difficulties

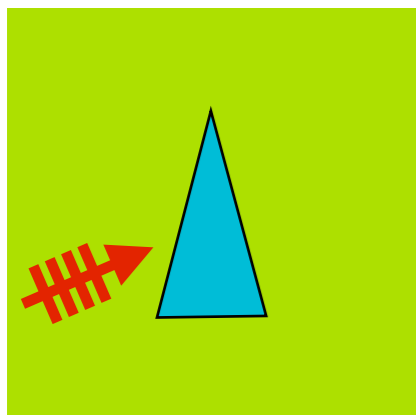
Future work



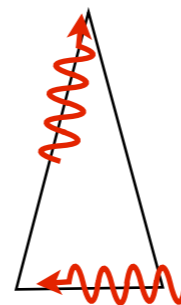
Variational-based approach
→
(multiscale- FEM)



- ✓ Mathematical challenges solved
- ✗ High mesh constraints
- ✓ Use of SCM



Multiscale asymptotic
boundary integral approach
→



- ✓ No high mesh constraints
- ✗ Adapt the mathematical difficulties

The black-hole is of "infinite" energy. What does it mean in the time domain ?

Thank you for your attention.